



# STK EOIR

## Model Description and Validation

**Authors:**

Robert Anderson  
Greg Cantwell

Space Dynamics Laboratory  
Utah State University Research Foundation  
1695 North Research Park Way  
North Logan, Utah 84341

**DOCUMENT NUMBER:** SDL/10-393  
**REVISION:** ORIGINAL RELEASE  
**DATE:** DECEMBER 9, 2010

---

## TABLE OF CONTENTS

<b>1. Introduction</b> .....	<b>1</b>
<b>2. Purpose</b> .....	<b>2</b>
<b>3. Overview</b> .....	<b>3</b>
3.1 Modeled Universe of Interest.....	3
3.2 Time .....	3
3.3 Spatial Coordinate System.....	3
3.4 Save and Restore.....	3
<b>4. Synthetic Scene Generator-Sensor Model</b> .....	<b>5</b>
4.1 Synthetic Scene Generator.....	5
4.1.1 Scene Generator to Sensor Interface.....	5
4.1.2 Scene Generator to Display .....	5
4.1.3 Geometric Operations .....	5
4.1.4 Radiometric Operations .....	6
4.1.5 Shapes & Surface Tessellation.....	9
4.1.6 Radiance Calculations.....	14
4.2 Scene Generator Processing Options .....	15
4.2.1 Coarse .....	15
4.2.2 Smooth.....	15
4.2.3 Bit Map .....	15
4.3 Modeled Universe of Interest Object Descriptions.....	16
4.3.1 Central Bodies.....	16
4.3.2 Stars.....	17
4.3.3 Satellites.....	17
4.3.4 Aircraft.....	18
4.3.5 Ground Vehicles .....	18
4.3.6 Missile and Missile Systems.....	19
<b>5. Sensor Model</b> .....	<b>20</b>
5.1 Sensor Model Overview .....	20
5.2 Field of View and Spatial Sampling Grid.....	21
5.3 Spectral Bandpass and Spectral Sampling Grid.....	23
5.4 Radiance Responsivity.....	24
5.5 Irradiance Responsivity .....	25
5.6 Optical Transfer Functions .....	25
5.6.1 Optical System OTF .....	25
5.6.2 Line-of-Sight Jitter OTF .....	27
5.6.3 System OTF .....	27
5.7 System Point Spread Function .....	27
5.8 Ensquared Energy .....	28

5.9	Radiometric Sensitivity.....	28
5.10	Saturation .....	29
5.11	Sensor Response .....	30
5.11.1	Response to Scene Generator Extended Area Sources .....	30
5.11.2	Response to Scene Generator Point Sources .....	30
5.11.3	Dark offset .....	30
5.11.4	Sensor Noise and Scene Photon Noise .....	31
5.11.5	Saturation .....	31
5.11.6	Total Response.....	31
5.12	Static Metrics .....	31
5.12.1	Detector Footprint Modulation Transfer Function .....	34
5.13	Dynamic Metrics Involving a Target.....	35
5.13.1	Point Source Targets and Backgrounds .....	35
5.13.2	Point Source Detection Criteria and Point Source Signal-to-Noise Ratio .....	36
5.13.3	Extended Area Targets.....	37
5.13.4	Summary of Dynamic Metrics Involving Targets .....	39
<b>6.</b>	<b>Scene Generator Validation.....</b>	<b>41</b>
6.1	Geometric.....	41
6.1.1	FOV – Projected Angles—Distance Ordering.....	41
6.1.2	Distance Ordering & Obscuration .....	43
6.1.3	Bitmap – Registration .....	47
6.2	Area Radiometric Equation.....	48
6.2.1	Background.....	48
6.2.2	Self-Radiance—Emissivity and Effective Temperature.....	50
6.2.3	Reflected .....	51
6.2.4	Point Radiometric Equation.....	55
6.2.5	SRF .....	59
<b>7.</b>	<b>Sensor Model Validation .....</b>	<b>76</b>
7.1	Angular Extent of Field Of View.....	76
7.2	Ideal Field Of View .....	76
7.2.1	Point Source .....	77
7.2.2	Extended Area Source.....	79
7.3	Numerical Integration over Wavelength.....	80
7.4	Uniform Extended Source Response .....	82
7.4.1	Dark Offset.....	83
7.4.2	Peak Radiance Responsivity .....	83
7.4.3	Sensor Dark Noise .....	85
7.4.4	Scene Photon Noise .....	86
7.4.5	Saturation .....	87
7.5	Point Source Response.....	88
7.5.1	Diffraction Limited Point Spread Function .....	88
7.5.2	Point Spread Function with Aberrations.....	91
7.5.3	Point Spread Function with Defocus .....	96

---

7.5.4	Point Spread Function with Line-of-Sight Jitter .....	100
7.5.5	Ensquared Energy .....	104
7.6	Static Metrics .....	105
7.7	Dynamic Metrics Involving a Target.....	107
7.7.1	Stationary Target against a Uniform Background .....	107
7.7.2	Satellite Point Source Target .....	109
7.8	SNR Access Constraint.....	110

---

## 1. INTRODUCTION

STK EOIR provides computer automation support for people who specify, develop, or operate systems that include electro-optical/infrared sensors. STK EOIR's physics-based models rapidly and interactively calculate medium-fidelity results, allowing users to quickly explore a wide set of possible alternatives to discover a best solution to the problem at hand. As the best solutions are determined, the user can, as necessary, select higher fidelity models within STK EOIR or revert to other, more traditional phenomenology codes within a more restricted solution space.

STK EOIR provides the following advantages:

- STK EOIR incorporates all necessary components for modeling sensor-based systems into a single program, saving users the task of compiling results from separately operated programs.
- A single, trained user can operate STK EOIR in all its aspects. Teams of subject experts are not required.
- STK EOIR enables sensor modeling to take place over an incredible diversity of applications and range of scales—serving needs ranging from Ballistic Missile Defense to Space Situational Awareness to Civil Space Exploration anywhere in the Solar System.
- As a maintained COTS product, the development costs are distributed across all users.

---

## 2. PURPOSE

This document describes the equations and algorithms used in the STK EOIR model and validates that the software implements them. In some cases, this document compares STK EOIR's model results against independent models. This information will aid users in determining whether the modeling fidelity produced by STK EOIR is sufficient for their modeling needs.

The software architecture and detailed codes of STK EOIR remain proprietary and subject to use agreements.

---

## 3. OVERVIEW

The STK EOIR program operates on a modeled universe of interest (MUI) with up to six independent synthetic scene generator—sensor model pairs (SSG-SMP). SSG-SMPs may be placed within the MUI and operated so as to produce images of the MUI. For instance, an SSG-SMP could be placed on a satellite orbiting the Earth and generate images of the Earth.

All SSG-SMPs view the same MUI, at the same instant of time, but usually from different viewing geometries.

Note that the number of SSG-SMPs is fixed when the EOIR software is compiled. It can readily be changed, but the practical number of SSG-SMP pairs is very dependent on the user's computational resources.

### 3.1 MODELED UNIVERSE OF INTEREST

The user selects objects displayed in the STK Object Browser, i.e. objects previously created in STK, for inclusion in the STK EOIR MUI.

The STK EOIR MUI consists of the Sun, any of the planets in the solar system, the Earth's moon, and a star field. The user can add or remove any of the objects, except the Sun, from the MUI. Likewise, the user can include up to 16 satellites, orbiting any of the Central Bodies in the MUI. The user can include up to six vehicles, air or ground<sup>1</sup>, residing on any of the included central bodies. The user can include up to six single or multistage<sup>1</sup>, surface-to-surface missiles on the Earth. Up to six SSG-SMPs can be included and reside on any of the sun, planets, moon, satellites, vehicles or missiles.

Future versions will include other planet's moons, asteroids, the zodiacal light, and a galactic background image. Future versions may also relax the above limits on the number of objects simulated in the STK EOIR MUI. The practical, maximum number of SSG-SMP pairs that can be simultaneously simulated is quite dependent on the user's computational resources.

### 3.2 TIME

STK EOIR utilizes the current STK date and time step value. Internal STK EOIR time is maintained as a double precision J2000 date and fraction of a day. J2000 is an astronomical time keeping convention that denotes the date/time since noon (12:00 pm) on January 1, 2000.

### 3.3 SPATIAL COORDINATE SYSTEM

STK EOIR uses the positions and orientations of simulated objects as calculated by STK and thus corresponds to STK's notion of coordinates.

### 3.4 SAVE AND RESTORE

When a user saves the current state of an STK simulation, STK EOIR automatically saves its internal state to a file with the same name but having an .SCD file extension.

When a user restores a saved STK simulation, STK EOIR seamlessly restores its internal state using the file of the same name but having an .SCD file extension.

---

<sup>1</sup> Disabled for initial release.

---

Saved STK EOIR simulation files reside in the same folder as the corresponding STK .SC file. Sensor models can also be saved and restored independent of simulations. This allows a sensor model to be defined once and then readily be incorporated into multiple scenarios.



---

## 4. SYNTHETIC SCENE GENERATOR-SENSOR MODEL

### 4.1 SYNTHETIC SCENE GENERATOR

The following sections describe synthetic scene generation with respect to a single SSG-SMP.

#### 4.1.1 Scene Generator to Sensor Interface

The scene generator's output to the sensor model is a two-dimensional array of spectral radiance vectors. Each (spectral radiance vector) element of the array represents one angular sample as described in Section 4.1.3 below. Each spectral radiance vector is a set of  $N$  spectral radiance values in units of  $\text{W cm}^{-2} \text{sr}^{-1} \mu\text{m}^{-1}$ . Each of the  $N$  spectral radiance values corresponds to the  $N$  wavelength intervals from  $\lambda_{\min}$  to  $\lambda_{\max}$ , as defined by the sensor model. STK EOIR can model scenes and sensor operation in the spectral range from  $0.28 \mu\text{m}$  to  $28.0 \mu\text{m}$ .

#### 4.1.2 Scene Generator to Display

The scene generator's output can be directed to the computer display, should the user wish to observe the input scene to the sensor model. This mode requires less processing than when the sensor model is turned on.

One scene generator sample is output to one display pixel. To produce this display pixel value, the scene generator radiance vector is integrated over the bandwidth and converted to irradiance ( $\text{W cm}^{-2}$ ) at sensor aperture. This irradiance is dynamic range compressed. If Automatic Gain Control (AGC) is turned on, the compression forces the greatest and least pixel values to fit within the range of 0-255. AGC tends to function as an infinitely capable image intensifier and can produce strange effects for images with constant or almost constant radiance, i.e. low contrast scenes.

If AGC is turned off, the pixels are brightness and contrast processed with user selectable constants. These constants are selectable by sliders, with each successive discrete position representing a multiplicative factor of about 30 from the previous button. The compression forces the pixel value to fit within the range of 0-255. Dimmer values are clipped to 0 and brighter values are clipped to 255.

Of course, the display function ignores the fact that the human eye will not respond to ultraviolet or infrared wavelengths. The display represents the compressed irradiance value.

Point sources are already maintained as irradiances but must still be integrated over the bandwidth. Point source locations are digitized to the nearest pixel location for display. Each point source is added to the irradiance already in the pixel.

#### 4.1.3 Geometric Operations

Synthetic Scene Generation operates on objects in the MUI that reside within or are intersected by the sensor's view frustum. The latter being an orthogonal pyramid whose angular dimensions correspond to the sensor's Field of View (FOV) and whose central axis corresponds to the sensor's Line of Sight (LOS) as determined by STK.

The volume within the view frustum is sampled in orthogonal angular directions at a frequency determined by the sensor parameters. The sensor model defines a pixel's instantaneous field of view (IFOV) in each of two orthogonal, angular dimensions—nominally horizontal and vertical.

---

The scene generator's angular sampling frequency is four times that of the sensor's IFOV. Thus, each sensor pixel encompasses 4x4 or 16 scene generator samples.

In the sensor's body coordinate system, the positive Z axis is the LOS. The X axis is the horizontal extent of the focal plane, and the Y axis is the vertical extent of the focal plane. A sample direction can be equally expressed as a  $\theta, \phi$  pair in the body coordinate system, as an X, Y position on the focal plane, or as an  $\alpha, \beta$  angle on the focal plane.

Each directional sample terminates on the surface of the nearest encountered object in the MUI. The MUI is centered within a sphere with a diameter 1000 times Neptune's orbit, effectively the "bowl of the sky". Thus, if no planet, satellite, or other object is encountered, the directional sample terminates on the surface of that large sphere. For each directional sample, there is a corresponding terminating object and object's surface coordinate. The surface coordinates for the "bowl of the sky" are the astronomical coordinates of Right Ascension and Declination.

It is on the "bowl of the sky" that the future galactic image will be "painted".

#### 4.1.4 Radiometric Operations

STK EOIR's imaging radiometer sensor model simulates the physics of a sensor that measures photon (radiant energy) flux. The Scene Generator calculates the photon (radiant energy) flux for each angular sample in  $W\ cm^{-2}\ sr^{-1}\ \mu m^{-1}$ . This includes the surface radiance of the terminating object, at the sampled point, and any radiance added or removed along the sample path by traversing an atmosphere.

The Scene Generator simulates sources of thermal radiant flux via either the Planck function or, as in the case of the sun, by an incorporated, measured spectral radiance vector. The Planck function calculation utilizes the object's surface temperature and surface emissivity at the sample point. An expandable table allows additional spectral radiance vectors to be supplied and assigned to represent the self-radiance of objects. The measured solar spectral radiance vector is the 0<sup>th</sup> entry in the table. Missile object plume spectra are an example for using this tabular capability. [The current STK EOIR release does not yet provide a user interface for accessing this functionality.]

The Scene Generator also computes the reflection of radiant flux, originating elsewhere, off the surfaces of MUI objects. Reflection depends on the surface's optical properties as determined by the surface material type.

Before either self-radiance or reflected radiances are computed, the surfaces of objects (other than the galaxy) are initialized to a "basement" radiance corresponding to the sum of: integrated starlight, zodiacal light, and air glow. In the following, radiances were scaled to approximate data given in, "The 1997 reference of diffuse night sky brightness", Ch. Leinert, S. Bowyer, L.K. Haikala, M.S. Hanner, M.G. Hauser, A.-Ch. Levasseur-Regourd, I. Mann, K. Mattila, W.T. Reach, W. Schlosser, H.J. Staude, G.N. Toller, J.L. Weiland, J.L. Weinberg, and A.N. Witt

- Integrated starlight is simulated by a scaled 3900K blackbody curve
- Zodiacal light is simulated as the scaled sum of solar reflection off of a dark mineral [literally it uses the Mars surface material properties] plus 250K self-radiance
- Airglow is currently simulated as 3 spectral lines at: 0.5577 $\mu m$ , 0.630 $\mu m$ , and 0.589 $\mu m$  scaled to have an integrated visible irradiance value of  $5.1 \times 10^{-18}\ W/cm^2$ . An expected

future enhancement would be to provide a continuum spectrum per the above mentioned document

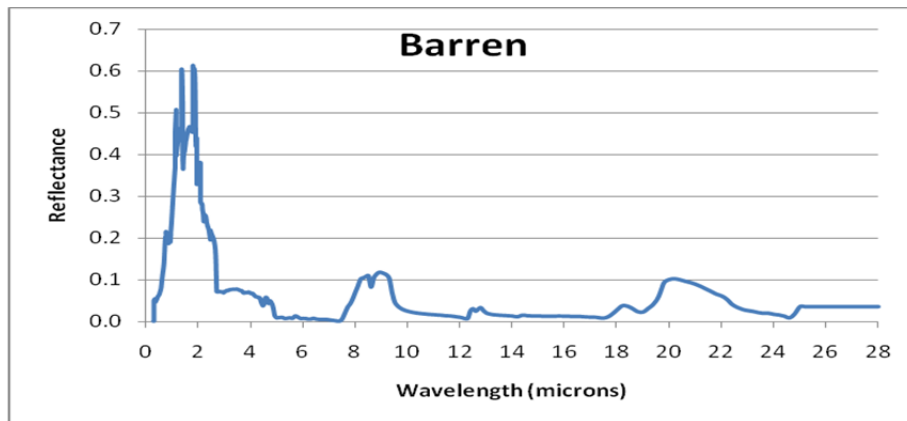
Future versions will replace this airglow model with a measured spectrum extending into the infrared. Also application of the airglow component needs to be related to proximity of Earth's atmosphere.

#### 4.1.4.1 Surface Optical Properties of Materials

The general issues of reflection for a material are that its surface will 1) differentially absorb radiant flux by wavelength, i.e. the surface has a color, and 2) the radiant flux arriving from some input direction will reflect into outgoing directions according to surface properties of the material.

A surface that scatters the incoming flux equally into all outgoing directions is referred to as Lambertian, e.g., a sheet of white copy paper. A surface that reflects incoming light as does a mirror is referred to as specular. This characteristic of the proportion of flux in the outgoing direction versus the incoming direction is incorporated within a surface property called the bi-directional reflectance distribution function (BRDF). In the most general case, BRDF is a function of wavelength as well as incoming and outgoing directions; however, for many materials, especially natural materials, it is practical to treat BRDF as a function of direction alone.

STK EOIR simulates differential absorption by wavelength through a Spectral Reflectance Function (SRF) wherein a value of 0 at a wavelength is 0% reflection (100% absorption) and a value of 1 at a wavelength is 100% reflection (0% absorption). SRF's for specific materials are described in 0.



The surface spectral emission (used in conjunction with self-radiance) is calculated as  $1 - \text{SRF}_\lambda$ . Surface materials are assumed to have no transparency. In the general case:

$$\text{Absorption} + \text{Reflection} + \text{Transmission} = 1$$

$$\text{Absorption} = \text{Emission}$$

$$\text{Therefore if Transmission} = 0, \text{Emission} = 1 - \text{Reflection}$$

EOIR's BRDF function uses a modified Phong Reflection Model, in that backscatter is simulated, in addition to forward scatter. Four parameters control:

- $k_0$  - Spectral vs. Lambertian nature of the surface

- $k_1$  - Relative strength of forward scatter vs. backscatter
- $\alpha$  - Sharpness of the forward (reflected) scatter peak
- $\beta$  - Sharpness of the back scatter peak

The BRDF function is normalized such that reflected flux is conserved. Every arriving photon will be reflected, in some direction.

$$BRDF = (k_0 + (1 - k_0) * (k_1 \beta e^{-\pi \beta (\hat{I} \cdot \hat{O})} + (1 - k_1) \alpha e^{-\pi \alpha (\hat{O} \cdot \hat{R})}) / \pi \quad (1)$$

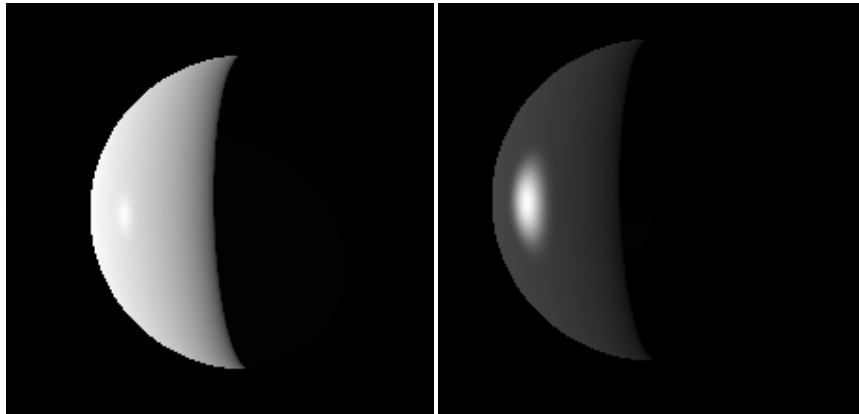
where:

$\hat{I}$  is the incoming light ray unit vector (from the light source)

$\hat{O}$  is the outgoing light ray unit vector (to the sensor)

$\hat{N}$  is the surface normal unit vector

$\hat{R}$  is the reflected light ray unit vector  $\hat{R} = \hat{N}(2\hat{I} \cdot \hat{N}) - \hat{I}$



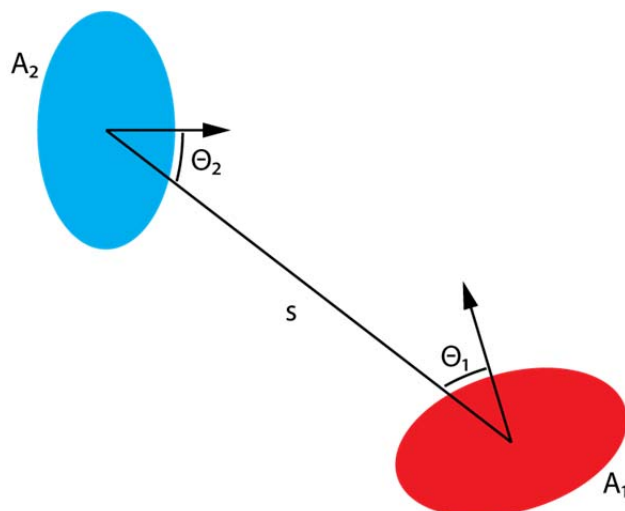
A future enhancement would be to allow the user to select from a list of BRDF models, e.g. the same list supported by MODTRAN 4.

#### 4.1.4.2 Radiometric Coupling between Surfaces

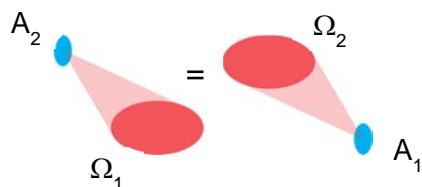
The radiometric coupling between two units of surface area is called throughput.

$$\Gamma = nA_1 \cos(\theta_1) A_2 \cos(\theta_2) / s^2 \quad (2)$$

$\Gamma = nA\Omega$  where  $\Omega$  is the projected solid angle of the other surface as seen from surface A, and  $n$  is the index of refraction of the media being transited by the coupling ray along  $s$ .



Either  $A_1$  or  $A_2$  can be the viewing surface and the projected solid angle is that of the opposite surface. This is known as the “invariance of throughput”.



Radiant flux is the product of radiance and throughput

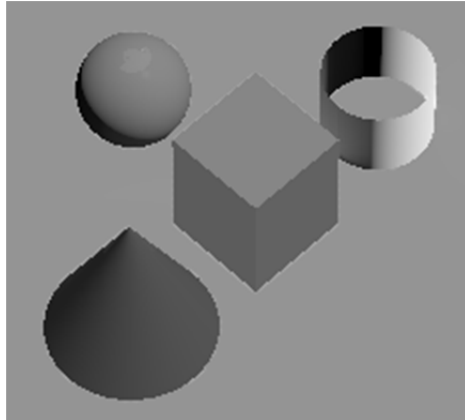
$$\Phi_\lambda = L_\lambda \tau_\lambda \Gamma = L_\lambda n_\lambda \tau_\tau \Omega A \tag{3}$$

### 4.1.5 Shapes & Surface Tessellation

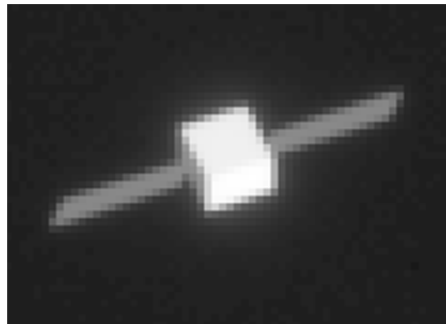
#### 4.1.5.1 Shapes

Object shapes can be one of the simple geometrics: sphere, oblate, box, plate, cylinder, cone or coupler (cone frustum). Each of the simple geometric shapes is parameterized with dimensions.

There is also a shape type called None. Assigning the shape None to an object, removes it from the geometric and radiometric calculations while retaining its position and orientation calculations. It is often convenient to assign the parent object to which a sensor is attached as shape None. Since a sensor cannot (currently) image its parent object, this speeds up radiometric calculation with little or no effect on the results.



Object may also be composite shapes constructed from one or more of the simple geometrics or other composite shapes at specified offsets and orientations with respect to one another.



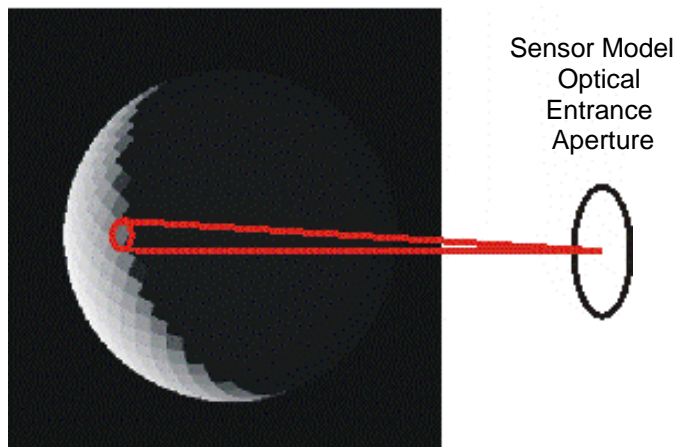
For Central Bodies (see Section 4.3.1) the dimensions are preset to known physical values and cannot be altered by the user. For satellites and vehicles, the dimensions can be set by the user. Missiles are inherently composite shapes that the Missile and Missile System STK EOIR property pages allow the user to define.

In a future revision of STK EOIR, the GUI will likewise enable users to predefine composite shapes for satellites, aircraft, and ground vehicles.

#### 4.1.5.2 Surface Tessellations

Each object's surface is divided into small units of approximately equal area. These small units of area,  $dA$ , are utilized for computing radiometric coupling. Each such  $dA$  can have a unique material type and temperature. Based on its parent shape's location and orientation, each such  $dA$  has a location and surface normal vector.

Synthetic Scene  
[Coarse Mode]



#### 4.1.5.3 Radiance Calculations

##### ***Resolved Area Sources***

The spectral radiance of a unit of surface area  $dA$  for a resolved object, without atmosphere, is modeled as follows:

$$L_{\lambda} = \left[ \sum_{i=src} (E_{\lambda}(i) * (\hat{I}(i) \cdot \hat{N}) * BRDF(\hat{I}(i), \hat{N}, \hat{O})) + E_{\lambda}^{bkg} / \pi \right] * SRF_{\lambda} + \epsilon_{\lambda} B_{\lambda}(T) \quad (4)$$

Where:

$SRF_{\lambda}$  is the surface's Spectral Reflectance at wavelength  $\lambda$

$\epsilon_{\lambda}$  is the surface's Spectral Emittance at wavelength  $\lambda$

$B_{\lambda}(T)$  is the Planck function for self radiance at wavelength  $\lambda$  at the surface's effective temperature

$$B_{\lambda}(T) = \frac{2hc^2}{\lambda^5} * \frac{1}{\exp\left(\frac{hc}{\lambda kT}\right) - 1} \quad (5)$$

Where:

$h$  is Planck's constant

$c$  is the speed of light

$k$  is Boltzmann's constant

$T$  is the effective temperature in Kelvin

$E_{\lambda}^{bkg}$  is the spectral, general background irradiance multiplied by a Hemispherical-Directional Reflectance modeled as  $1/\pi$ . The background spectral irradiance simulates integrated stellar, zodiacal light, and air glow components.

$\hat{I}(i)$  is the unit input light ray vector from source  $i$

$\hat{N}$  is the surface's unit normal vector

$\hat{O}$  is the unit output light ray vector from the surface to the observer, i.e. the sensor or some other unit of surface area being illuminated by this surface

$BRDF(\hat{I}(i), \hat{N}, \hat{O})$  is the surface's BRDF function for the input-output direction pair

$(\hat{I}(i) \cdot \hat{N})$  is the direction cosine for the incoming light ray

$E_{\lambda}(i)$  is the spectral irradiance from the  $i^{\text{th}}$  source that is capable of illuminating the surface, i.e. equations (5), (6), or (7).

The illuminating sources  $E_{\lambda}(i)$  for  $dA$  are modeled as either point sources or as area sources. Point sources are defined in this model to be area sources whose projected solid angle is less than the minimum solid angle of either the sun or moon as seen from the Earth. Point source radiance calculations are faster to perform than area source calculations but less accurate for non-spherical objects. The selected solid angle for deciding point vs. area causes the sun and moon to be treated as point sources for typical simulations. Stars are truly point sources but only illuminate other objects in this model through the general background irradiance, integrated stellar component.

Geometric processing culls out potential point sources that are eclipsed, relative to  $dA$ , by other objects.

### **Point Source**

Sun:

$$E_{\lambda}^{sun} = L_{\lambda}^{tab} d\Omega^{sun} \quad (6)$$

where  $L_{\lambda}^{tab}$  is a measured tabular spectral radiance (ASTM E-490) for the sun, and  $d\Omega^{sun}$  is the projected solid angle of the sun as seen from the point source.

Other:

$$E_{\lambda}^{other} = \left[ E_{\lambda}^{sun} * SRF_{\lambda} * \left( \frac{2}{3\pi} \right) * Phase(\psi) + \epsilon_{\lambda} B_{\lambda}(T) \right] * d\Omega^{other} \quad (7)$$

Where:

$SRF_{\lambda}$  is the overall spectral reflectance for the object; effectively a spectral albedo

$\left( \frac{2}{3\pi} \right)$  is the effective BRDF of a projected Lambertian sphere

$Phase(\psi) = (\sin(\psi) + (\pi - \psi) * \cos(\psi))/\pi$  is the phase function, as in phases of the moon, for a sphere.  $\psi$  is the angle between the sun and the observer with the vertex of the angle at the observed point source

$\epsilon_{\lambda}$  is the overall spectral emittance of the point source



$B_\lambda(T)$  is the Planck function for self-radiance at wavelength  $\lambda$  at the point source's effective temperature  $T$

$d\Omega^{\text{other}}$  is the projected solid angle of the point source as seen from the surface, where the object is represented by a sphere whose radius is the volumetric mean radius of the object's true shape

Geometric processing eliminates the reflected solar component, if the sun is eclipsed relative to the Point Source, by some other object

Canned spectral vector:  $E_\lambda = L_\lambda^{\text{tab-other}} d\Omega^{\text{other}}$  where  $L_\lambda^{\text{tab-other}}$  is a user provided tabular spectral radiance for the object.

### Area Source

$$E_\lambda(i) = \sum_{tess=k} \left[ \left[ \sum_{src=j} E_\lambda(j) * (\hat{I}(j) \cdot \hat{N}(k)) * BRDF(\hat{I}(j), \hat{N}(k), \hat{O}) + \frac{E_\lambda^{bkg}}{\pi} \right] * SRF_\lambda(k) + \epsilon_\lambda(k) B_\lambda(T(k)) \right] d\Omega(k) \quad (8)$$

Where:

$\sum_{tess}$  is the sum over the area source's tessellations that are capable of illuminating the surface  $dA$

$\sum_{src=j}$  is the sum over all the other sources that are capable of illuminating the  $k^{\text{th}}$  tessellation

The spectral radiance of a unit of surface area  $dA$  for a resolved object, with atmosphere, is modeled as follows:

$$L_\lambda = \left[ \left[ \sum_{i=src} \left( T_\lambda^{\text{In}}(i) * E_\lambda(i) * (\hat{I}(i) \cdot \hat{N}) * BRDF(\hat{I}(i), \hat{N}, \hat{O}) + \frac{\text{DownWelling}_\lambda(i)}{\pi} + \frac{E_\lambda^{bkg}}{\pi} \right) * SRF_\lambda + \epsilon_\lambda B_\lambda(T) \right] * T_\lambda^{\text{Out}} + L_\lambda^{\text{path}} + \sum_{i=src} L_\lambda^{\text{scatter}}(i) \right] \quad (9)$$

Where:

$T_\lambda^{\text{In}}(i)$  is the spectral transmission along the line of sight from illuminating source  $i$  to  $dA$

$T_\lambda^{\text{Out}}$  is the spectral transmission along the line of sight from  $dA$  to the observer (sensor).

$L_\lambda^{\text{path}}$  is the self-radiance of the atmosphere into the line of sight from  $dA$  to the observer (sensor). This component is only calculated for  $\lambda \geq 4.0 \mu\text{m}$ . It is computed by integrating Schwarzschild's equation, using layer data from MODTRAN's US Standard 1976 atmospheric model and treating the atmosphere as a uniformly mixed gas with a single mass absorption coefficient. This is fast but produces less accurate results around the spectral lines of non-uniformly mixed gasses such as  $\text{O}_3$ .

---

$L_{\lambda}^{scatter}$  is the diffuse light scattered into the line of sight from  $dA$  to the observer (sensor). It is computed based on single scatter of light originating at the illuminating source  $i$ , using layer data from MODTRAN 4's US Standard 1976 atmospheric model. This component is only calculated for  $\lambda \leq 4.0 \mu\text{m}$ .

$DownWelling_{\lambda}(i)$  is the diffuse, hemispherical down-welling light that illuminates shadows as well as augmenting directly illuminated areas. It consists of Rayleigh scattering, which produces the blue of the sky, and aerosol (Mie) scattering, which produces the white haze of the sky. This component affects objects such as the Earth's surface by illuminating and reflecting off that surface into the line of sight. Scatter is this same nature of light but is injected into the line of sight directly from the atmosphere.

$DownWelling$  is only calculated for  $\lambda \leq 4.0 \mu\text{m}$ . Note: The  $DownWelling$  component is disabled in the current EOIR release, in order to match MODTRAN results. Why this should be so is under investigation.

## 4.1.6 Radiance Calculations

### 4.1.6.1 Point Sources

For imaged point sources the spectral irradiance is calculated as  $\text{W cm}^{-2} \mu\text{m}^{-1}$ . The scene generator maintains an imaged point source list separate from the two-dimensional angular sampling used for area sources. Point sources on this list are those that fall within the sensor Field of View after apparent position calculation. STK corrects the locations of stars and planets for apparent position and provides them to EOIR.

Point sources have an  $\alpha, \beta$  focal plane coordinate and thus can be located between area source angular samples. Point sources also have an angular velocity in focal plane coordinates that can account for motion during sensor integration time. Motion blur of point sources (streaks) will be incorporated into a future STK EOIR release.

The spectral irradiance of Imaged Point Sources is calculated as follows:

$$\text{For imaged stars } E_{\lambda} = m0 * B_{\lambda}(T) \quad (10)$$

Where:

$B_{\lambda}(T)$  is the Planck function at wavelength  $\lambda$  and the star's effective temperature  $T$

$m0$  = converts Planck function radiance to an irradiance that corresponds correctly to the star's visual magnitude and temperature, i.e.  $m0$  is the projected solid angle of the star.

STK's star catalog contains the values of  $T$  and  $m0$  that EOIR uses.

Distant area sources are the non-stellar objects whose angular subtense is less than that of the scene generator spatial (angular) sample. There are two calculation modes for imaged distant area sources: Simple (lower fidelity, faster) and Detailed (higher fidelity, slower).

Simple distant area sources are calculated exactly as described for Point Sources, in 4.1.5.3 above, which illuminate some  $dA$ . That is, the lower fidelity approach reduces the source to a Lambertian sphere of equivalent volumetric radius and calculates the radiance from a single  $dA$  equivalent to the projected area of that sphere, including the solar phase function. The sun is the only external illuminating source considered. If the sun is eclipsed relative to the point source, it

---

contributes no illumination. Self-radiance of the distant area source is calculated based on the equivalent sphere, an overall emittance, and an overall effective temperature.

Higher fidelity, point sources within the field of view are computed as a summation over all of the source's tessellations that are visible to the observer (sensor). The sun is the only external illuminating source considered. If the sun is eclipsed relative to the point source, it contributes no illumination. Reflection is calculated tessellation-by-tessellation using each tessellation's SRF and BRDF. Self-radiance is calculated tessellation-by-tessellation using each tessellation's emittance and effective temperature. This is necessarily a slower calculation but is more accurate where an exacting optical cross section of an object is desired. This mode is applied automatically to satellites and missile objects where, for instance, obscuration of the plume by the hardbody would not be at all represented by the simple sphere described in the prior paragraph. Other point source objects designated as targets are also automatically calculated in this fashion when the STK Report Generator is selected with the point source as a designated target object.

$$E_{\lambda} = \sum_{tess=k} [E_{\lambda}^{sun} * (\hat{I}^{sun} * \hat{N}(k)) * SRF_{\lambda}(k) * BRDF(\hat{I}^{sun}, \hat{N}(k), \hat{O}) + \epsilon_{\lambda}(k)B_{\lambda}(T(k))] * d\Omega(k) \quad (11)$$

## 4.2 SCENE GENERATOR PROCESSING OPTIONS

### 4.2.1 Coarse

In coarse mode, each spectral radiance vector for directional samples that terminate on the surface of the same  $dA$  has the same value. That value is the calculated spectral radiance at the center of the  $dA$ . This is a faster scene generation mode.

### 4.2.2 Smooth

In smooth mode, the directional samples are interpolated from the values of the radiance vectors of surrounding  $dA$ 's. The radiance vector at the center of each  $dA$  is the same value previously described. This is a slower scene generation mode.

### 4.2.3 Bit Map

MUI object surfaces can be overlaid with a bitmap of materials at some higher resolution. The Earth bitmap, for instance, is at 0.93 kilometer resolution, whereas the surface tessellations are about 785 km on a side. The interpolation as described in Section 4.2.2, above, is applied, however the material type of the tessellation is removed from the calculation and the bitmap supplied material is used instead. The SRF, BRDF, and emissivity are thus affected. This is the slowest scene generation mode.

Note that the surface self-radiation is also affected, in that each material type has an emissivity. Also, land versus water has separate thermal model temperatures.

Bitmaps are currently available for Earth, the Moon, and Mars. The Earth bitmap is derived from data available at the University of Maryland's "1 Km Land Cover" website. The Moon and Mars bitmaps were derived from processing high resolution digital images.

There are higher and lower resolution versions of each bitmap. The higher or lower resolution map is selected based on ground sample distance.

---

## 4.3 MODELED UNIVERSE OF INTEREST OBJECT DESCRIPTIONS

### 4.3.1 Central Bodies

Central Body objects available in STK EOIR are the Sun and the planets in the solar system—Mercury, Venus, Earth, Mars, Jupiter, Saturn, Uranus, Neptune. The Earth's moon is also available. Moons of the other planets will be available in future releases.

The STK EOIR architecture allows any Central Body to have an atmosphere model, but currently only the Earth's atmosphere is implemented. The Earth GUI allows the user to select from 2 atmospheric models:

#### 4.3.1.1 Simple Atmosphere

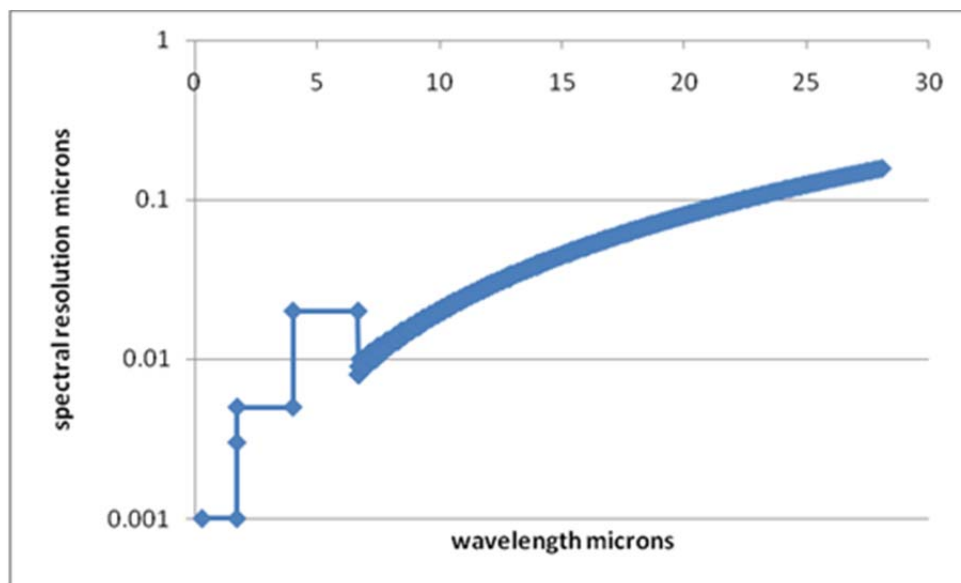
The "Simple" model calculates transmission and downwelling hemispherical irradiance (from the blue sky) using the equations in "SMARTS2. A Simple Model of the Atmospheric Radiative Transfer of Sunshine: Algorithms and performance assessment", by Christian Gueymard.

Single scatter into the line of sight is calculated using an approach evolved from "Display of the Earth Taking into Account of Atmospheric Scattering" by Nishita, Sirai, Tadamura and Nakamae.

Atmospheric self-radiance is calculated at wavelengths greater than 4  $\mu$  by integrating Swcharzschild's equation.

The first step to all of the preceding atmospheric calculations is to calculate the air mass intervening between sensor and target. This involves computing a line integral of atmospheric density along the light ray, through a spherical atmosphere. The layer thicknesses and layer densities are those specified in the US Standard 1976 atmosphere. Air mass is calculated separately for water vapor and ozone, since these are not uniformly distributed. Separate air mass calculation for aerosol distribution will be incorporated in a future release.

The spectral resolution of the Simple model is as follows:



---

#### 4.3.1.2 MODTRAN

MODTRAN 4 has been integrated into the developmental EOIR to the point of being able to generate images. It provides higher fidelity results but at the cost of significant execution speed.

MODTRAN 5 integration is currently in progress in a developmental EOIR.

It is anticipated that a future release will offer the option of using MODTRAN in scene generation.

#### 4.3.1.3 Thermal Models

The Earth's thermal model is based on "Monthly Mean Diurnal Cycles in Surface Temperature over Land for Global Climate Studies", A. Ignatov and G. Gutman of NOAA/NESDIS, *Journal of Climate* Vol. 12, 1999. Monthly Mean relates to the fact that the daily variability of weather and cloud cover has been averaged out. Their approach models the diurnal cycle seasonally and latitudinally using only the daily temperature maximum and minimum as parameters.

EOIR has tables of max and min temperatures by latitude region and month. The max and min are interpolated from this table for specific latitudes and days. There are separate tables for land and water.

For other Central Bodies, the daytime temperature is modeled, per "Brightness Temperatures of the Lunar Surface, The Clementine Long-Wave Infrared Global Data Set", S. L. Lawson and B. M. Jakosky, Laboratory for Atmospheric Space Physics, as

$$T_{ss} \cos^{1/4}(\varphi) \tag{12}$$

Where,

$T_{ss}$  is the sub-solar temperature in K for the Central Body

$\Phi$  is the angle off of the sub-solar point

The night time temperature is modeled, as a  $T^{1/4}$  temperature decay based on time in total shadow, tied to reported minima. This part is still under development.

#### 4.3.2 Stars

Stars are those occurring in the Hipparcos and Tyco catalogs, as provided by STK. Stars are simulated as point sources with blackbody spectral irradiance according to the star's effective temperature and visual magnitude, as described in 4.1.6.1. Stars are located at their appropriate apparent positions as determined by STK.

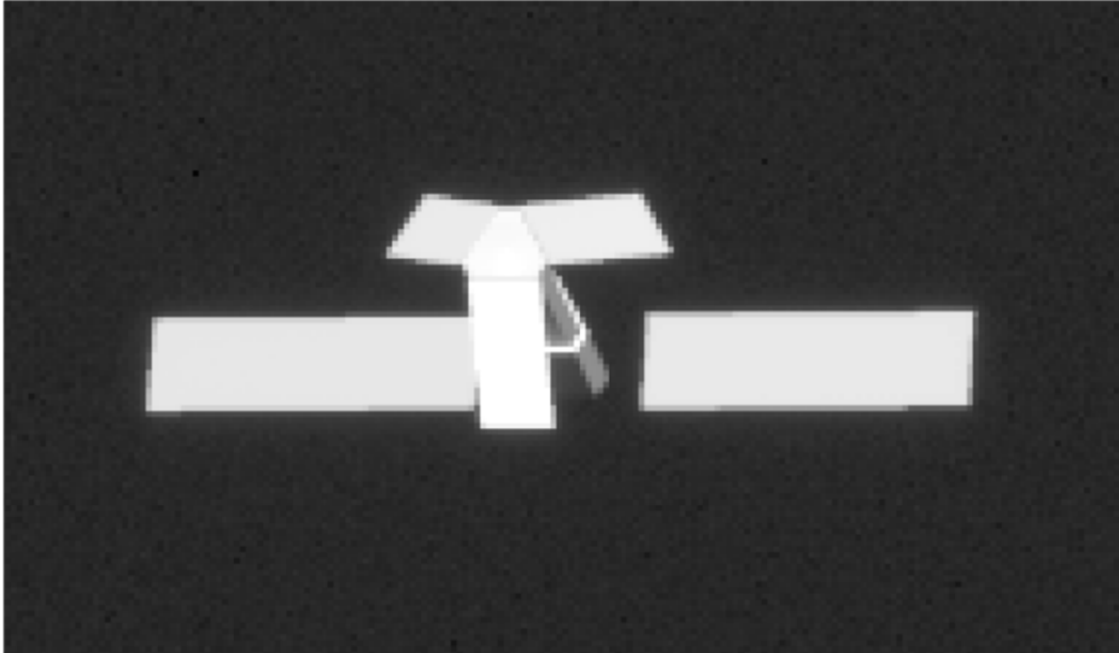
#### 4.3.3 Satellites

Up to 16 independent satellites can be simulated. [This number is fixed when the EOIR software is compiled. It can readily be increased.]

STK EOIR uses the satellite position and orientation that are calculated by STK. User selections, such as orbit propagator model, are transparent to STK EOIR, except to the extent that they affect the resulting position and orientation.

The user can control satellite shape, dimensions, surface material, and temperature.

Shapes available are described in 4.1.5.1. There are selectable composite shapes representing LEO Earth Observing, LEO communications, and GEO communications satellites.



Surface materials available are: Gray Body, Burnished Aluminum, Aluminum MLI, Gold MLI, Silver MLI, Solar Panel, Black Thermal Control, and White Thermal Control as described in 0. Custom materials can be developed upon request.

The current thermal model has a fixed temperature for the entire satellite. The composite satellites have a variety of temperatures for different components, and represent average equilibrium temperatures for LEO and GEO orbits. An expected future enhancement will have the temperatures of the surface equilibrate to the incoming and outgoing heat fluxes at the surface location.

#### **4.3.4 Aircraft**

Up to 6 independent aircraft can be simulated. The total number of aircraft and ground vehicles must be equal to or less than 6. [This number is fixed when the EOIR software is compiled. It can readily be increased.]

STK EOIR uses the aircraft position and orientation that are calculated by STK. User selections, such as orbit propagator model, are transparent to STK EOIR, except to the extent that they affect the resulting position and orientation.

The user can control satellite shape, dimensions, surface material, and temperature.

Shapes available are described in 4.1.5.1. Other standard vehicle shapes are under development.

Surface materials available are: Aluminum, Burnished Aluminum, Gold, Gray Body, Mixed Forest Camouflage, Silver, Soil Camouflage, Water Camouflage as described in 0. Custom materials can be developed upon request.

The current thermal model has a fixed temperature for the entire aircraft.

#### **4.3.5 Ground Vehicles**

[Incorporation of Ground Vehicles has been deferred to a future release.]

---

Up to 6 independent ground vehicles can be simulated. The total number of aircraft and ground vehicles must be equal to or less than 6. [This number is fixed when the EOIR software is compiled. It can readily be increased.]

STK EOIR uses the ground vehicle position and orientation that are calculated by STK.

The user can control ground vehicle shape, dimensions, surface material, and temperature.

Shapes available are described in 4.1.5.1. Other standard vehicle shapes are under development.

Surface materials available are: Aluminum, Burnished Aluminum, Gold, Gray Body, Mixed Forest Camouflage, Silver, Soil Camouflage, and Water Camouflage as described in 0. Custom materials can be developed upon request.

The current thermal model has a fixed temperature for the entire ground vehicle.

#### **4.3.6 Missile and Missile Systems**

[Incorporation of Missile Systems has been deferred to a future release.]

Up to 6 independent Missiles and/or Missile Systems as defined by STK's Missile Model Tool can be simulated. These Missiles/Missile Systems can be comprised of up to 18 stages, where Post Boost Vehicles and Reentry Vehicles are counted as stages. [These numbers are fixed when the EOIR software is compiled. They can readily be increased.]

STK EOIR uses the location, velocity, and orientation as calculated by STK.

Users can construct the shapes of stages by "stacking up" successive shape primitives, (see 4.1.5.1).

Each stage can have a rocket exhaust plume. This is an automatically generated shape that attaches to the trailing end of a stage. The shape is a sphere (nearest the stage) with an attached tangent cone with pointed end directed away from the stage. The plume scales itself to the size of the associated stage. The user can override the default scale factors for plume length and width.

The user can specify plume on and plume off times that are relative to the stages active lifetime. Time 0 is launch time for the first stage and is separation time for successive stages.

The user can assign a temperature to the plume. The body of the plume acts as a solid graybody with 0.99 emittance. The plume emits self-radiance utilizing the Planck function and the assigned temperature.

In a future version of STK EOIR, the spectral radiance of the plume can be set via a user provided table of radiance versus wavelength.

Note that this plume model does not evolve either spatially or radiometrically over time. It should be set by the user to represent some average behavior of interest. The plumes of successive stages can be user adjusted to demonstrate the effects of changing altitude on the plume.

---

## 5. SENSOR MODEL

The following sections describe the sensor model with respect to a single SSG-SMP.

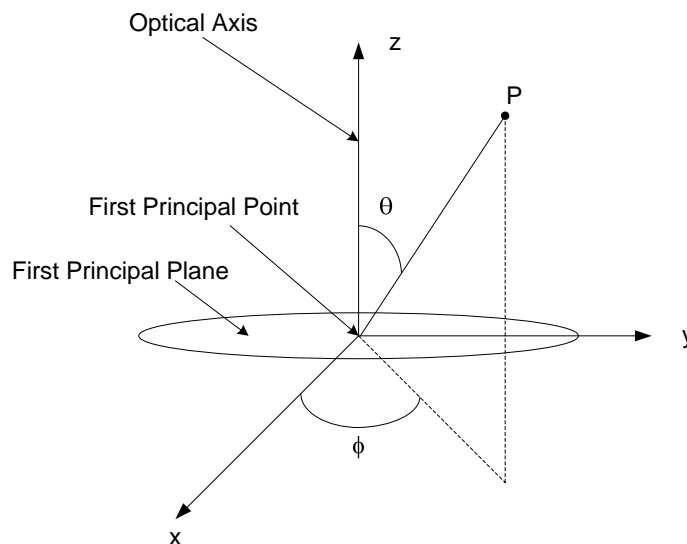
### 5.1 SENSOR MODEL OVERVIEW

The sensor is a generic imaging radiometer. The sensor is modeled as a single equivalent thick lens followed by a focal plane array. The single lens acts as the aperture stop (and entrance pupil). The field stop is coincident with the focal plane array. The aperture stop is circular and the field stop is rectangular. The focal plane array is an array of individual detectors (pixels) with uniform characteristics (dimensions, responsivity, noise, etc.).

The following limitations and assumptions apply to the sensor. Other assumptions may be stated in the sections which follow.

1. Scene radiation is assumed to be incoherent and un-polarized.
2. Scatter internal to the sensor is assumed to be negligible.
3. Sensor responsivity is assumed to be linear (up to the point of saturation if saturation effects are enabled).
4. The scene to be imaged is assumed to be effectively at infinite distance from the sensor (i.e. far enough away that rays from elements in the scene are focused at the focal length of the optical system).
5. Optical systems with central obscuration are not modeled.
6. Objects in the scene are treated as stationary during the period of a sensor integration time.
7. The model assumes 100% fill factor for the FPA pixels.
8. The detectors are assumed to be photon detectors.

The sensor body coordinate system is shown below.

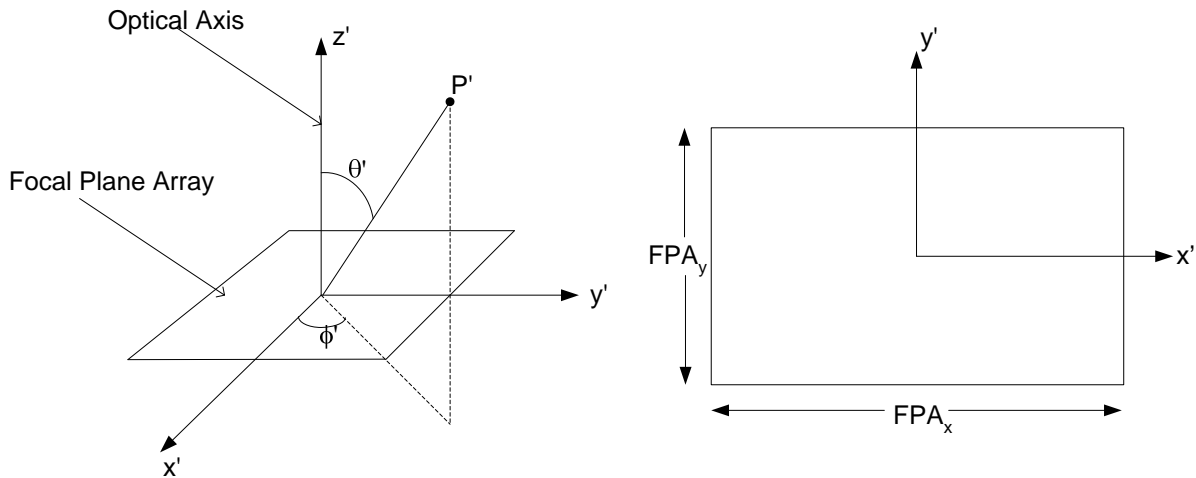


The origin of the sensor body coordinate system is the first principal point of the optical system. The z-axis points along the optical axis and away from the sensor (toward the scene). The x-y plane is in the first principle plane of the optical system. A direction from the sensor entrance



aperture to a point  $P$  in object space may be specified with the angles  $(\theta, \phi)$ . For a rectangular field of view (FOV) it is convenient to specify the direction using azimuth and elevation angles  $(\alpha, \beta)$ . Let  $\vec{F}$  be the vector from the origin to  $P$ . The azimuth angle  $\alpha$  is defined as the angle made by the projection of  $\vec{F}$  onto the  $x$ - $z$  plane with the  $z$ -axis and the elevation angle  $\beta$  is defined as the angle made by the projection of  $\vec{F}$  onto the  $y$ - $z$  plane with the  $z$ -axis. The  $x$ -direction is referred to as the horizontal direction, the  $y$ -direction as the vertical direction.

The focal plane array (FPA) coordinate system is shown below.



The origin of the FPA coordinate system is at the center of the FPA with the  $x'$ -axis along the FPA width, the  $y'$ -axis along the FPA height, and the  $z'$ -axis along the optical axis. Primed coordinates are used to designate focal plane coordinates. The  $x'$  and  $y'$  axes of the FPA coordinate system are exactly aligned with the respective axes of the sensor body coordinate system.

## 5.2 FIELD OF VIEW AND SPATIAL SAMPLING GRID

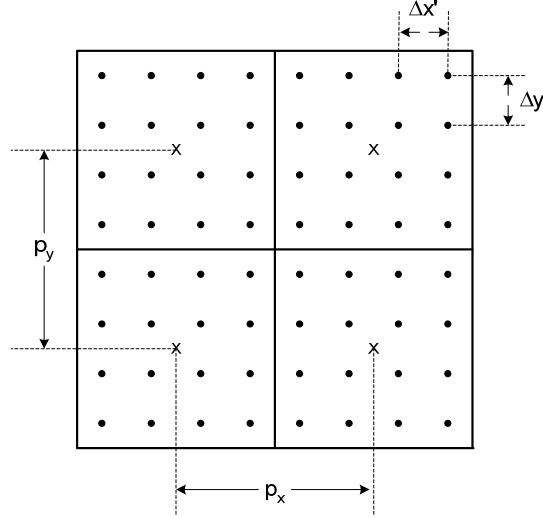
Two angles specify the full angular extent of the sensor field of view in two orthogonal directions, nominally horizontal and vertical. The sensor model uses an ideal spatial response which is unity within the FOV and zero outside the FOV. Users specify the number of sensor pixels in the horizontal and vertical directions. Each sensor pixel is sampled with four samples in each direction, for a total of 16 samples per sensor pixel. The sample intervals in the focal plane coordinate system are uniform and given by

$$\Delta x' = \frac{p_x}{4} \quad (13)$$

$$\Delta y' = \frac{p_y}{4} \quad (14)$$

where  $\Delta x'$  and  $\Delta y'$  are the sample intervals in the  $x'$  (horizontal) and  $y'$  (vertical) directions, respectively, and  $p_x$  and  $p_y$  are the pixel pitch in the  $x'$  and  $y'$  directions, respectively.

The figure below shows the spatial sampling grid in the FPA coordinate system for four adjacent sensor pixels.



A position in the FPA coordinate system  $(x', y')$  is related to a direction in object space  $(\alpha, \beta)$  as follows

$$\alpha = -\arctan\left(\frac{x'}{f}\right) \quad (15)$$

$$\beta = -\arctan\left(\frac{y'}{f}\right) \quad (16)$$

where  $f$  is the effective focal length of optical system and  $x'$ ,  $y'$  and  $f$  are all expressed in the same units.

The sampling grid in object space consists of the set of  $(\alpha, \beta)$  angles corresponding to each sample in the FPA sampling grid. The angular sample intervals in object space are non-uniform because the sample intervals in the FPA coordinate system are uniform and the arctangent function is a nonlinear function. Object space angular sample intervals are slightly larger for sample positions near the center of the field-of-view (the optical axis). An upper bound for the sample intervals in object space is approximately

$$\Delta\alpha \approx \frac{\Delta x'}{f} = \frac{p_x}{4f} [\text{radians}] \quad (17)$$

$$\Delta\beta \approx \frac{\Delta y'}{f} = \frac{p_y}{4f} \text{ [radians]} \quad (18)$$

where  $p_x$ ,  $p_y$ , and  $f$  are all expressed in the same units. Therefore, an approximate lower bound for the sample frequencies in object space is

$$\xi_{samp,\alpha} = \frac{1}{\Delta\alpha} \approx \frac{4f}{p_x} \text{ [cycles/radian]} \quad (19)$$

$$\xi_{samp,\beta} = \frac{1}{\Delta\beta} \approx \frac{4f}{p_y} \text{ [cycles/radian]} \quad (20)$$

and the maximum spatial frequencies in the synthetic scene in horizontal and vertical directions which can be represented without aliasing are  $\frac{\xi_{samp,\alpha}}{2}$  and  $\frac{\xi_{samp,\beta}}{2}$ .

The full-angle field of view of the sensor in the horizontal and vertical directions is related to the number of pixels, the pixel pitch, and the focal length by

$$FOV_H = 2\arctan\left(\frac{N_x p_x}{2f}\right) \quad (21)$$

$$FOV_V = 2\arctan\left(\frac{N_y p_y}{2f}\right) \quad (22)$$

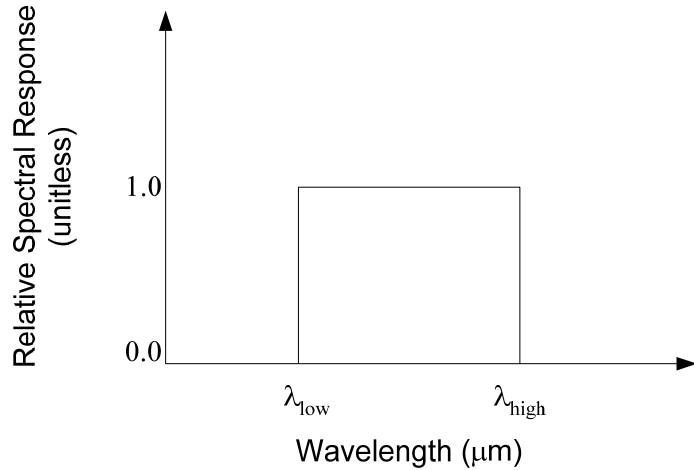
The on-axis instantaneous field of view (IFOV), or full-angle extend of one pixel in the horizontal and vertical directions is

$$IFOV_H = 2\arctan\left(\frac{p_x}{2f}\right) \quad (23)$$

$$IFOV_V = 2\arctan\left(\frac{p_y}{2f}\right) \quad (24)$$

### 5.3 SPECTRAL BANDPASS AND SPECTRAL SAMPLING GRID

The sensor spectral bandpass is defined by two wavelengths,  $\lambda_{low}$  and  $\lambda_{high}$ . These two wavelengths specify the low and high edges of the spectral bandpass, respectively. The sensor model uses an ideal spectral response which is unity within the spectral bandpass and zero outside the spectral bandpass.



Users specify the number of discrete spectral intervals within the spectral bandpass,  $N_{intervals}$ , to be used by the model for all spectral quantities relevant to the SSG-SMP. The spectral sampling grid is defined as  $\lambda_i = \lambda_{low} + i * \Delta\lambda$ , ( $i = 0, 1, \dots, N_{intervals} - 1$ ), where  $\Delta\lambda$  is the spectral sample interval given by  $\Delta\lambda = \frac{\lambda_{high} - \lambda_{low}}{N_{intervals}}$ .

#### 5.4 RADIANCE RESPONSIVITY

The sensor response to a spatially uniform extended area source is

$$r = \int \frac{L_{\lambda}^{scene}(\lambda) \pi \tau_{opt}(\lambda) A_d \eta(\lambda) \lambda t_i}{(4(F/\#)^2 + 1) hc} d\lambda \quad [\text{electrons}] \quad (25)$$

where,  $r$  is the sensor response,  $L_{\lambda}^{scene}(\lambda)$  is the scene spectral radiance at sensor entrance aperture,  $\lambda$  is the wavelength,  $\tau_{opt}(\lambda)$  is the spectral transmittance of optical subsystem,  $A_d$  is the detector active area,  $\eta(\lambda)$  is the spectral quantum efficiency,  $t_i$  is the integration time,  $F/\#$  is the  $f$ -number,  $h$  is Planck's constant, and  $c$  is the speed of light.

The absolute sensor radiance responsivity is defined as

$$\mathfrak{R}_L(\lambda) = \frac{\pi \tau_{opt}(\lambda) A_d \eta(\lambda) \lambda t_i}{(4(F/\#)^2 + 1) hc} \quad [\text{electrons}/(\text{W}/(\text{cm}^2 \text{ sr}))] \quad (26)$$

Given  $\mathfrak{R}_L(\lambda)$ , the peak radiance responsivity,  $\mathfrak{R}_{peak,L}$ , is defined as

$$\mathfrak{R}_{peak,L} = \max_{\lambda} (\mathfrak{R}_L(\lambda)) \quad (27)$$

and the peak normalized relative spectral response,  $RSR(\lambda)$ , is defined as

$$RSR(\lambda) = \frac{\mathfrak{R}_L(\lambda)}{\mathfrak{R}_{peak,L}} \quad (28)$$

With these definitions the sensor response to a spatially uniform extended area source can be written

$$r = \mathfrak{R}_{peak,L} \int L_{\lambda}^{scene}(\lambda) RSR(\lambda) d\lambda \quad (29)$$

As stated above, the relative spectral response,  $RSR(\lambda)$ , is modeled as ideal, i.e. unity within the spectral bandpass and zero outside the spectral bandpass. In the STK EOIR sensor model the user does not supply values for  $\tau_{opt}(\lambda)$  and  $\eta(\lambda)$ . In order to satisfy the constraint that  $RSR(\lambda) = 1$  within the spectral bandpass the following assumption is made about the product  $\tau_{opt}(\lambda)\eta(\lambda)$

$$\tau_{opt}(\lambda)\eta(\lambda) = \frac{0.8\lambda_{low}}{\lambda} \quad (30)$$

Given this assumption the absolute radiance responsivity is modeled as

$$\mathfrak{R}_L(\lambda) = \frac{\pi A_d 0.8\lambda_{low} t_i}{(4(F/\#)^2 + 1)hc} \quad [\text{electrons}/(\text{W}/(\text{cm}^2 \text{ sr}))] \quad (31)$$

## 5.5 IRRADIANCE RESPONSIVITY

The peak irradiance responsivity is defined as

$$\mathfrak{R}_{peak,E} = \frac{\mathfrak{R}_{peak,L} ENSQ}{IFOV_H IFOV_V} [\text{electrons}/(\text{W}/\text{cm}^2)] \quad (32)$$

where  $ENSQ$  is the fractional ensquared energy defined in Section 5.8,  $IFOV_H$  is the instantaneous field of view (IFOV) in the horizontal direction, and  $IFOV_V$  is the IFOV in the vertical direction.

## 5.6 OPTICAL TRANSFER FUNCTIONS

The system optical transfer function (OTF) is modeled as the product of the optics OTF and high-frequency line of sight jitter OTF.

### 5.6.1 Optical System OTF

The optical system optical transfer function (OTF) is a product of three terms: the diffraction OTF, the Hufnagle optical quality factor (OQF) which models degradations due to aberrations, and the defocus OTF.

$$OTF_{optics}(\xi) = OTF_{diff}(\xi) OQF(\xi) OTF_{defocus}(\xi) \quad (33)$$

Each of the terms of the optics OTF is discussed below.

#### 5.6.1.1 Diffraction OTF

The diffraction OTF is given by

$$\begin{aligned}
 OTF_{diff}(\xi) &= \frac{2}{\pi} \left\{ \arccos(\xi / \xi_{cutoff}) - \xi / \xi_{cutoff} \left[ 1 - (\xi / \xi_{cutoff})^2 \right]^{1/2} \right\}, & \xi \leq \xi_{cutoff} \\
 OTF_{diff}(\xi) &= 0, & \xi > \xi_{cutoff}
 \end{aligned}
 \tag{34}$$

where  $\xi$  is the spatial frequency,  $\xi_{cutoff}$  is the optical system spatial frequency cutoff given by  $\frac{1}{\lambda_{diff} F / \#}$  where  $\lambda_{diff}$  is the diffraction wavelength. The diffraction OTF is always positive so the OTF is the same as the MTF.

### 5.6.1.2 Hufnagle OQF

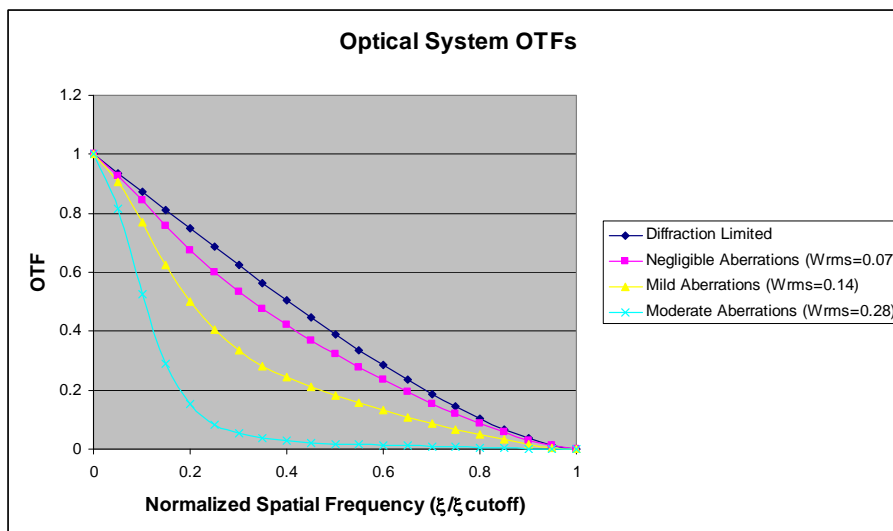
The Hufnagle optical quality factor is used to model aberrations of the optical system. The optical quality factor (OQF) is given by

$$OQF(\xi) = e^{- (2\pi W_{rms})^2 \left( 1 - e^{-2n^2 (\xi / \xi_{cutoff})^2} \right)^2 }
 \tag{35}$$

where  $\xi$  is the spatial frequency,  $\xi_{cutoff}$  is the optical system spatial frequency cutoff given by  $\frac{1}{\lambda_{diff} F / \#}$  where  $\lambda_{diff}$  is the diffraction wavelength,  $W_{rms}$  is the rms wavefront error expressed as a multiple of  $\lambda_{diff}$  wavelengths, and  $n$  is the number of bumps over the exit pupil (set to 3 by the model).

Four predefined levels of aberration using the Hufnagle OQF are available: Diffraction Limited, Negligible, Mild, and Moderate. The names are somewhat arbitrary. The four levels of aberration correspond to  $W_{rms}=0.0$ ,  $W_{rms}=0.07$ ,  $W_{rms}=0.14$ , and  $W_{rms}=0.28$ , respectively. Plots of  $OTF_{optics}(\xi) = OTF_{diff}(\xi) OQF(\xi)$  for the four predefined levels of aberration are shown below.

These plots effectively assume  $OTF_{defocus}(\xi) = 1$  (zero longitudinal defocus).



---

### 5.6.1.3 Defocus OTF

The defocus OTF is an approximation given by

$$OTF_{defocus}(\xi) = 2J_1(x) / x \quad (36)$$

where  $J_1(x)$  is the first-order Bessel function of the first kind,  $x = \frac{\pi\delta\xi(\xi_{cutoff} - \xi)}{(F/\#)\xi_{cutoff}}$  and  $\delta$  is the

longitudinal defocus. This approximation is used for up to 2.2  $\lambda_{diff}$  waves peak-to-peak wavefront error due to defocus. For larger amounts of defocus (for greater than 2.2  $\lambda_{diff}$  waves peak-to-peak wavefront error) the following approximation is used

$$OTF_{diff}(\xi)OTF_{defocus}(\xi) = 2J_1(x) / x \quad (37)$$

where  $x = \frac{\pi\delta\xi}{(F/\#)}$ . Note that the second approximation is for the product  $OTF_{diff}(\xi)OTF_{defocus}(\xi)$  and not just  $OTF_{defocus}(\xi)$ .

### 5.6.2 Line-of-Sight Jitter OTF

High-frequency line-of-sight jitter is modeled using a Gaussian OTF as

$$OTF_{jitter}(\xi) = e^{-2(\pi\sigma\xi)^2} \quad (38)$$

where  $\sigma$  is the rms random angular displacement in mrad and  $\xi$  is the spatial frequency in cycles/mrad.

### 5.6.3 System OTF

The two-dimensional system OTF is

$$OTF_{system}(\xi_x, \xi_y) = OTF_{optics}\left(\sqrt{\xi_x^2 + \xi_y^2}\right) OTF_{jitter}\left(\sqrt{\xi_x^2 + \xi_y^2}\right) \quad (39)$$

## 5.7 SYSTEM POINT SPREAD FUNCTION

The system point spread function (PSF) is the two-dimensional Fourier transform of the system OTF.

$$PSF_{system}(x', y') = \mathfrak{F}\mathfrak{F}\left\{OTF_{system}(\xi'_x, \xi'_y)\right\} \quad (40)$$

where  $\mathfrak{F}\mathfrak{F}\{V\}$  is the two-dimensional Fourier transform of  $V$ ,  $x'$  and  $y'$  are coordinates in the FPA coordinate system, and  $\xi'_x$  and  $\xi'_y$  are image space spatial frequencies in the FPA coordinate system.

## 5.8 ENSQUARED ENERGY

The fractional ensquared energy (fraction of the total power in a point source which falls on a single pixel centered on the point source) is defined as

$$ENSQ = \frac{\int_{-py/2}^{py/2} \int_{-px/2}^{px/2} PSF_{system}(x', y') dx' dy'}{\int_{-\infty}^{\infty} \int_{-\infty}^{\infty} PSF_{system}(x', y') dx' dy'} \quad (41)$$

where  $p_x$  and  $p_y$  are the pixel pitch in the  $x'$  and  $y'$  directions and  $PSF_{system}$  is the system point spread function given by Eqn. (40). Because of the way  $PSF_{system}$  is defined

$\int_{-\infty}^{\infty} \int_{-\infty}^{\infty} PSF_{system}(x', y') dx' dy' = 1$ , therefore,

$$ENSQ = \int_{-py/2}^{py/2} \int_{-px/2}^{px/2} PSF_{system}(x', y') dx' dy' \quad (42)$$

## 5.9 RADIOMETRIC SENSITIVITY

Radiometric sensitivity is defined using aperture-referred quantities. Users specify sensitivity in terms of the sensor dark noise equivalent radiance (NER) or dark noise equivalent irradiance (NEI). Sensor dark noise refers to the sensor noise when viewing a ‘dark’ scene with zero photon flux input to the sensor. In a physical sensor the dark noise may include contributions from thermal self-emissions, detector dark current, read-out noise, etc..

STK EOIR allows users to model the theoretical or measured relationship between sensitivity and sensor integration time. In a physical sensor the sensitivity depends on many other parameters besides integration time, e.g. F/#, detector area, detector quantum efficiency, detector noise, etc. However, unlike integration time these parameters are frequently fixed by the sensor design and are unchangeable once the sensor is built. The simple theoretical relationship used by the model between NEI (or NER), and integration time,  $T_{int}$ , is  $NEI \propto \frac{1}{\sqrt{T_{int}}}$ . The user specifies a

reference NEI (or NER) value,  $NEI_{ref}$ , and the sensor integration time,  $T_{ref}$ , for which  $NEI_{ref}$  is valid. This pair of values,  $(T_{ref}, NEI_{ref})$ , is referred to as a Sensitivity Reference Pair. Users must specify at least one Sensitivity Reference Pair and may specify up to eight. The Sensitivity Reference Pairs define points on a curve. Let  $(t_1, NEI_1), (t_2, NEI_2), \dots, (t_n, NEI_n)$  be  $n$  Sensitivity Reference Pairs entered by the user which have been sorted such that  $t_1 < t_2 < t_3 < \dots < t_n$ . The operating NEI (or NER),  $NEI_{current}$ , is determined by interpolation or extrapolation of the data in the Sensitivity Reference Pairs at the operating integration time,  $T_{current}$ , as follows.



$$NEI_{current} = \begin{cases} NEI_1 \sqrt{\frac{t_1}{t_{current}}}, & t_{current} \leq t_1 \\ \frac{(NEI_k - NEI_{k-1})(t_{current} - t_{k-1})}{t_k - t_{k-1}} + NEI_{k-1}, & t_{k-1} < t_{current} < t_k \\ NEI_n \sqrt{\frac{t_n}{t_{current}}}, & t_{current} \geq t_n \end{cases} \quad (43)$$

If only one Sensitivity Reference Pair is supplied the operating NEI is calculated as

$$NEI_{current} = NEI_{ref} \sqrt{\frac{T_{ref}}{T_{current}}} \quad (44)$$

## 5.10 SATURATION

As with sensitivity, saturation is defined using aperture-referred quantities. Users specify saturation in terms of the saturation equivalent irradiance (SEI) or saturation equivalent radiance (SER). STK EOIR allows users to model the theoretical or measured relationship between saturation and sensor integration time in a similar manner to radiometric sensitivity. The simple theoretical relationship used by the model between SEI (or SER), and integration time,  $T_{int}$ , is

$SEI \propto \frac{1}{T_{int}}$ . The user specifies a reference SEI (or SER) value,  $SEI_{ref}$ , and the sensor integration

time,  $T_{ref}$ , for which  $SEI_{ref}$  is valid. This pair of values,  $(T_{ref}, SEI_{ref})$ , is referred to as a Saturation Reference Pair. Users must specify at least one Saturation Reference Pair and may specify up to eight. The Saturation Reference Pairs define points on a curve. Let  $(t_1, SEI_1)$ ,  $(t_2, SEI_2)$ ,  $\dots$ ,  $(t_n, SEI_n)$  be  $n$  Saturation Reference Pairs entered by the user which have been sorted such that  $t_1 < t_2 < t_3 < \dots < t_n$ . The operating SEI (or SER),  $SEI_{current}$ , is determined by interpolation or extrapolation of the data in the Saturation Reference Pairs at the operating integration time,  $T_{current}$ , as follows.

$$SEI_{current} = \begin{cases} SEI_1 \frac{t_1}{t_{current}}, & t_{current} \leq t_1 \\ \frac{(SEI_k - SEI_{k-1})(t_{current} - t_{k-1})}{t_k - t_{k-1}} + SEI_{k-1}, & t_{k-1} < t_{current} < t_k \\ SEI_n \frac{t_n}{t_{current}}, & t_{current} \geq t_n \end{cases} \quad (45)$$

If only one Saturation Reference Pair is supplied the operating SEI is calculated as

$$SEI_{current} = SEI_{ref} \frac{T_{ref}}{T_{current}} \quad (46)$$

---

## 5.11 SENSOR RESPONSE

### 5.11.1 Response to Scene Generator Extended Area Sources

The sensor response to spectral radiance from extended area sources, which in general is spatially non-uniform, is modeled as

$$r_L(m, n) = \frac{1}{A_d} \int_{\Delta A'(m, n)} \int_{\Delta \lambda} (L_\lambda^{scene}(x', y', \lambda) \mathfrak{R}_L(\lambda)) \otimes PSF_{system}(x', y') d\lambda dA' \quad (47)$$

where  $r_L(m, n)$  is the response for pixel  $(m, n)$ ,  $L_\lambda^{scene}(x', y', \lambda) = L_\lambda^{scene}(\alpha(x'), \beta(y'), \lambda)$ ,  $\otimes$  is the convolution operator,  $\Delta A'(m, n)$  is the detector active area for pixel  $(m, n)$ . We are assuming linearity and shift invariance in order to represent the blurred image at the focal plane as a convolution of the  $PSF$  with the ideal image. When  $L_\lambda^{scene}(x', y', \lambda)$  is spatially uniform this reduces to Eqn. (29). Let the “effective radiance” be defined as

$$L^{scene}(x', y') = \int L_\lambda^{scene}(x', y', \lambda) RSR(\lambda) d\lambda \quad (48)$$

Then, expressing the convolution in the spectral domain and simplifying, the sensor response to radiance sources can be written as

$$r_L(m, n) = \frac{\Re_{peak, L}}{A_d} \int_{\Delta A'(m, n)} \mathfrak{F} \mathfrak{F}^{-1} \{ \mathfrak{F} \mathfrak{F} \{ L^{scene}(x', y') \} * OTF(\xi'_x, \xi'_y) \} dA' \quad (49)$$

### 5.11.2 Response to Scene Generator Point Sources

The sensor response to the spectral irradiance from a point source,  $E_\lambda^{ps}(\lambda)$ , is modeled as

$$r_E(m, n) = \frac{\Re_{peak, E} E^{ps} EOD(m, n, x'_{ps}, y'_{ps})}{ENSQ} \quad (50)$$

where,  $EOD(m, n, x'_{ps}, y'_{ps})$  is the fractional energy on detector  $(m, n)$  due to the point source centered at focal plane coordinates  $(x'_{ps}, y'_{ps})$  and is calculated as

$$EOD(m, n, x'_{ps}, y'_{ps}) = \int_{\Delta A'(m, n)} PSF_{system}(x' - x'_{ps}, y' - y'_{ps}) dA' \quad (51)$$

and  $E^{ps}$  is the point source effective irradiance defined as

$$E^{ps} = \int E_\lambda^{ps}(\lambda) RSR(\lambda) d\lambda \quad (52)$$

### 5.11.3 Dark offset

We will refer to the sensor response when viewing a dark scene with zero radiometric input to the sensor as the dark offset. In a physical sensor the dark offset may be non-zero due to effects

such as thermal self-emissions from the sensor, detector dark current, or a non-zero voltage bias. In the STK EOIR sensor model the dark offset is effectively subtracted from the modeled sensor response, giving a nominal sensor response of zero for zero radiometric input.

#### 5.11.4 Sensor Noise and Scene Photon Noise

The total number of noise electrons for pixel  $(m, n)$  is given by

$$ne_{total}(m, n) = \sqrt{ne_{dark}^2 + ne_{photon}(m, n)^2} \quad (53)$$

where  $ne_{total}$  is the total number of noise electrons,  $ne_{dark}$  is the number of sensor dark noise electrons, and  $ne_{photon}$  is the number of scene photon noise electrons. The dark noise,  $ne_{dark}$ , specifies the total internal sensor noise from all sources when there is zero radiometric input flux to the sensor. Dark noise electrons are computed as either  $ne_{dark} = NEI_{dark} \mathfrak{R}_{peak,E}$ , or  $ne_{dark} = NER_{dark} \mathfrak{R}_{peak,L}$ , depending on whether the user selects to input sensitivity in NEI or NER. The number of photon noise electrons is computed as

$$ne_{photon}(m, n) = \sqrt{r_L(m, n) + r_E(m, n)} \quad (54)$$

#### 5.11.5 Saturation

The number of saturation equivalent electrons ( $SEe^-$ ) is computed as either  $SEe^- = SEI * \mathfrak{R}_{peak,E}$ , or  $SEe^- = SER * \mathfrak{R}_{peak,L}$ , depending on whether the user selects to input saturation in SEI or SER. If the user elects to simulate without saturation then  $SEe^- = \infty$ .

#### 5.11.6 Total Response

The total sensor response for pixel  $(m, n)$  is computed as

$$r_{tot}(m, n) = \min[r_L(m, n) + r_E(m, n) + N(0, ne_{total}(m, n)), SEe^-] \quad (55)$$

where  $N(0, x)$  is a Gaussian random number with mean 0 and standard deviation  $x$  and  $\min\{x, y\}$  is the minimum function which returns the minimum of  $x$  and  $y$ .

### 5.12 STATIC METRICS

The following static metrics are available for display in STK reports.

**Table 1. Summary of Static Metrics**

Metric	Definition	Notes
Number of Pixels in Horizontal and Vertical Directions	Number of pixels entered by the user is passed through to the report unmodified.	

Geometric FOV in Horizontal Direction	The full-angle field of view in the horizontal direction, $FOV_H$ , entered by the user is passed through to the report unmodified.	
Geometric FOV in Vertical Direction	The full-angle field of view in the vertical direction, $FOV_V$ , entered by the user is passed through to the report unmodified.	
Geometric Field of View (FOV) Solid Angle	$\Omega_{FOV} = FOV_H FOV_V$	$FOV_H$ and $FOV_V$ are the full-angle field of view in horizontal and vertical directions entered by the user.
Geometric IFOV in Horizontal Direction	$IFOV_H = 2 \arctan\left(\frac{p_x}{2f}\right)$	Pixel pitch, $p_x$ , is calculated from Eqn. (21).
Geometric IFOV in Vertical Direction	$IFOV_V = 2 \arctan\left(\frac{p_y}{2f}\right)$	Pixel pitch, $p_y$ , is calculated from Eqn. (22).
Geometric Instantaneous Field of View (IFOV) Solid Angle	$\Omega_{IFOV} = IFOV_H IFOV_V$	
Effective FOV in Horizontal Direction	$EFOV_H = \frac{FOV_H}{\sqrt{ENSQ}}$	$ENSQ$ is ensquared energy calculated from Eqn. (42).
Effective FOV in Vertical Direction	$EFOV_V = \frac{FOV_V}{\sqrt{ENSQ}}$	$ENSQ$ is ensquared energy calculated from Eqn. (42).
Effective FOV Solid Angle	$\Omega_{EFOV} = \frac{\Omega_{FOV}}{ENSQ}$	$ENSQ$ is ensquared energy calculated from Eqn. (42).
Effective IFOV in Horizontal Direction	$EIFOV_H = \frac{IFOV_H}{\sqrt{ENSQ}}$	$ENSQ$ is ensquared energy calculated from Eqn. (42).
Effective IFOV in Vertical Direction	$EIFOV_V = \frac{IFOV_V}{\sqrt{ENSQ}}$	$ENSQ$ is ensquared energy calculated from Eqn. (42).
Effective Instantaneous Field of View (IFOV) Solid Angle	$\Omega_{EIFOV} = \frac{\Omega_{IFOV}}{ENSQ}$	$ENSQ$ is ensquared energy calculated from Eqn. (42).

Low and High Band Edge Wavelengths	Low and high band edge wavelengths entered by the user are passed through to the report unmodified.	
Peak Radiance Responsivity	Calculated from Eqn. (31).	This definition is based on assumptions made to ensure sensor RSR is a boxcar.
Peak Irradiance Responsivity	Calculated from Eqn. (32).	
Sensor Dark Noise Equivalent Irradiance (NEI)	Current sensor dark NEI calculated as explained in Section 5.9.	
Sensor Dark Noise Equivalent Radiance (NER)	Current sensor dark NER calculated as explained in Section 5.9.	
Saturation Equivalent Irradiance (SEI)	Current SEI calculated as explained in Section 5.10.	
Saturation Equivalent Radiance (SER)	Current SER calculated as explained in Section 5.10.	
Effective Focal Length	Effective focal length entered by the user is passed through to the report unmodified.	
F-number	F-number entered by the user is passed through to the report unmodified.	
Diffraction Wavelength	Diffraction wavelength specified by the user is passed through to the report unmodified.	
Airy Disk Diameter	$\frac{2.44\lambda_{diff}}{D_{enp}}$	$\lambda_{diff}$ is the diffraction wavelength, $D_{enp}$ is the entrance pupil diameter calculated as $D_{enp} = \frac{f}{F/\#}$
Rayleigh Resolution	$\frac{1.22\lambda_{diff}}{D_{enp}}$	$\lambda_{diff}$ is the diffraction wavelength, $D_{enp}$ is the entrance pupil diameter calculated as $D_{enp} = \frac{f}{F/\#}$
Sparrow Resolution	$\frac{\lambda_{diff}}{D_{enp}}$	$\lambda_{diff}$ is the diffraction wavelength, $D_{enp}$ is the entrance pupil diameter calculated as $D_{enp} = \frac{f}{F/\#}$

Ensquared Energy	Defined in Section 5.8.	
Diffraction OTF	Defined in Section 5.6.1.1.	
Optics OTF	Defined in Section 5.6.1	
Jitter OTF	Defined in Section 5.6.2.	
Horizontal Detector Footprint MTF	Defined in Section 5.12.1.	
Vertical Detector Footprint MTF	Defined in Section 5.12.1.	

### 5.12.1 Detector Footprint Modulation Transfer Function

A modulation transfer function (MTF) can be defined for the detector footprint which accounts for the spatial averaging performed by individual pixels. Detector footprint MTFs are not used internally by the STK EOIR computational engine; they are only output in STK EOIR reports. Although the detector footprint MTF is not used when computing the sensor response to the synthetic scene (see Section 5.11) defining a detector footprint MTF is nonetheless useful in that it allows a straightforward comparison of the spatial frequency filtering aspects of the detector with the optics and system level degradations such as line-of-sight jitter.

The horizontal detector footprint MTF is defined as

$$MTF_{\text{det},H}(\xi_x') = \left| \frac{\sin(\pi \xi_x' p_x)}{\pi \xi_x' p_x} \right| \quad (56)$$

where  $\xi_x'$  is the spatial frequency and  $p_x$  is the pixel pitch in the  $x'$  direction in the FPA coordinate system.

The vertical detector footprint MTF is defined as

$$MTF_{\text{det},V}(\xi_y') = \left| \frac{\sin(\pi \xi_y' p_y)}{\pi \xi_y' p_y} \right| \quad (57)$$

where  $\xi_y'$  is the spatial frequency and  $p_y$  is the pixel pitch in the  $y'$  direction in the FPA coordinate system.

## 5.13 DYNAMIC METRICS INVOLVING A TARGET

### 5.13.1 Point Source Targets and Backgrounds

A point source target is a target object that is angularly small compared with a single pixel; specifically, the solid angle  $\Omega_T$  subtended by the target is less than the effective IFOV solid angle<sup>2</sup>. The point target solid angle is given by

$$\Omega_T = \frac{A_T^*}{R^2} \quad (58)$$

where,

$A_T^*$  = the projected area of the target (as observed at the sensor) given by

$$A_T^* = \int_{A_{tgt}} \cos(\theta(\vec{x})) dA, A_{tgt} \text{ is the target surface area, } \theta(\vec{x}) \text{ is the angle between the vector in the direction of the sensor and the surface normal at point } \vec{x} \text{ on the target surface.}$$

For metrics involving point source targets the background is treated as uniform; i.e. spatial clutter is neglected. The following definitions are used.

$E_\lambda^{tgt}(\lambda)$  = target spectral irradiance at the sensor aperture given by Eqn. (11)

$L_\lambda^{bkg}(\lambda)$  = uniform apparent background spectral radiance at the sensor aperture from the area immediately behind the target given by Eqn. (4) or Eqn. (9)

The total sensor response for a target-containing-IFOV and the mean background-only-IFOV can be written as

$$r_{TGT} = \min \left\{ E^{tgt} \mathfrak{R}_{peak,E} + L^{bkg} \left( 1 - \frac{\Omega_T}{\Omega_{EIFOV}} \right) \mathfrak{R}_{peak,L}, \quad SEe^- \right\} \quad (59)$$

$$r_{BKG} = \min \left\{ L^{bkg} \mathfrak{R}_{peak,L}, \quad SEe^- \right\} \quad (60)$$

where,

$$E^{tgt} = \int_{\Delta\lambda} E_\lambda^{tgt}(\lambda) RSR(\lambda) d\lambda \quad (61)$$

$$L^{bkg} = \int_{\Delta\lambda} L_\lambda^{bkg}(\lambda) RSR(\lambda) d\lambda \quad (62)$$

$SEe^-$  = saturation equivalent electrons (when simulating without saturation  $SEe^- = \infty$ )

<sup>2</sup> For non-spherical objects the test for an extended area target is done using an approximation of  $\Omega_T$  rather than the exact projected solid angle.

---

$\min[\{x, y\}]$  = minimum function which returns the minimum of  $x$  and  $y$  (used to account for saturation).

In Eqn. (60) the fraction of target signal which spills into the background pixels due to diffraction, aberrations, etc. is neglected.

### 5.13.2 Point Source Detection Criteria and Point Source Signal-to-Noise Ratio

The following detection criterion for point sources is used as the basis for defining the point source signal-to-noise ratio.

*In order for the target to be detected the difference in sensor response for a target-containing-IFOV and the mean of the local surrounding IFOVs must be greater than the RMS deviations in the surrounding IFOVs by some factor  $k$ .*

That is for detection the following condition must be met

$$r_{TGT} - r_{BKG} > k\sigma \quad (63)$$

where,

$\sigma$  = RMS deviations in sensor response [electrons] for the local IFOVs surrounding the target-containing IFOV.

The RMS deviations in sensor response in the local IFOVs surrounding the target are due to sensor dark noise and scene photon noise (background clutter is neglected). That is

$$\sigma = \sqrt{ne_{dark}^2 + ne_{photon}^2 (L_{B,eff})} \quad (64)$$

where,

$ne_{dark}$  = sensor dark noise (for non-illumination conditions) [electrons]

$ne_{photon}$  = scene photon noise due to background radiance [electrons]

Defining the “signal” to be  $|r_{TGT} - r_{BKG}|$  the point source signal-to-noise ratio can be defined as

$$SNR_{ps} = \frac{|r_{TGT} - r_{BKG}|}{\sigma} \quad (65)$$

The detection criterion can be restated in terms of the point source SNR with the necessary condition for detection being

$$SNR_{ps} > k \quad (66)$$

Substituting Eqns. (59) and (60) into Eqn. (65) gives



$$SNR_{ps} = \frac{\left| \min \left\{ E^{igt} \mathfrak{R}_{peak,E} + L^{bkg} \left( 1 - \frac{\Omega_T}{\Omega_{EIFOV}} \right) \mathfrak{R}_{peak,L}, SEe^- \right\} - \min \left\{ L^{bkg} \mathfrak{R}_{peak,L}, SEe^- \right\} \right|}{\sigma} \quad (67)$$

When sensor saturation is neglected, (i.e.  $SEe^- = \infty$ ) Eqn. (67) can be rewritten as

$$SNR_{ps} = \frac{|E^{igt} - L^{bkg} \Omega_T|}{NEI_{tot}} \quad (68)$$

where the total noise equivalent irradiance (NEI) metric is defined as

$$NEI_{tot} = \frac{\sigma}{\mathfrak{R}_{peak,E}} \quad (69)$$

The scene photon noise equivalent irradiance (NEI) metric is defined as

$$NEI_{photon} = \frac{ne_{photon}(L^{bkg})}{\mathfrak{R}_{peak,E}} = \frac{\sqrt{L^{bkg} \mathfrak{R}_{peak,L}}}{\mathfrak{R}_{peak,E}} \quad (70)$$

Using Eqn. (64), Eqn. (70), and the definition of sensor dark noise Eqn. (69) can be rewritten as

$$NEI_{tot} = \sqrt{NEI_{dark}^2 + NEI_{photon}^2} \quad (71)$$

### 5.13.3 Extended Area Targets

When the projected solid angle subtended by the target at the sensor  $\Omega_T$  is greater than or equal to  $\Omega_{EIFOV}$  the target is considered to be an extended area target. For non-spherical objects the test for an extended area target is done using an approximation of  $\Omega_T$  rather than the exact projected solid angle.

In order to define the background for extended area targets a rectangular region is defined which contains the target of interest. Within this region all surface areas sampled by the regular spatial sampling grid which are not on the target are classified as part of the background.

The average target spectral radiance at the sensor is defined as

$$\bar{L}_{\lambda}^{igt}(\lambda) = \frac{1}{N_{igt}} \sum_{i \in S_{igt}} L_{\lambda}(\lambda, i) \quad (72)$$

where,

$L_{\lambda}(\lambda, i)$  = spectral radiance at the sensor aperture from surface area  $i$  given by Eqn. (4) or Eqn. (9)

$S_{tgt}$  = the set of unit surface areas  $dA$  on the extended area target sampled by the regular spatial sampling grid

$N_{tgt}$  = total number of surface areas in  $S_{tgt}$

The average background spectral radiance at the sensor is defined as

$$\bar{L}_{\lambda}^{bkg}(\lambda) = \frac{1}{N_{bkg}} \sum_{i \in S_{bkg}} L_{\lambda}(\lambda, i) \quad (73)$$

where,

$L_{\lambda}(\lambda, i)$  = spectral radiance at the sensor aperture from surface area  $i$  given by Eqn. (4) or Eqn. (9)

$S_{bkg}$  = the set of unit surface areas  $dA$  from the background within a rectangular region surrounding the target sampled by the regular spatial sampling grid

$N_{bkg}$  = total number of surface areas in  $S_{bkg}$

The “signal” radiance is defined to be

$$L_{signal} = \left| \min\{\bar{L}^{tgt}, SER\} - \min\{\bar{L}^{bkg}, SER\} \right| \quad (30)$$

where  $SER$  is the saturation equivalent radiance and

$$\bar{L}^{tgt} = \int_{\Delta\lambda} \bar{L}_{\lambda}^{tgt}(\lambda) RSR(\lambda) d\lambda \quad (74)$$

$$\bar{L}^{bkg} = \int_{\Delta\lambda} \bar{L}_{\lambda}^{bkg}(\lambda) RSR(\lambda) d\lambda \quad (75)$$

The extended source SNR is defined as

$$SNR_{ext} = \frac{\bar{L}_{signal}}{NER_{tot}} \quad (76)$$

where,

$$NER_{tot} = \sqrt{NER_{dark}^2 + NER_{photon}^2} \quad (77)$$

$$NER_{photon} = \frac{ne_{photon}(\bar{L}^{bkg})}{\mathfrak{R}_{peak,L}} = \sqrt{\frac{\bar{L}^{bkg}}{\mathfrak{R}_{peak,L}}} \quad (78)$$

$NER_{dark}$  = current sensor dark NER

$ne_{photon}(\bar{L}^{bkg})$  = scene photon noise electrons for the average background radiance

At the point of transition from a point source to an extended area source ( $\Omega_T = \Omega_{IFOV}$ ) the above definition allows for a smooth transition in SNR, i.e.  $SNR_{ps} = SNR_{ext}$  (assuming a uniform background).

### 5.13.4 Summary of Dynamic Metrics Involving Targets

**Table 2. Summary of Dynamic Metrics**

Metric	Definition	Notes
Range to Target	Distance between target and sensor.	
Effective Target Irradiance	Eqn. (61).	Only defined for point source targets.
Point Target Solid Angle	Eqn. (58).	Only defined for point source targets.
Scene Photon NEI	Eqn. (70).	For extended area targets this metric is calculated by converting the scene photon NER (using Eqn. (78) to NEI rather than using Eqn. (70).
Total NEI	Eqn. (71).	For extended area targets this metric is calculated by converting the total NER (using Eqn. (77)) to NEI rather than using Eqn. (71).
Effective Target Radiance	Eqn. (74).	Only defined for extended area targets.
Effective Background Radiance	Eqn. (62) or Eqn. (75).	Eqn. (62) is used for point source targets and Eqn. (75) is used for extended area targets.
Scene Photon NER	Eqn. (78).	For point source targets this metric is calculated by converting the scene photon NEI (using Eqn. (70)) to NER rather than using Eqn. (78).
Total NER	Eqn. (77).	For point source targets this metric is calculated by converting the total NEI (using Eqn. (71)) to NER rather than using Eqn. (77).
Signal to Noise Ratio	Eqn. (65) or Eqn. (76).	Eqn. (65) is used for point source targets and Eqn. (76) is used for extended area targets.
Geometric IFOV Footprint at Range to Target	$\Omega_{IFOV} R^2$	$\Omega_{IFOV}$ is the geometric IFOV solid angle, R is the range to target

---

Effective IFOV Footprint at Range to Target	$\Omega_{EIFOV} R^2$	$\Omega_{EIFOV}$ is the effective geometric IFOV solid angle, R is the range to target
---	----------------------	--

---

## 6. SCENE GENERATOR VALIDATION

Validation mostly consists of a set of "physics experiments" conducted in the modeled universe, such that each element of the radiance and irradiance equations is exercised in isolation of the other elements. This demonstrates that the code implements the equations correctly. The user must judge whether the equations used are adequate to his purpose. [User comments on possible better equations are welcome.]

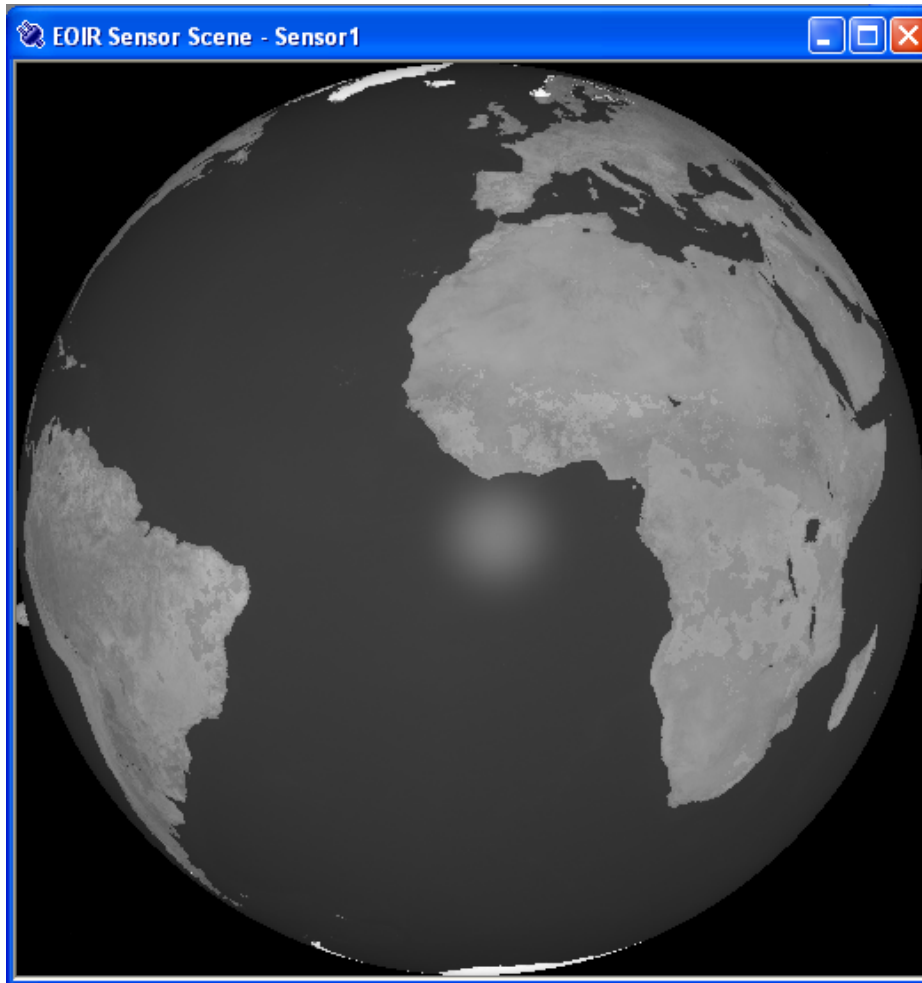
The experiments mostly demonstrate relative behavior as opposed to absolute behavior. The experiments are tied to absolute measurements as follows:

- The modeled integral solar irradiance is compared to the accepted Solar Constant
- The modeled integral irradiance of a star and planet are compared to the same models presented in an "Applied Optics" paper
- The modeled spectral radiance of an Earth viewing scenario is compared to a MODTRAN run of the same scenario

### 6.1 GEOMETRIC

#### 6.1.1 FOV – Projected Angles—Distance Ordering

1. Run STK EOIR
2. Load V\_Test1.sc – a sensor on a geosynchronous satellite observing the earth at full moon near the spring equinox

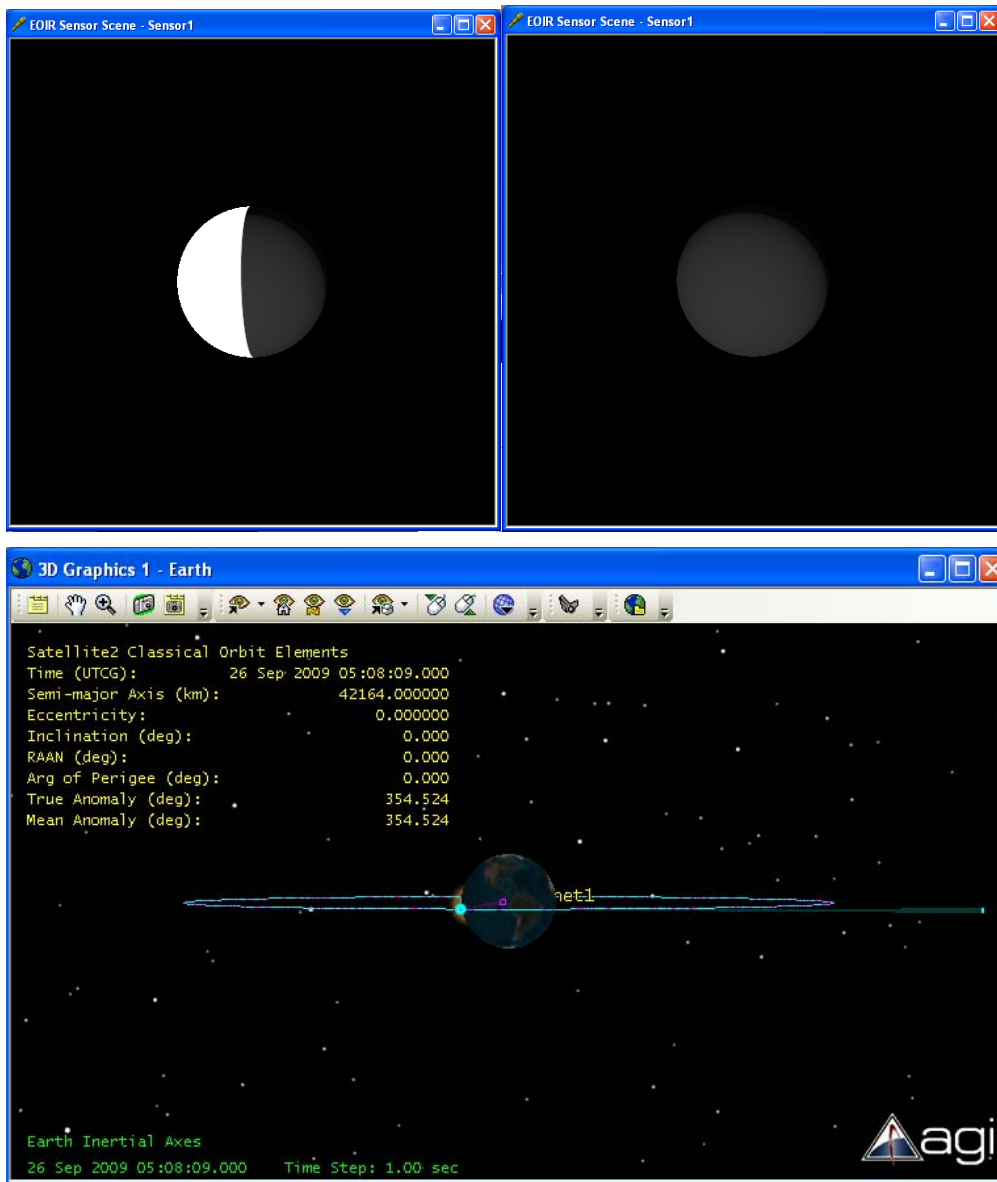


3. The moon should be at about the 8:00 position, behind the Earth
4. Note that the Earth exactly fills the  $17.4008^\circ$  Field of View [ $2 * \text{asin}(6378.1 \text{ km}/42164.2 \text{ km})$ ]
5. Click on both the Earth and moon. Note that the moon is at a greater distance than the Earth and is partially obscured by the Earth [Note: Step 4 above uses the center distance, while Step 5 gives the surface distance]
  - Earth distance = 35,786.1 km (42,164.2 - 6378.1) @ scene pixel  $256_x$   $256_y$
  - Moon distance =  $\sim 415,181$  km @ scene pixel  $3_x$   $309_y$
6. Click on the upper and lower edges of the moon, to get the scene pixel Y coordinates.
  - $3_x$   $302_y$
  - $3_x$   $315_y$

Note that the moon subtends  $(315-302+1 = 14)$  scene samples. [ $\# \text{ samples} * \text{IFOV}/4 = 14 * 2.3911 \times 10^{-3}/4 = 0.4795^\circ$ , while  $2 * 1737.53 \text{ km}/415181 \text{ km} = 0.4796^\circ$ ]. Note that this is a reasonable angular subtense for the moon, given a digitization uncertainty of  $1/2$  synthetic scene pixel =  $0.017^\circ$ .

## 6.1.2 Distance Ordering & Obscuration

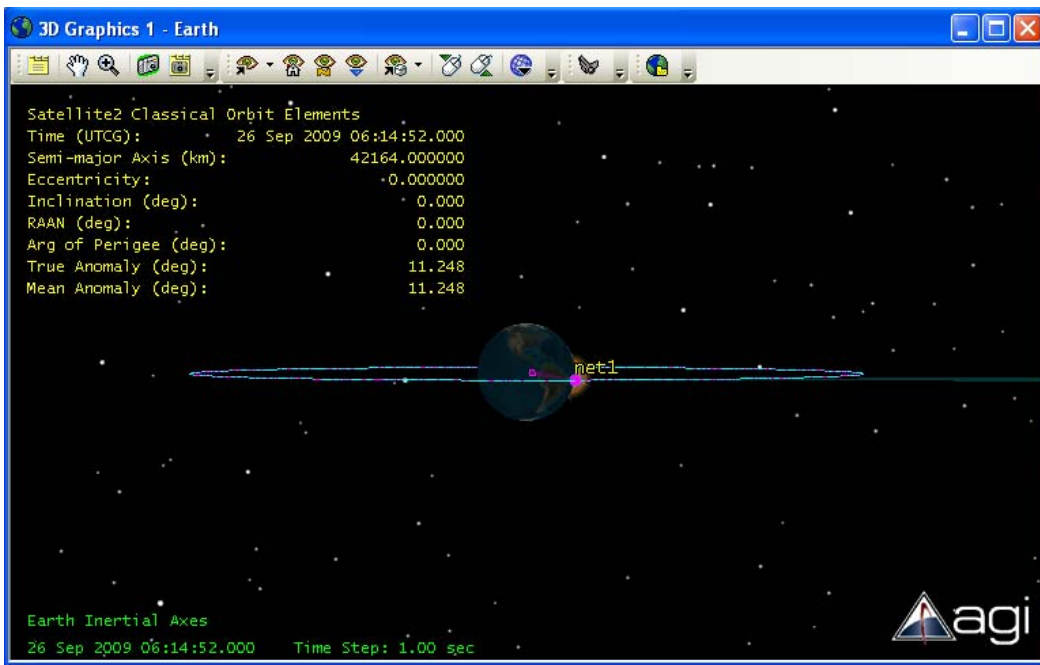
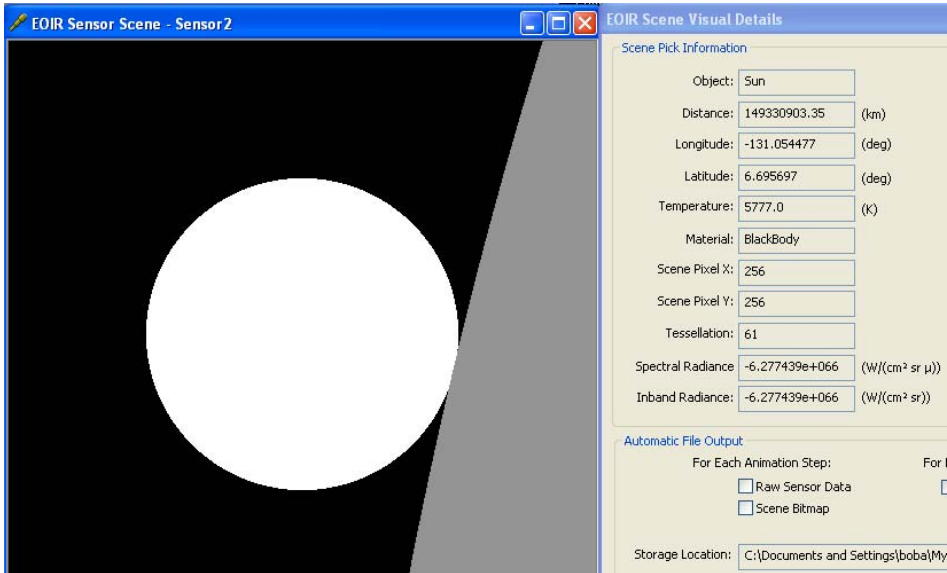
1. Run STK EOIR.
2. Load V\_Test2.sc – a sensor on a geosynchronous satellite #1 observes geosynchronous satellite #2 as it is eclipsed by the Earth's shadow.
3. Change the current time to 05:08:09. At this time satellite #2 has just become eclipsed. Note the true anomaly  $v = 354.524^\circ$ . One second earlier in time satellite #2 can just see the last bit of sunset. Note the true anomaly  $v = 354.519^\circ$ .



4. Change the current time to 06:14:52. At this time satellite #2 is still eclipsed. Note the true anomaly  $v = 11.253^\circ$ . One second later in time satellite #2 can just observe sunrise. Note the true anomaly  $v = 11.248^\circ$ .

In the following calculations, 1 AU (Astronomical Unit) is used as shorthand to mean the *current* solar distance. This was determined by "clicking" on the View Dialog image of the

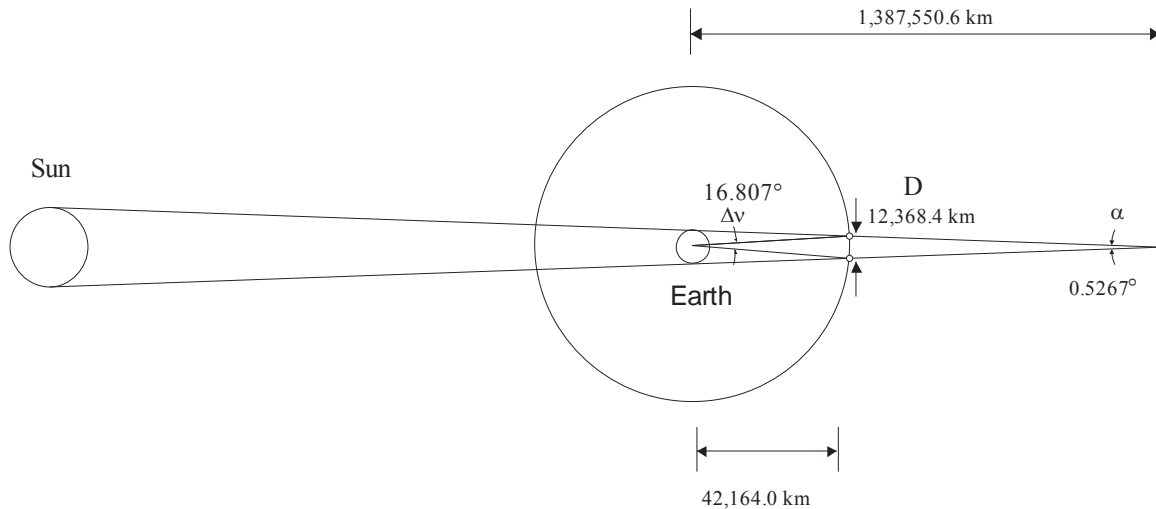
sun in an alternate scenario version V\_Test2\_debug.sc. This version places a sensor on the 2nd satellite, that is imaging the sun. 1AU = "click" distance + solar radius



5. Therefore  $\Delta v_{\text{measured}} = 16.729^\circ$ , using the averaged true anomalies.

To calculate the delta true anomaly for crossing the Earth's shadow:





$$\text{Shadow Length} = \frac{1AU * R_{earth}}{R_{sun} - R_{earth}} = \frac{150,026,893.4 * 6378.0}{695,990 - 6378.0} = 1,387,550.6 \text{ km}$$

$$\alpha = 2 * \frac{6378.0}{1,387,550.6} = 9.187 \times 10^{-3} \text{ rad} = 0.5267^\circ$$

$$D = \alpha * (1,387,550.6 - 42,164.0) = 12,368.4 \text{ km}$$

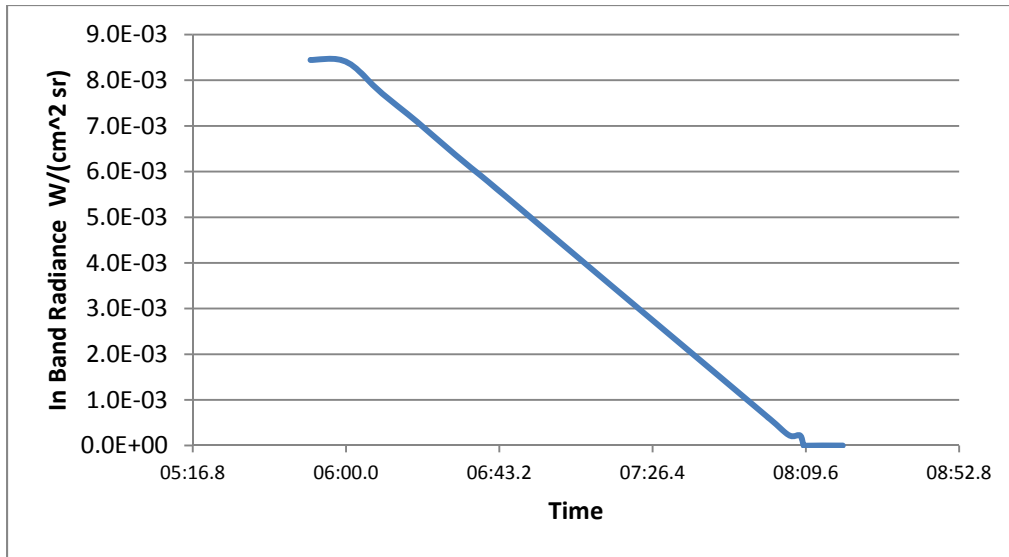
$$\Delta v = \frac{12,368.4}{42,164.0} = 2.933 \times 10^{-1} \text{ rad} = 16.807^\circ \text{ computed}$$

$$\Delta v_{\text{computed}} / \Delta v_{\text{measured}} = 1.005$$

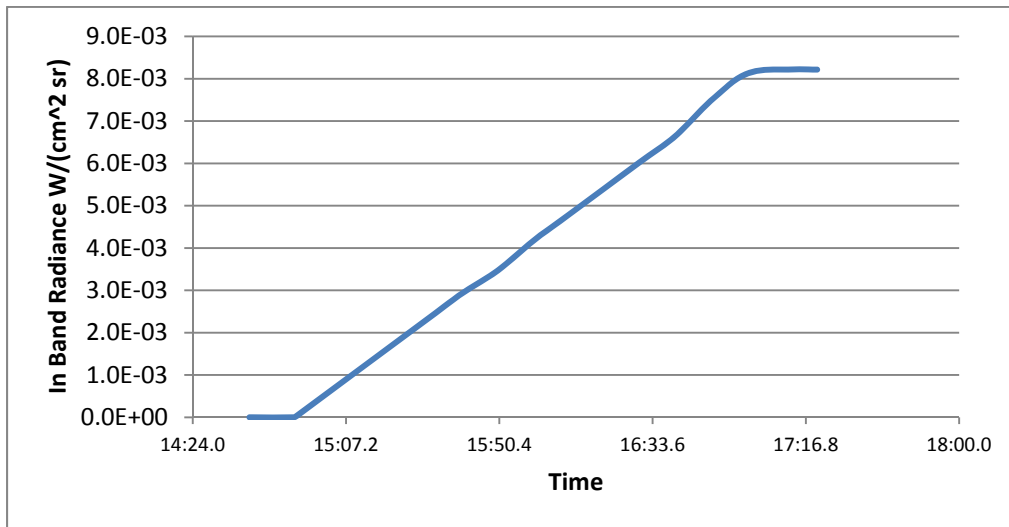
## 6. Penumbra

This part of the test measures the changing illumination on the observed satellite and the duration of the change during sunset and sunrise. The illumination is measured by clicking on the left (illuminated) edge of the satellite image at a series of time steps:

### a. Sunset



b. Sunrise



- c. Expected duration of sunset or sunrise can be approximated using the fact that the satellites are geosynchronous. Therefore their angular rate is

$$\frac{360}{24 * 60 * 60} = 0.004166667 \text{ deg/sec}$$

and the sun's angular diameter is

$$2 * \frac{695,990.0}{150,026,411.4} = 0.5316^\circ$$

therefore the time to traverse the sun's angular diameter is

$$\frac{0.5316}{0.004166667} = 127.58 \text{ sec or } 2:07.6$$

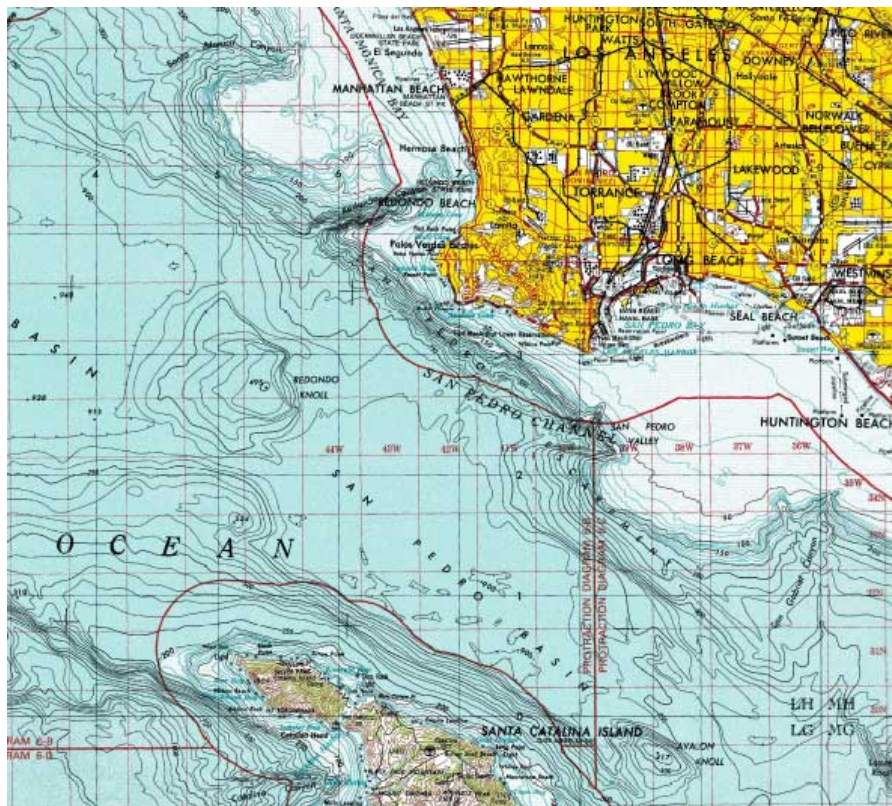
As simulated for sunset, the time delta from start to end is

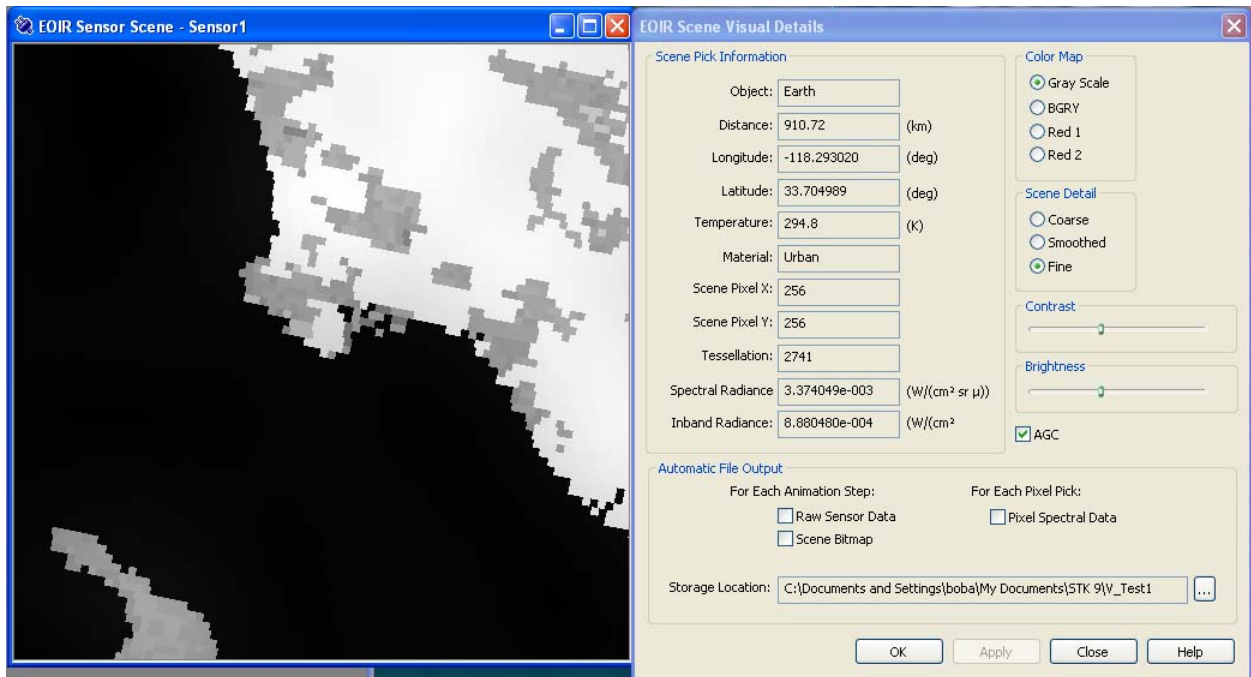
$$5:08:08 - 5:05:59 = 2:09$$

---

### 6.1.3 Bitmap – Registration

1. Run EOIR.
2. Load V\_Test3.sc – a sensor on a polar orbiting satellite with the sub satellite point over Los Angeles. A Target Object has been placed at the longitude & latitude of the Point Fermin Lighthouse, Long = -118.294°, Lat = 33.705°.
3. Using the Detail Dialog, click on the centermost pixel (256 x 256).
4. The Detail Dialog coordinates are Long = -118.293°, Lat = 33.705°.
5. Note that the centermost pixel location is within the 1 km bitmap pixel that most closely approximates Point Fermin. [A subsequent test looking at a location near the equator and the mouth of the Amazon River, shows a longitudinal offset of the bitmap of about 2.5 km. This is under investigation.]





## 6.2 AREA RADIOMETRIC EQUATION

### 6.2.1 Background

1. Run EOIR.

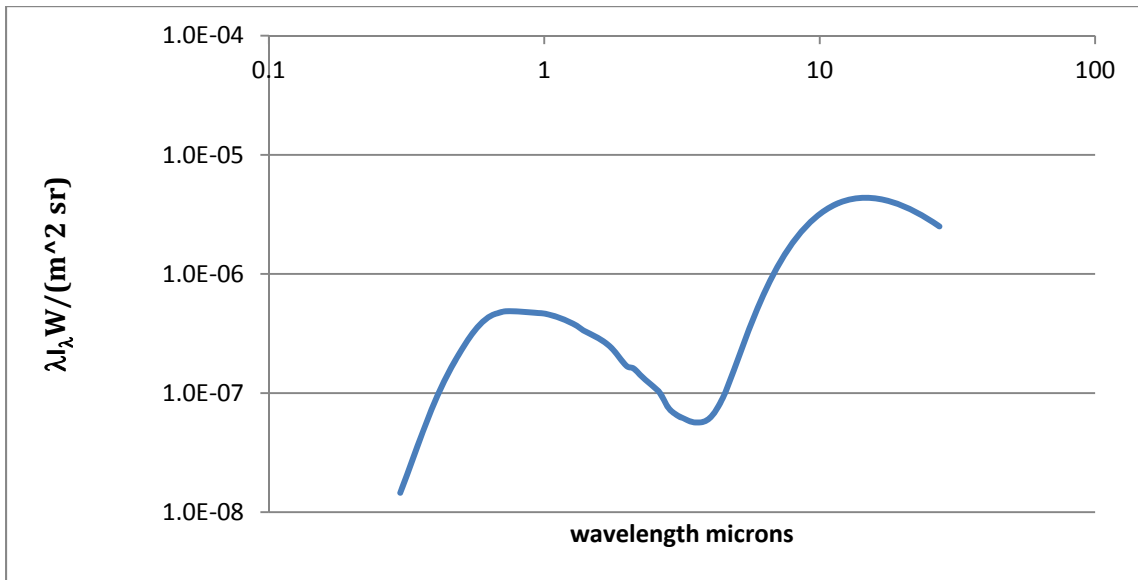
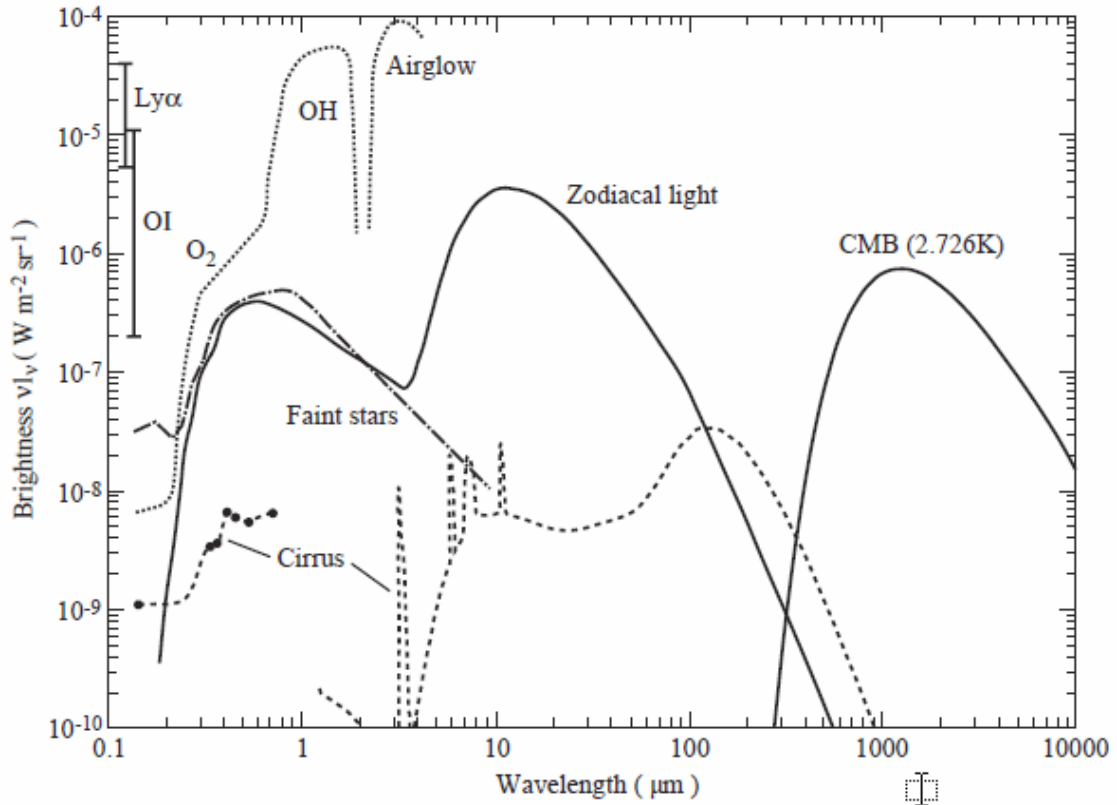
- 
2. Load V\_SRF\V\_SRF\_AC.sc – Aircraft #4 is the viewing target. There is a sensor on Aircraft #1 for viewing Aircraft #4. Aircraft #2 acts as a light source. The Aircraft are all at 0° Longitude and 0° latitude on the dark side of the Earth, during new moon. There is no atmosphere.
  3. Set Aircraft #2 to a temperature of 0 K so that it has no self-radiance.
  4. Set Aircraft #4 to 100% Gray Body Reflectance and 0 K temperature.
  5. Set the sensor's bandpass to 0.3 to 20.3 μm with 200 intervals
  6. On the Details Dialog, check the "For Each Pixel Pick" box.
    - a. Be sure to press the Apply button, so the check takes effect.
  7. Click on Aircraft #4's image.
  8. Exit EOIR
  9. Open EOIR\_ClickData.txt.
  10. Copy the radiance entries, corresponding to the wavelengths, to A\_Test.xlsx, 6.2.1 worksheet

In interpreting the following, note that Fig.1 of, “The 1997 reference of diffuse night sky brightness”, Ch. Leinert, S. Bowyer, L.K. Haikala, M.S. Hanner, M.G. Hauser, A.-Ch. Levasseur-Regourd, I. Mann, K. Mattila, W.T. Reach, W. Schlosser, H.J. Staude, G.N. Toller, J.L. Weiland, J.L. Weinberg, and A.N. Witt, represents each source component separately, whereas EOIR produces the sum of sources. Also note that EOIR is representing the Faint Stars and Zodiacal Light components only.

The spreadsheet converts the usual EOIR units to those used in the above paper, given the relationship:

$$\nu I_\nu = \lambda I_\lambda$$

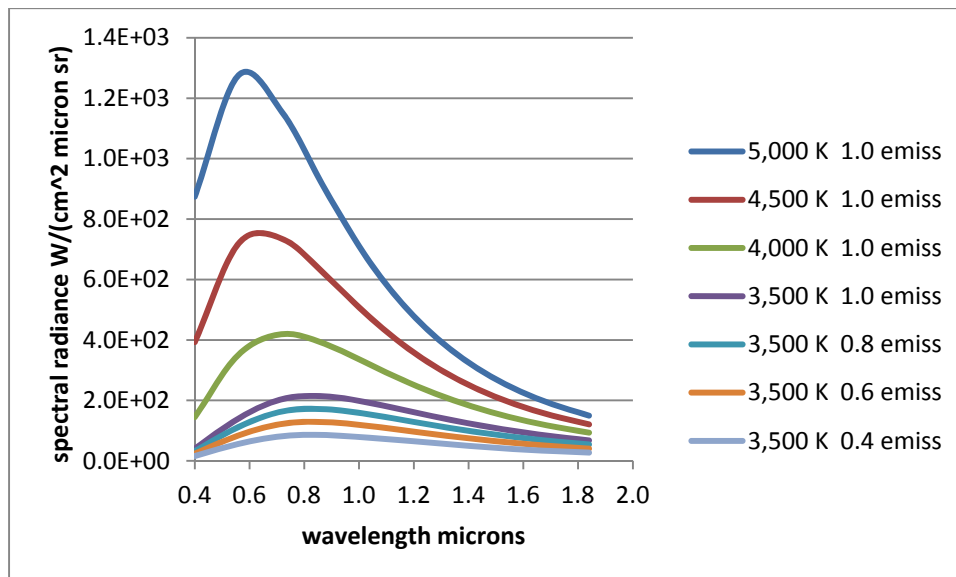
where the paper uses  $I_\lambda$  for spectral radiance



## 6.2.2 Self-Radiance—Emissivity and Effective Temperature

1. Run EOIR.

2. Load V\_SRF\V\_SRF\_AC.sc – Aircraft #4 is the target for viewing. There is a sensor on Aircraft #1 for viewing Aircraft #4. The aircraft are all at 0° Longitude and 0° latitude on the dark side of the Earth, during new moon. There is no atmosphere.
3. Set Aircraft #2 to a temperature of 0 K, such that it emits no radiance, and Aircraft #1 has a shape of None, such that it emits no radiance.
4. Set the sensor's bandpass to 0.4 to 2.0  $\mu\text{m}$  with 10 intervals.
5. On the Details Dialog, check the "For Each Pixel Pick" box.
  - a. Be sure to press the Apply button, so the check takes effect.
6. Set Aircraft #4 to 0% Gray Body Reflectance and 5000 K temperature
  - a. 0% Reflectance = 1.0 Emissivity
  - b. Emissivity = 1.0 - Reflectance
7. Reset time to recalculate the Scene, then Click on Aircraft #4.
8. Repeat the above 2 steps for a series of Temperatures and Emissivities.
9. Exit EOIR
10. Open EOIR\_ClickData.txt.
11. Copy the radiance entries, corresponding to the wavelengths, to A\_Test.xlsx, Self Rad worksheet.
12. Note linear change with Emissivity (1-SRF)
13. Note comparison of Planck function at various Teff's



## 6.2.3 Reflected

### 6.2.3.1 Source Radiance

The observer views the target, which is illuminated by a source at different source radiances. The observer and target remain constant.

1. Run EOIR
2. Load V\_SRF\V\_SRF\_Refl\_AC.sc – Aircraft #3 is the target for viewing. There is a sensor on Aircraft #1 for viewing Aircraft #3. Aircraft #2 acts as a light source. The vehicle/aircraft are all at 0° Longitude and 0° latitude on the dark side of the Earth, during new moon. There is no atmosphere
3. Aircraft #3's graybody reflectance is set to 100%.
4. Aircraft #3's temperature is set to 0 K.
5. Aircraft #2's temperature is set to 4990 K.
6. Aircraft #2's reflectance is set to 0%.
7. Click on Aircraft #3's image and note the in-band spectral radiance.
8. Repeat Steps 6 and 7 for a succession of Aircraft #2 reflectances. Note that the reflected spectral radiance from Aircraft #3 always changes in proportion to the Emissivity of Aircraft #2

Reflectance	Radiance
0% [emittance = 1.0]	1.000552e-003
33.33% [emittance = 0.6667]	6.670758e-004
50% [emittance = 0.5]	5.002879e-004
66.67% [emittance = 0.3333]	3.335000e-004

### 6.2.3.2 Sum of Sources

The observer views the target first illuminated by 1 source, then by 2 identical sources, at very slight position offsets from one another. The observer and target remain constant.

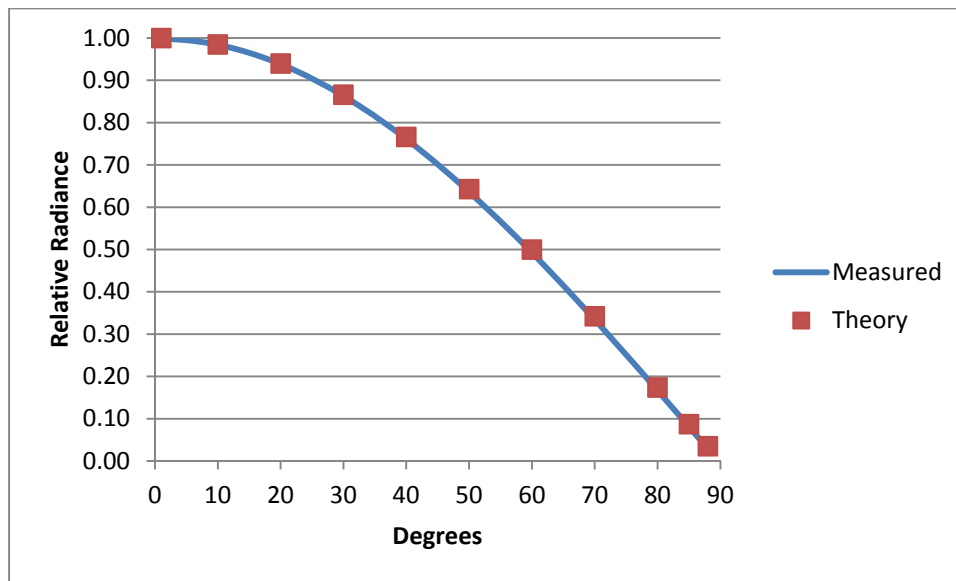
1. Run EOIR.
2. Load V\_SRF\V\_2Source\_AC.sc – Aircraft #4 is the target for viewing. There is a sensor on Aircraft #1 for viewing Aircraft #4. Aircraft #2 & #3 act as light sources. The vehicle/aircraft are all at 0° Longitude and 0° latitude on the dark side of the Earth, during new moon. There is no atmosphere.
3. Set Aircraft #4 to a Gray Body Reflectance of 100%.
4. Set Aircraft #4's temperature to 0 K.
5. Set Aircraft #2 to a temperature of 6000 K and a Gray Body Reflectance of 0%.
6. Set Aircraft #3 to a temperature of 0 K.
7. Click on the time Reset -- to refresh the Sensor Scene.
8. Click on Aircraft #4's image and note the in-band radiance (1.479e-3 W/(cm<sup>2</sup> sr)).
9. Set Aircraft #3 to a temperature of 6000 K and a Gray Body Reflectance of 0%.
10. Click on the time Reset -- to refresh the Sensor Scene.
11. Click on Aircraft #4's image and note the peak spectral radiance has now doubled (2.959e-3 W/(cm<sup>2</sup> sr)).



### 6.2.3.3 Projected solid angle (cosine law)

The observer is fixed relative to the target. The illumination source is at a constant distance but at a succession of different angles relative to the target's surface normal.

1. Run EOIR.
2. Load B\_Test1\_AC.sc – Aircraft #3 is the target for viewing. There is a sensor on Aircraft #1 for viewing Aircraft #3. Aircraft #2 acts as a light source. The aircraft are all at 0° Longitude and 0° latitude on the dark side of the Earth, during new moon. There is no atmosphere.
3. Set Aircraft #3 to Gray Body Reflectance of 100%.
4. Aircraft #2 is set to a temperature of 5,000 K and Gray Body Reflectance of 0%.
5. The Scene Detail mode is set to Smoothed on the Details Dialog.
6. Enter a series of altitudes and longitude offsets into both waypoints for Aircraft #2 such that a constant distance is maintained from the center of Aircraft #3, while the incidence angle of illumination of Aircraft #2 onto Aircraft #3 changes [see worksheet 6.2.3.3 of A\_Test.xlsx].
7. Note the radiance at the center of Aircraft #3 by clicking close to scene sample 256x, 256y.
8. Copy the radiance entries, corresponding to altitudes and longitude offsets, to A\_Test.xlsx, Cosine worksheet



### 6.2.3.4 Projected solid angle (inverse square law)

The observer views an area source target at a succession of distances to test inverse square fall off of irradiance. The reflected illumination and self-radiance of the target remain constant.

Note that the following test requires that EOIR be recompiled to access an internal report. This test cannot be performed using the released version of EOIR.

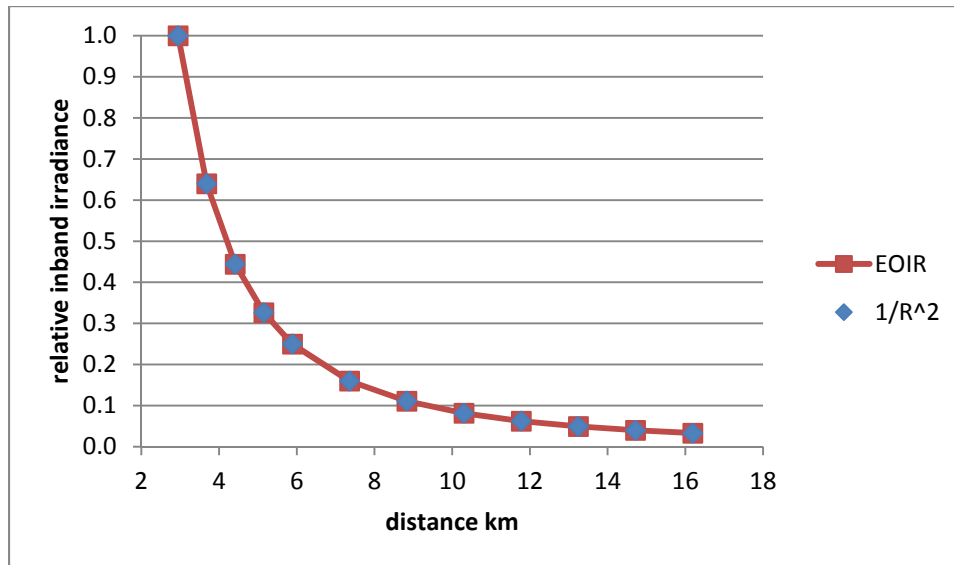
1. Compile EOIR and rebuild with

- a. TRACK\_IRRAD defined & IRRAD\_OBJECT = Satellite #2

This calculates the inband irradiance at aperture by summing all scene generator pixel irradiances corresponding to Satellite #2

- b. `SetDebugOutput(true);`

2. Run EOIR.
3. Load V\_Phase2.sc – a sensor on a geosynchronous satellite #1 observes geosynchronous satellite #2 at a succession of distances. Satellite #2 changes its argument of the ascending node to set various inter-satellite distances.
4. Satellite #2 should be fully illuminated.
5. Satellite #2's Gray Body Reflectance should be set to 100%.
6. Select the sensor band with the narrower FOV such that Satellite #2 appears as an area source.
7. The calculated values are written to a test file, each time the image is updated
8. Input a succession of RAAN values for Satellite #2 (argument of the ascending node).
9. Exit EOIR and Plot the distance vs. irradiance values. Note the inverse square relationship

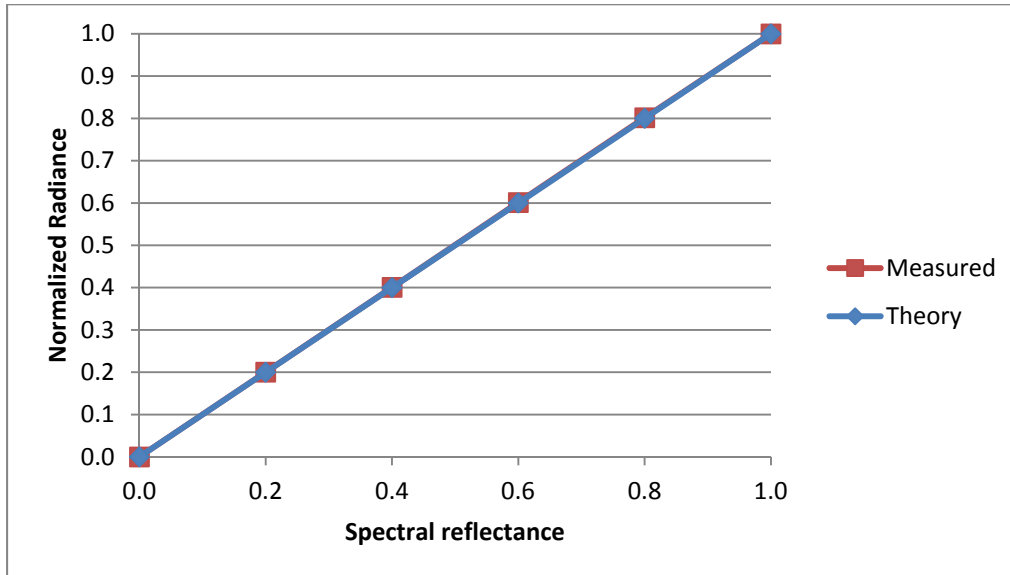


### 6.2.3.5 SRF

The observer views the target, while target's SRF is run through a succession of values from 0 to 1. The observer and illumination source remain constant.

1. Run EOIR.
2. Load V\_SRF\_AC.sc – Aircraft #4 is the target for viewing. There is a sensor on Aircraft #1 for viewing – Aircraft #4. Aircraft #2 acts as a light source. The vehicles are all at 0° Longitude and 0° latitude on the dark side of the Earth, during new moon. There is no atmosphere.
3. Aircraft #2 is set to a temperature of 5,000 K and reflectance of 0.0 (Planck radiance).

4. Successively enter a set of Gray Body Reflectance values from 0% to 100% for Aircraft #4.
5. At each reflectance, click on – Aircraft #4’s image and record its radiance and the reflectance to Excel spreadsheet A\_Test.xlsx, SRF sheet. The figure below plots SRF vs. Normalized Radiance from the spreadsheet.



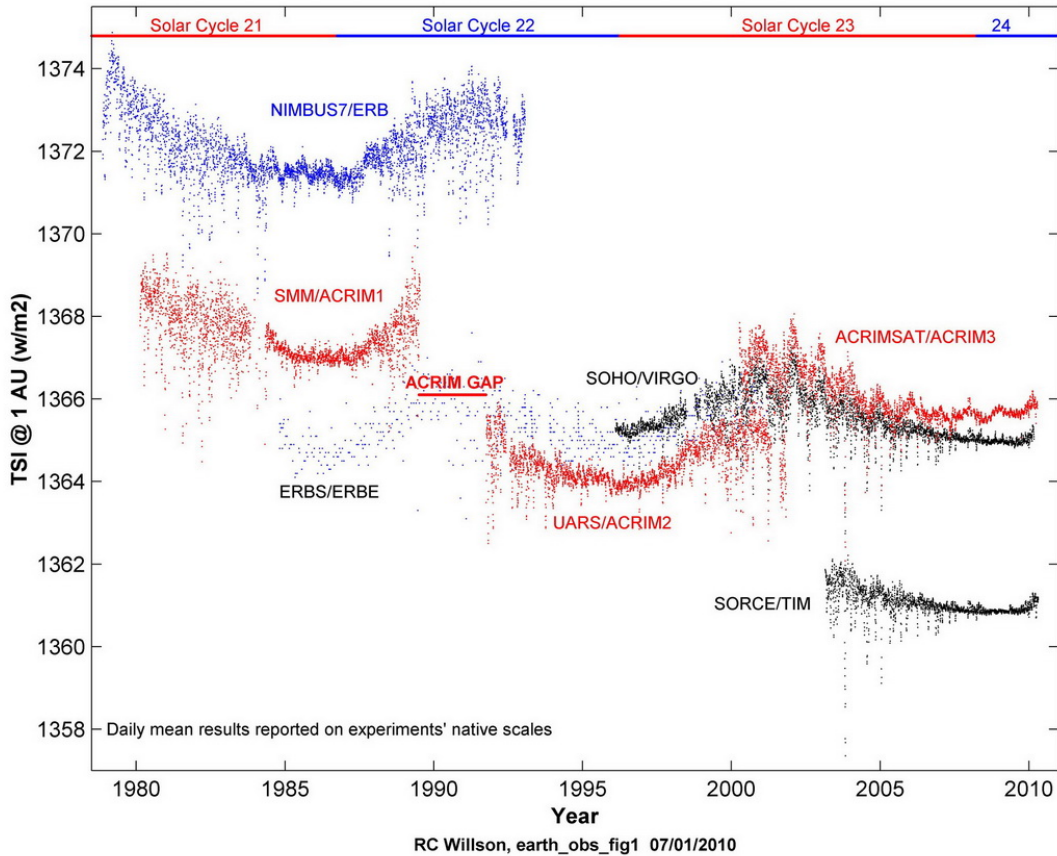
## 6.2.4 Point Radiometric Equation

### 6.2.4.1 Solar Constant

1. Run EOIR.
2. Load V\_SolarConstant2.sc – a sensor on the Earth’s surface on the equator with no atmosphere, stares at the sun on spring equinox.
3. Click on the sun in the center of the display and note its integrated band irradiance of  $0.1378 \text{ W cm}^{-2}$  and the "click" distance to sun = 148,988,587.22.
4. Using  $1 \text{ AU} = 149,597,871.464$ , the distance corrected irradiance is:
 
$$0.1378 * (148,988,587.22/149,597,871.464)^2 = 0.1367 \text{ W cm}^{-2}.$$

For comparison, note the following figure taken from the ACRIM (Active Cavity Radiometer Irradiance Monitor) website <http://acrim.com/Index.htm>:

## TOTAL SOLAR IRRADIANCE MONITORING RESULTS: 1978 to Present



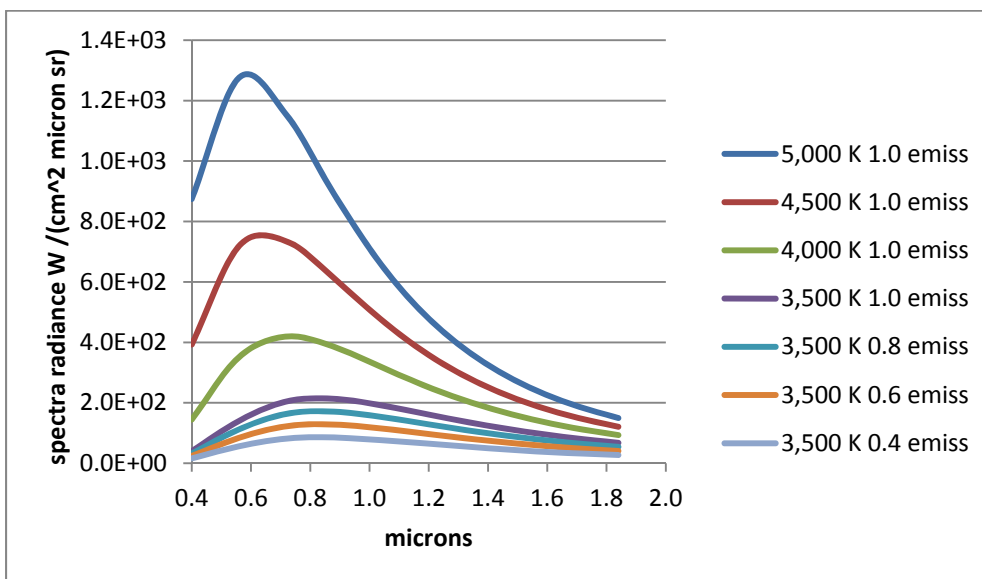
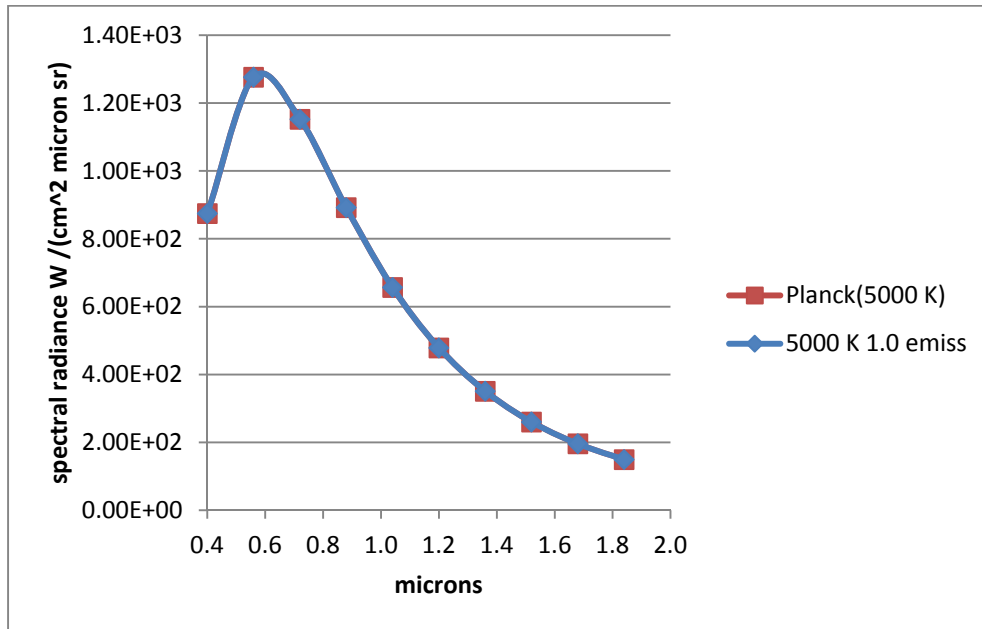
### 6.2.4.2 Self-Radiance

View a point source's self-radiance, with no external illumination. The global background radiance and Earth's self-radiance are still present but are insignificant compared to the selected point source self-radiance.

1. Run EOIR.
2. Load V\_Phase.sc – a sensor on a geosynchronous Satellite #1 observes geosynchronous Satellite #2 . Satellite #2 is in the Earth's shadow.
3. The sensor's bandpass should already be set to 0.4 to 2.0  $\mu\text{m}$  with 10 intervals.
4. Set satellite #2 to 0% Gray Body Reflectance [1.0 emittance] and 5000 K temperature.
5. Click on Satellite #2's image at its center, in the Scene Dialog.
6. Repeat the above 2 steps for a series of Temperatures and emittances.
7. Exit EOIR.
8. Open "EOIR\_ClickData.txt".
9. Copy the radiance entries, corresponding to the wavelengths, to A\_Test.xlsx, Planck worksheet.

10. Note comparison of Planck function at various  $T_{\text{eff}}$ 's.

11. Note linear change with emittance (1-Reflectance).



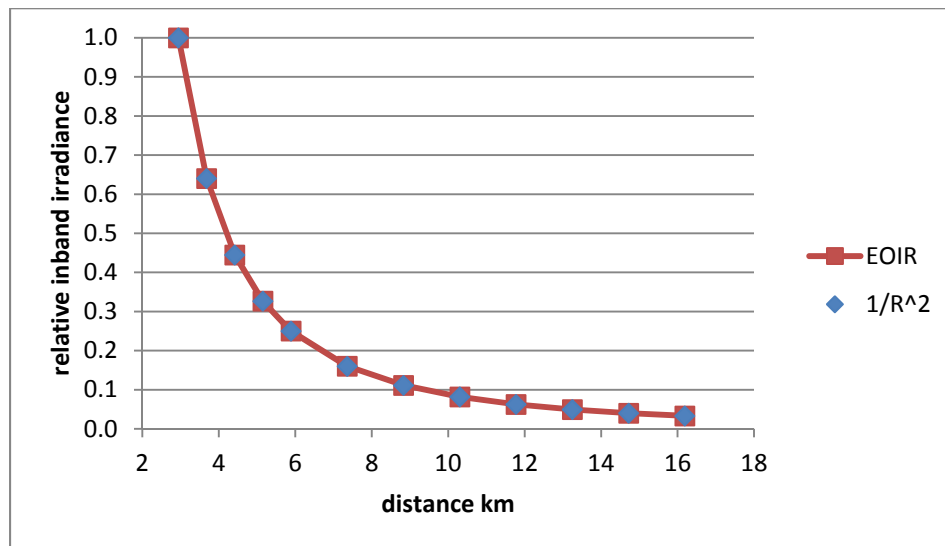
### 6.2.4.3 Reflected

Note that while this test recompiles EOIR to access an internal report, it could be performed by "clicking" on the satellite image in the Detail Dialog.

#### ***Projected solid angle (inverse square law)***

A point source target is viewed at a succession of distances to observe inverse square fall off of irradiance. The reflected illumination and self-radiance of the target remain constant.

1. Compile EOIR and rebuild with
  - a. `TRACK_IRRAD` defined & `IRRAD_OBJECT = Satellite #2`  
This calculates the inband irradiance at aperture corresponding to Satellite #2
  - b. Note that `sgltnDetailed = true` // default in the code for satellites
  - c. `SetDebugOutput(true);`
2. Run EOIR.
3. Load `V_Phase2.sc` – a sensor on a geosynchronous satellite #1 observes geosynchronous satellite #2 at a succession of distances. Satellite #2 changes its argument of the ascending node to set various inter-satellite distances.
4. Satellite #2 should be fully illuminated.
5. Satellite #2's Gray Body Reflectance should be set to 100%.
6. Select the sensor band with the wider FOV such that Satellite #2 appears as a point source.
7. The calculated values are written to a test file, each time the image is updated
8. Input a succession of RAAN values for Satellite #2 (argument of the ascending node).
9. Exit EOIR and Plot the distance vs. irradiance values. Note the inverse square relationship

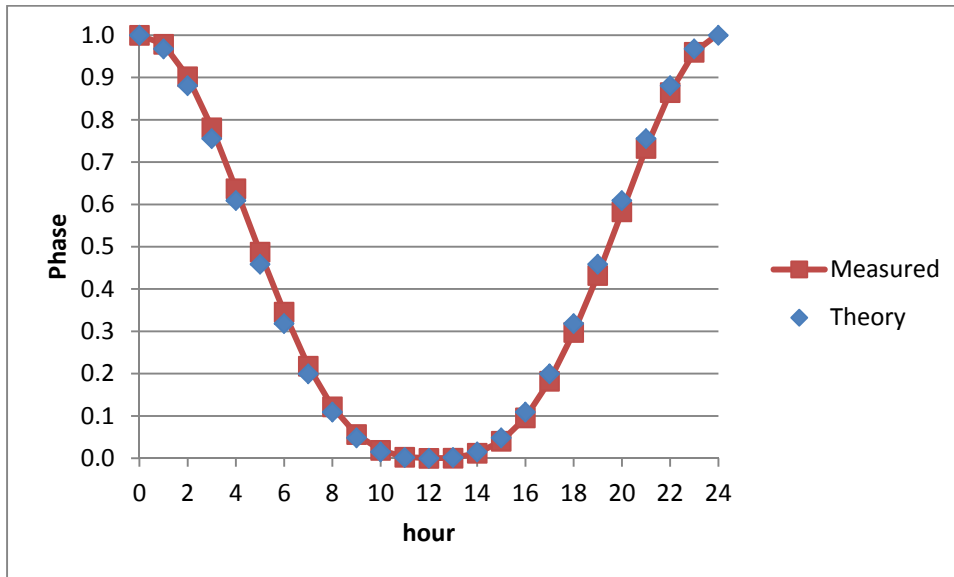


### ***Phase Law***

The phase law for illumination of a Lambertian sphere is demonstrated

1. Run EOIR.
2. Load `V_Phase3.sc` – a sensor on a geosynchronous Satellite #1 observes geosynchronous Satellite #2 over 24 hours at 1 hour intervals. Satellite #2 changes its phase angle with respect to the sun thru 360° in this time.
3. Step time by 1 hour and click on Satellite #2's point image, recording the in band W/cm<sup>2</sup> value versus time.

- a. During the darker phases, turn off AGC and increase brightness until Satellite #2 can be seen



## 6.2.5 SRF

### 6.2.5.1 Detailed vs Simple

This validation shows the code systems for calculating irradiances from area sources and from both the simple and detailed point source calculations all produce consistent results (see 4.1.6.1). The geometry between observer and observed remains the same across the three cases. Sensor image magnification is changed to switch between point and area source images.

A compile switch is set to force the simple calculation for satellites, instead of the default detailed point source calculation. This option is not available in the production version of EOIR.

#### 1. Compile EOIR and rebuild with

- a. `TRACK_IRRAD` defined & `IRRAD_OBJECT = Satellite #2`

This calculates the inband irradiance at aperture corresponding to Satellite #2

- b. `sgltnDetailed = false` // for satellites

- c. `SetDebugOutput(true);`

#### 2. Run EOIR

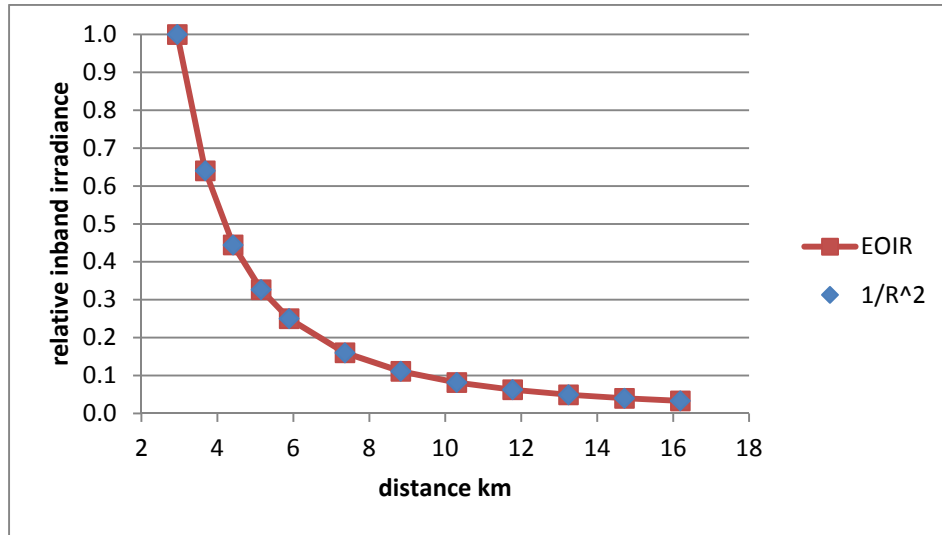
3. Load `V_Phase2.sc` – a sensor on a geosynchronous satellite #1 observes geosynchronous satellite #2 at a succession of distances. Satellite #2 changes its argument of the ascending node to set various inter-satellite distances

4. Satellite #2 should be fully illuminated

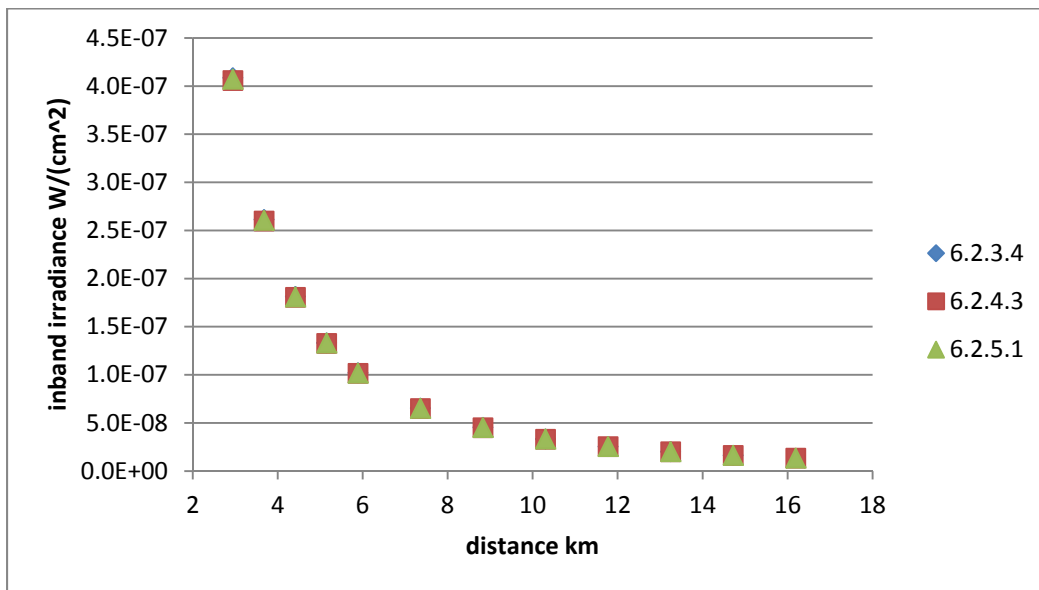
5. Satellite #2's Gray Body Reflectance should be set to 100%.

6. Select the sensor band with the wider FOV such that Satellite #2 appears as a point source

7. Click on the point source image of satellite #2 in the display.
8. From the Detail Dialog record the distance and peak inband irradiance of satellite #2.
9. Repeat the above 2 steps for a succession of RAAN values for Satellite #2 (argument of the ascending node).
10. Plot the distance vs. irradiances together with the area source irradiance and the simple point source irradiance experiments above.



The following plot compares the result, directly in irradiance, of the 3 different methods used in 6.2.3.4, 6.2.4.3, and 6.2.5.1



### 6.2.5.2 Benchmark Tests

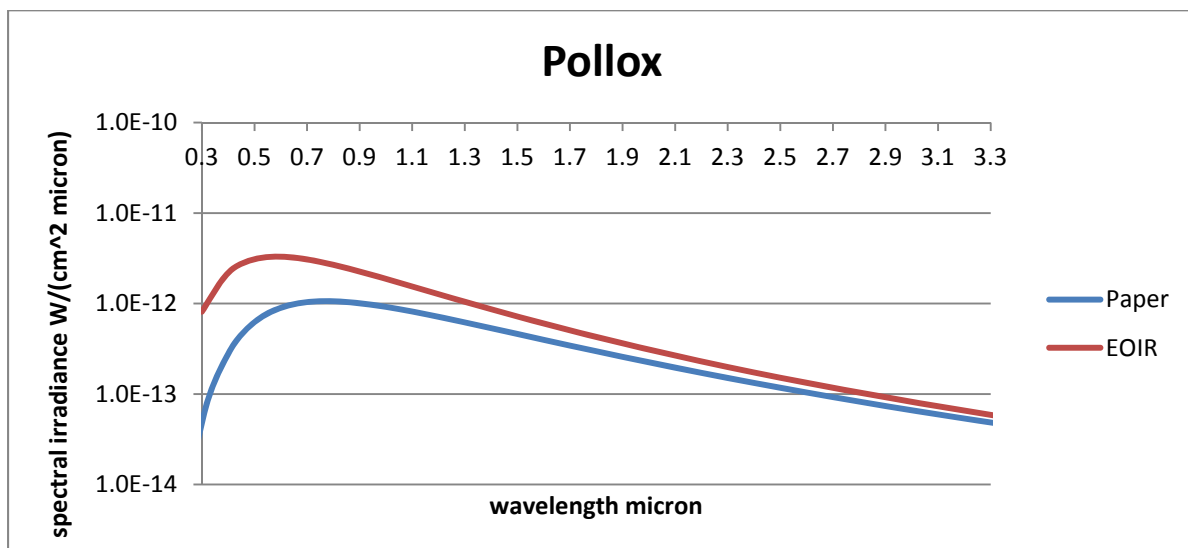
This test compares EOIR's representation of the star Pollux to a model published in Applied Optics.

1. Run EOIR.



2. Load V\_Star.scd – a sensor on a geosynchronous satellite is targeted inertially at a star.
3. A bright star, which is Pollux (Catalog 37,826), is centered at RA 07h 45m 19.4s Dec +28° 01' 35".
4. Set the Sensor's bandpass to 0.3 to 5.3 microns, with 50 intervals.
5. On the Details Dialog, check the "For Each Pixel Pick" box.
6. Click the Apply button, so the check takes effect.
7. Note the peak spectral irradiance, 3.294-12 at 0.6  $\mu\text{m}$  and compare to Pollux plot for Fig 1 (b) in "Spectral Irradiance from Stars and Planets, above the Atmosphere, from 0.1 to 100.0 Microns", Applied Optics, Vol 1., No. 4, July 1962.

The stellar temperature in the referenced paper (3750 K) differs from that used by EOIR (4,937.9 K), as provided by the STK Hipparcos star catalog. The visual magnitude of Pollux is listed as 1.21 in the paper, whereas a more recent value would be 1.15 (brighter). The more modern data makes the star's representation in EOIR both brighter and bluer.

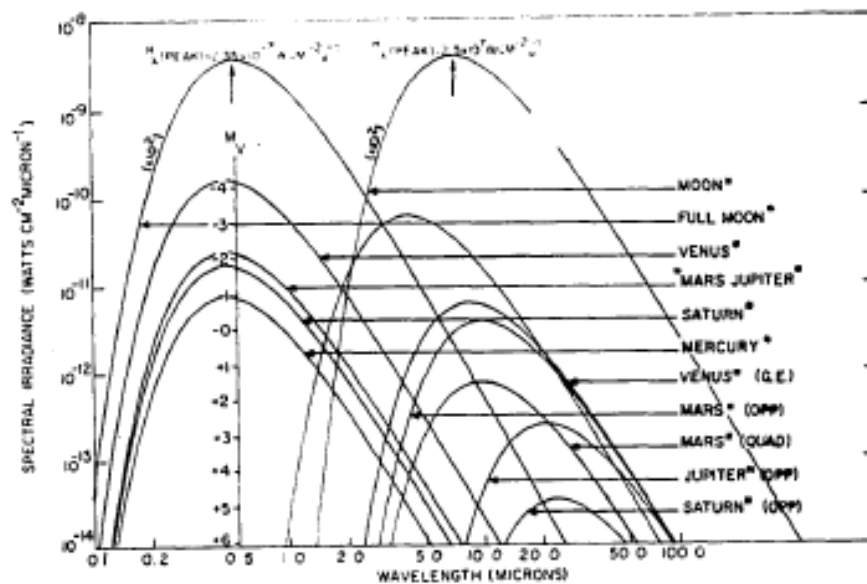
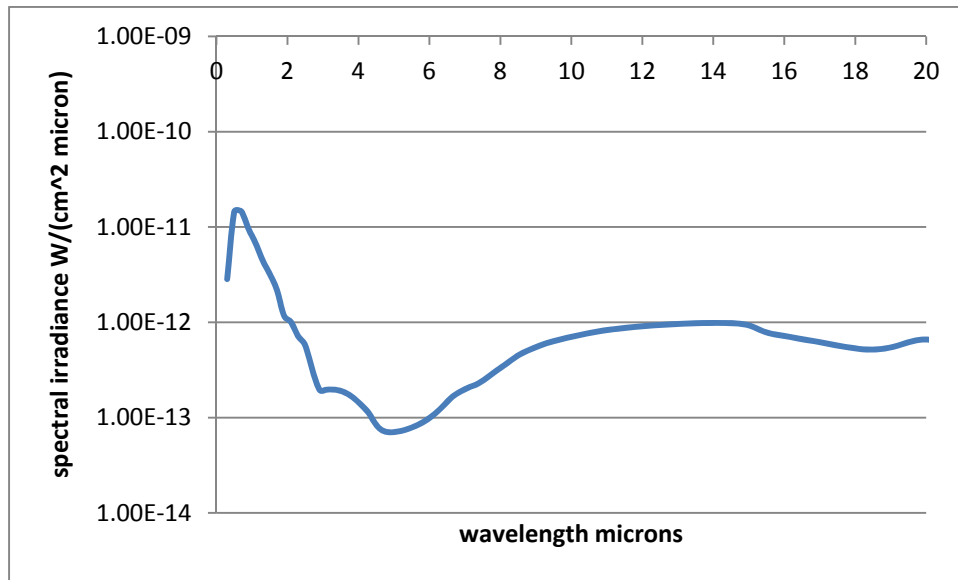


### 6.2.5.3 Planet as Point Source

This test compares EOIR's representation of Mars to a model published in Applied Optics.

1. Run EOIR
2. Load V\_Mars2.sc – a sensor on a geosynchronous satellite is targeted on Mars, at 27 November 1990, a date at which Mars' average opposition distance from Earth obtains.
3. Click on the target, Mars.
4. The EOIR reflected light peak is further in the red than the paper since EOIR uses *spectral* reflectance, while the paper uses a spectrally flat albedo.
5. On the Details Dialog, check the "For Each Pixel Pick" box.
6. Click the Apply button, so the check takes effect.
7. Click on the target, Mars.

8. Plot the resulting click file.
9. Note the peak spectral irradiance due to solar reflection,  $1.698 \times 10^{-11}$  at  $0.6 \mu\text{m}$  and compare to Mars plot for Fig 1 (b) in "Spectral Irradiance from Stars and Planets, above the Atmosphere, from 0.1 to 100.0 Microns", Applied Optics, Vol 1., No. 4, July 1962.
10. Note the peak spectral irradiance due to self-radiance,  $9.85 \times 10^{-13}$  at  $14.1 \mu\text{m}$  and compare to Mars (opposition) plot for Fig 1 (b) in "Spectral Irradiance from Stars and Planets, above the Atmosphere, from 0.1 to 100.0 Microns", Applied Optics, Vol 1., No. 4, July 1962. Also, in EOIR Mars has lower self-radiance, since its average temperature is set to 210 K (<http://nssdc.gsfc.nasa.gov/planetary/factsheet/marsfact.html>) instead of the 285 K used in the reference paper.



---

Figure 1 (b)

In comparing these two plots, note that 1) EOIR shows the sum of reflection and self-radiance rather than plots of 2 separate calculations, and 2) the wavelength scale for EOIR is linear, whereas the report's wavelength scale is logarithmic.

---

#### 6.2.5.4 Atmosphere – MODTRAN 4 comparison

This test requires a developer's debug version of EOIR compiled with the TRACK\_MODTRAN flag set. This option is not available in the production version of EOIR.

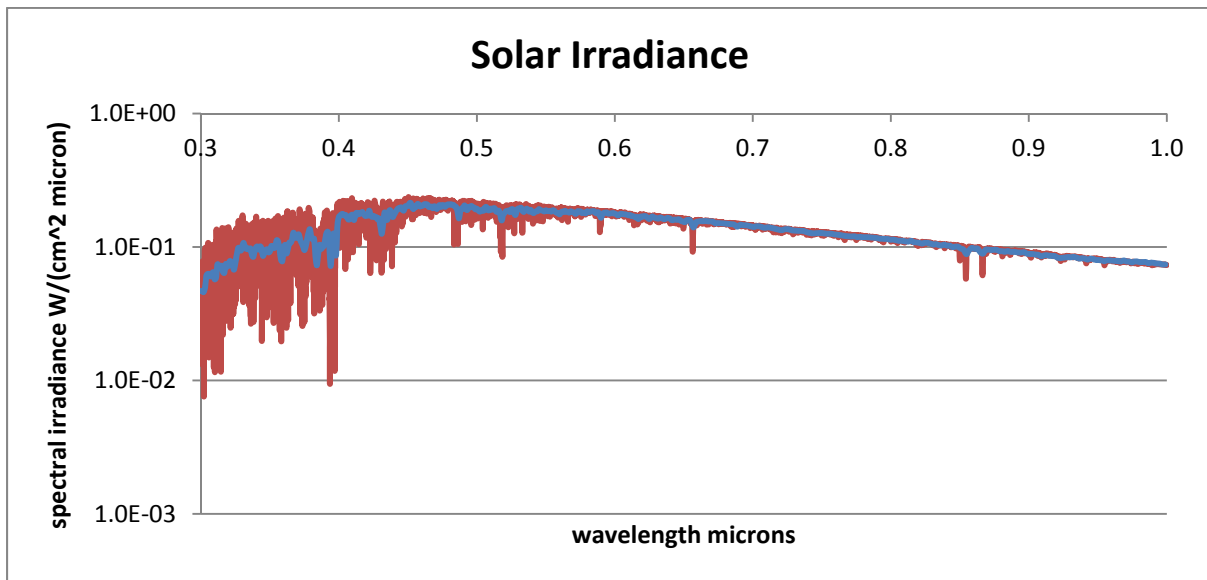
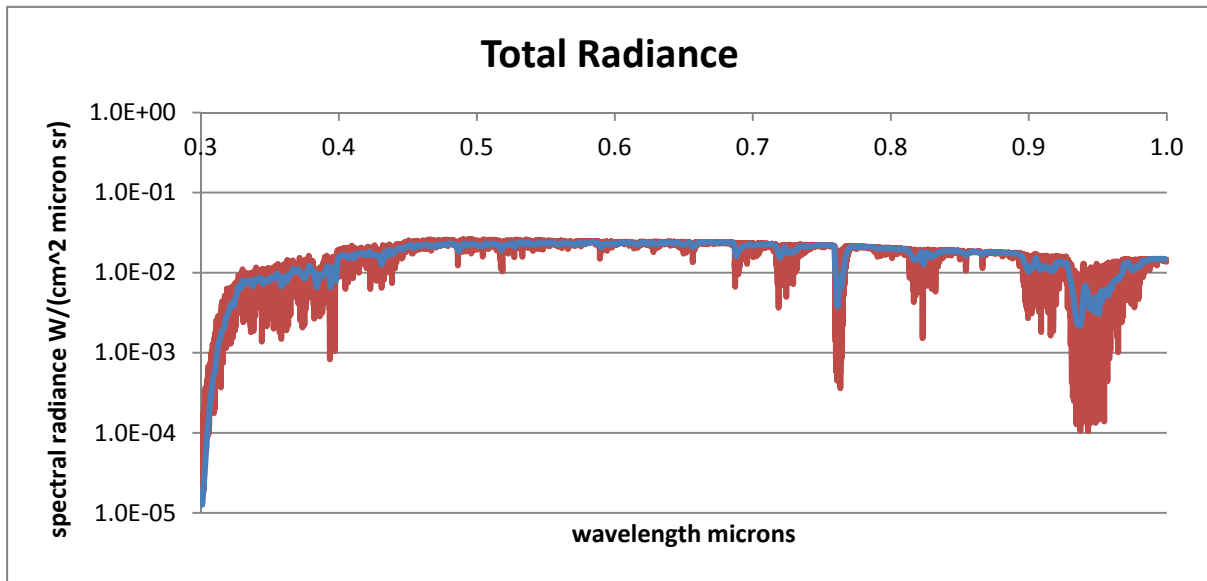
1. Recompile EOIR with the TRACK\_MODTRAN flag set.
2. Run EOIR.
3. Load Atmos\_Test3.scd – a sensor on a LEO satellite looks at a vehicle target at 0° Longitude and 0° latitude from straight overhead. The sun is also straight overhead. The vehicle's surface is a 0.8 reflective graybody.
4. Give several Ticks until the vehicle shows up in Geometric Mode.
5. Select the wavelength band pass and number of spectral intervals:
  - a. 0.3  $\mu\text{m}$  to 1.0  $\mu\text{m}$  with 700 intervals or
  - b. 1.0 m to 4.0 m with 600 intervals or
  - c. 4.0 to 28.0 with 600 intervals.
6. Select Radiometric input mode.
7. After EOIR's calculation is done, click the vehicle.
8. Exit EOIR.
9. Import "EOIR\_debug.txt" into Excel and graph wavelength vs. radiance.

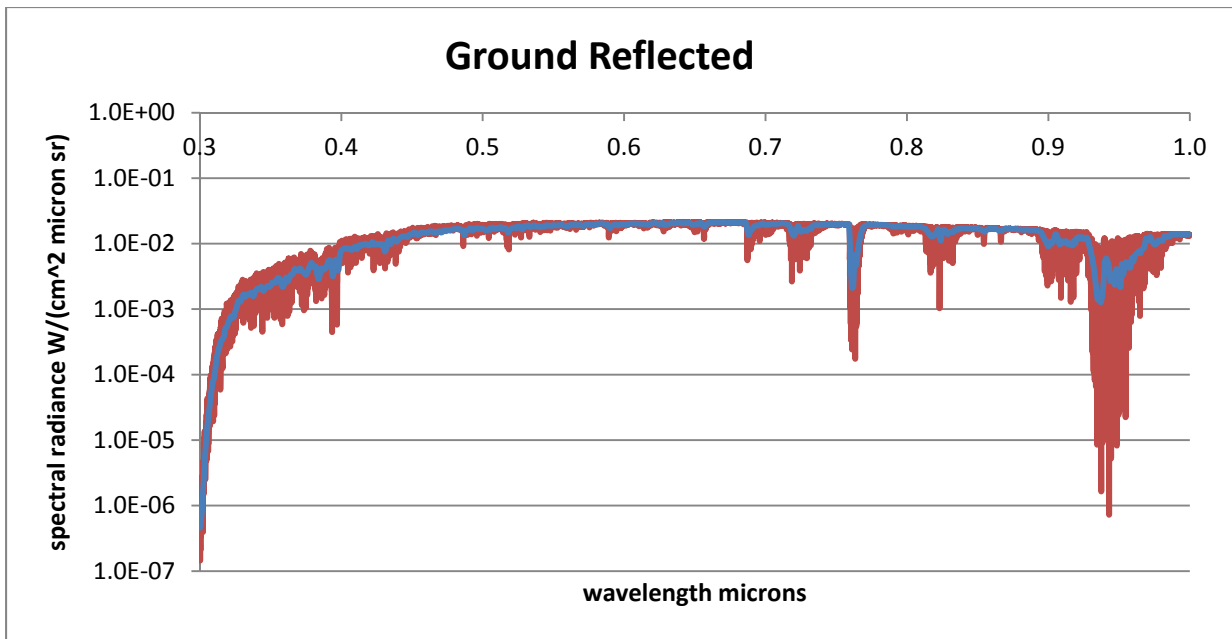
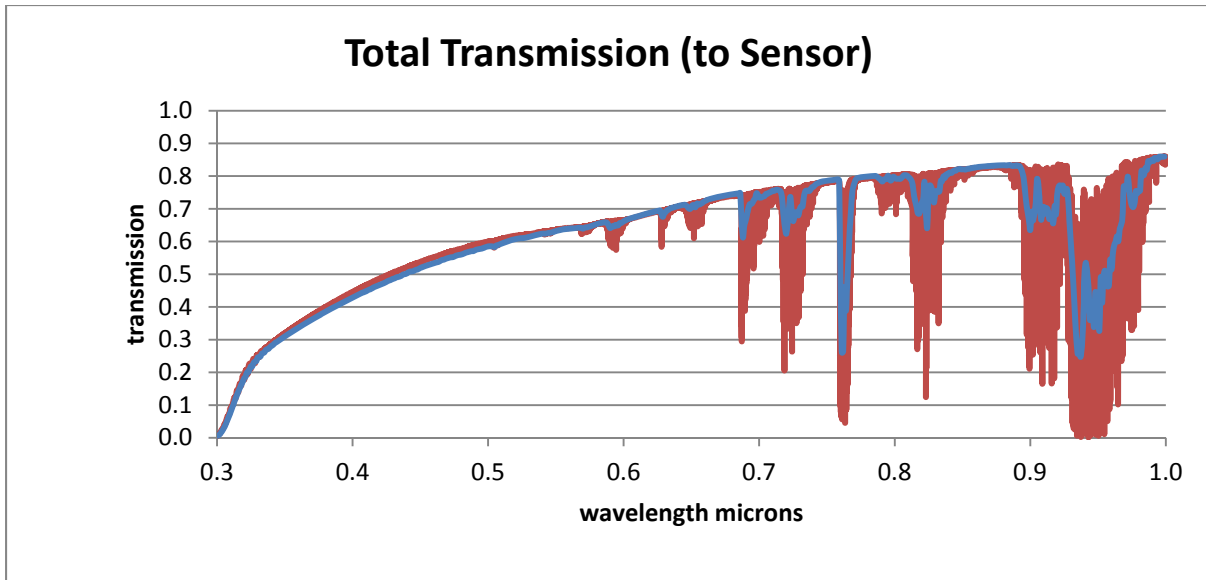
The common test case utilized for the following comparison between EOIR and MODTRAN 4 is as follows:

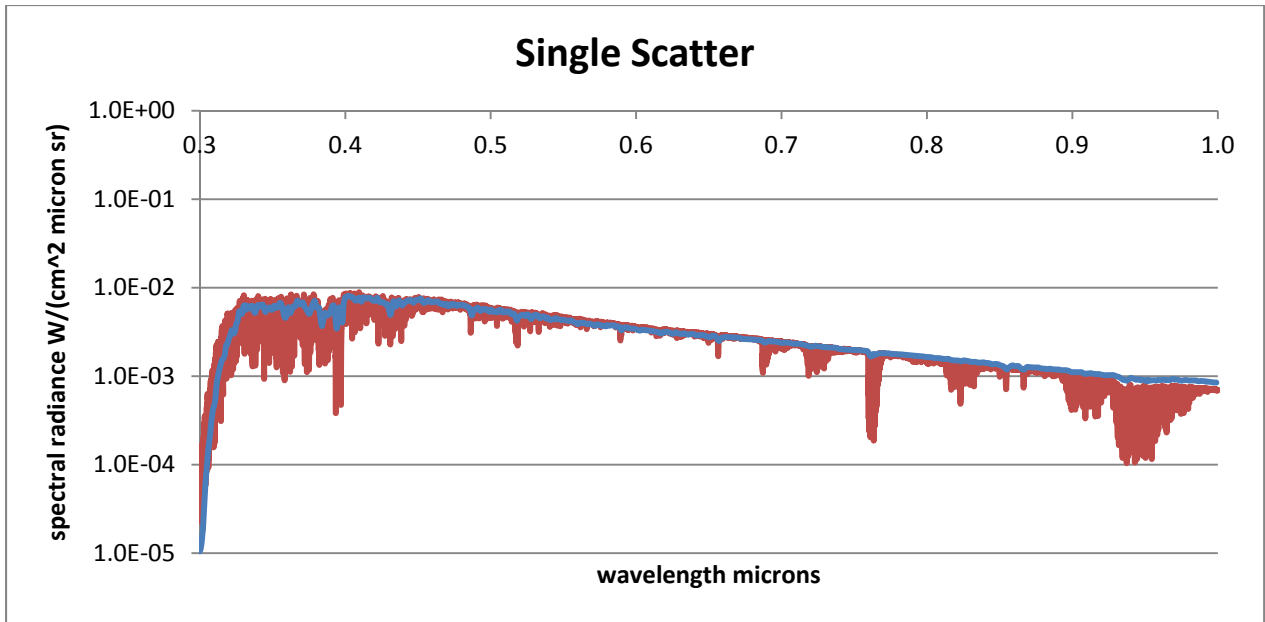
- Space to Earth geometry
- 0° Latitude, 0° Longitude
- Day 93
- US Standard 1976 Atmosphere
- 23 km meteorological visibility
- 46% relative humidity
- Single solar scatter
- 80% reflective Lambertian surface

In the following, the Total Radiance is shown first, then various familiar components that appear in a MODTRAN .tape6 report. MODTRAN4 values appear in red while EOIR values appear in blue.

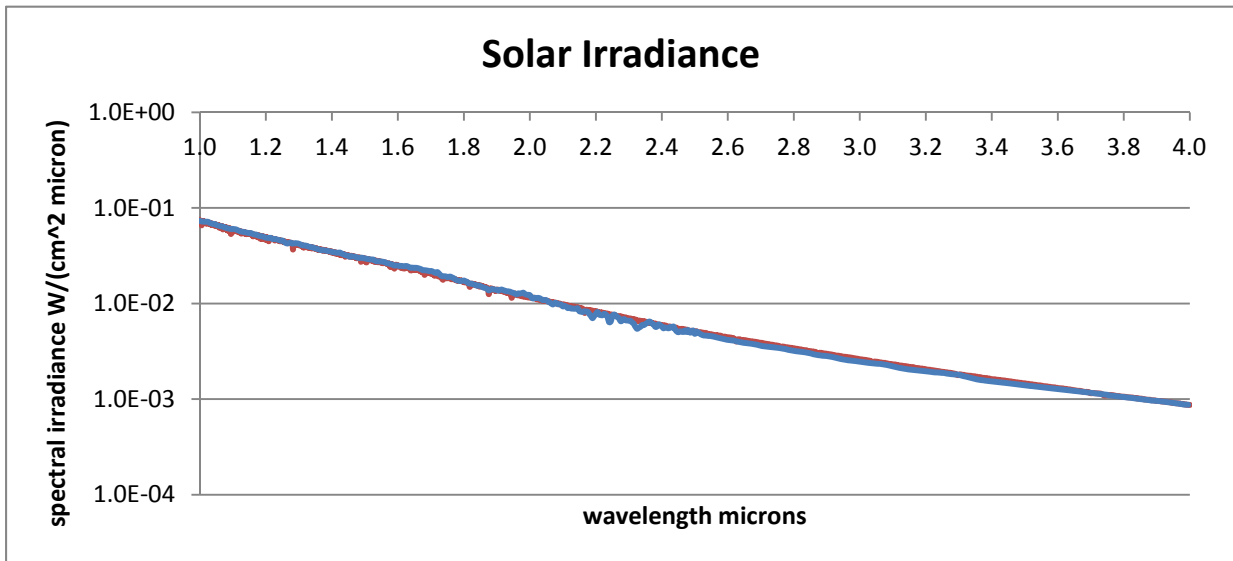
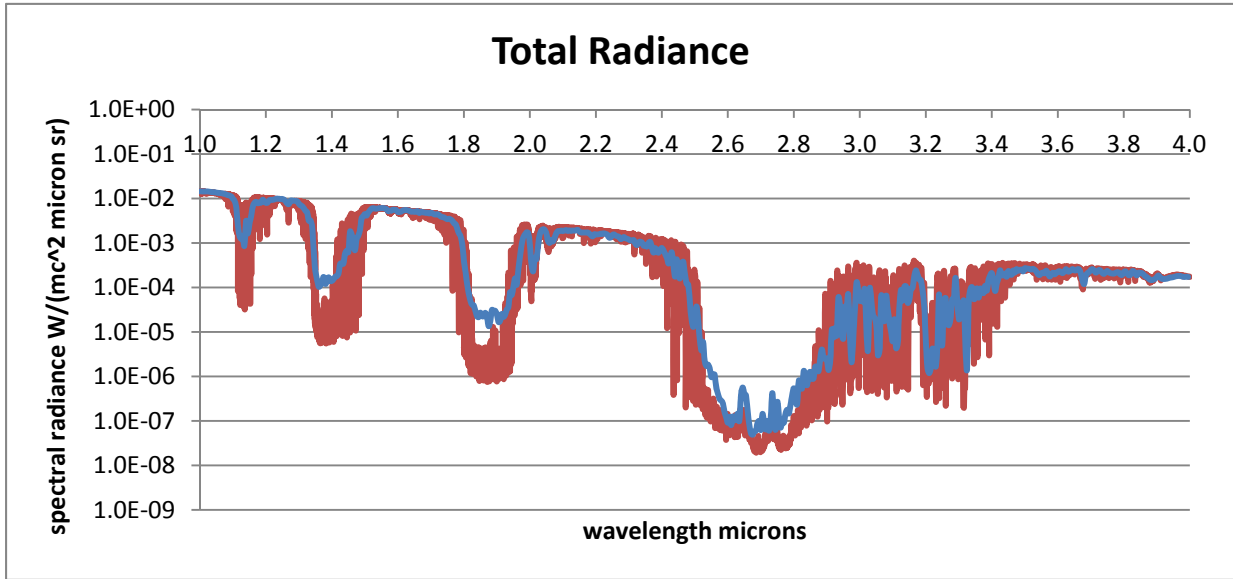
*0.3  $\mu\text{m}$  to 1.0  $\mu\text{m}$  comparison*



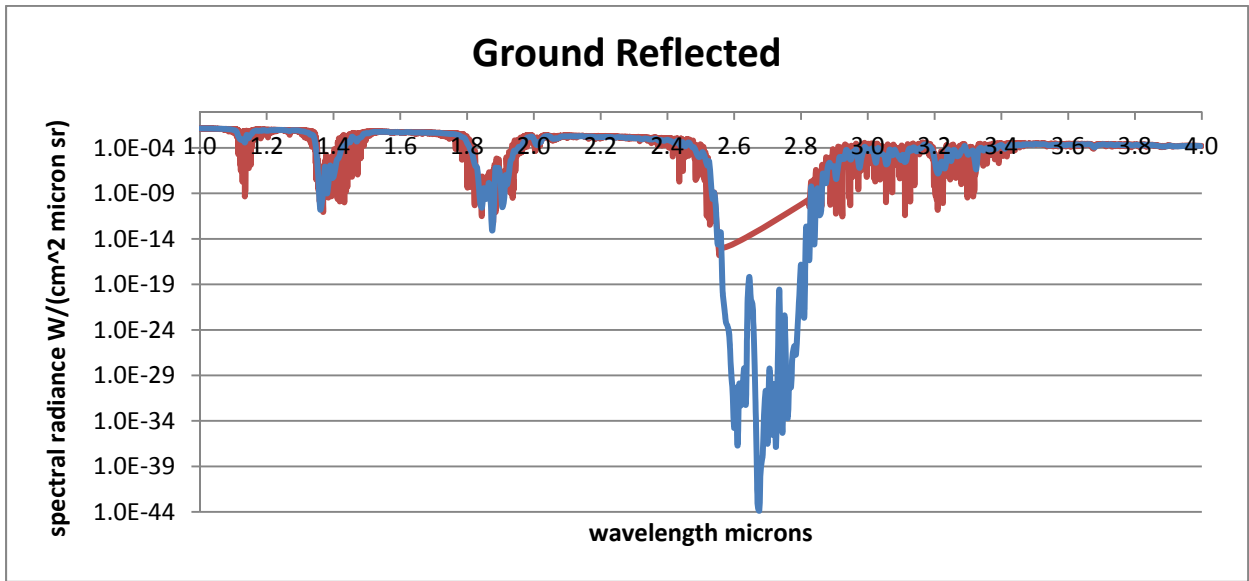
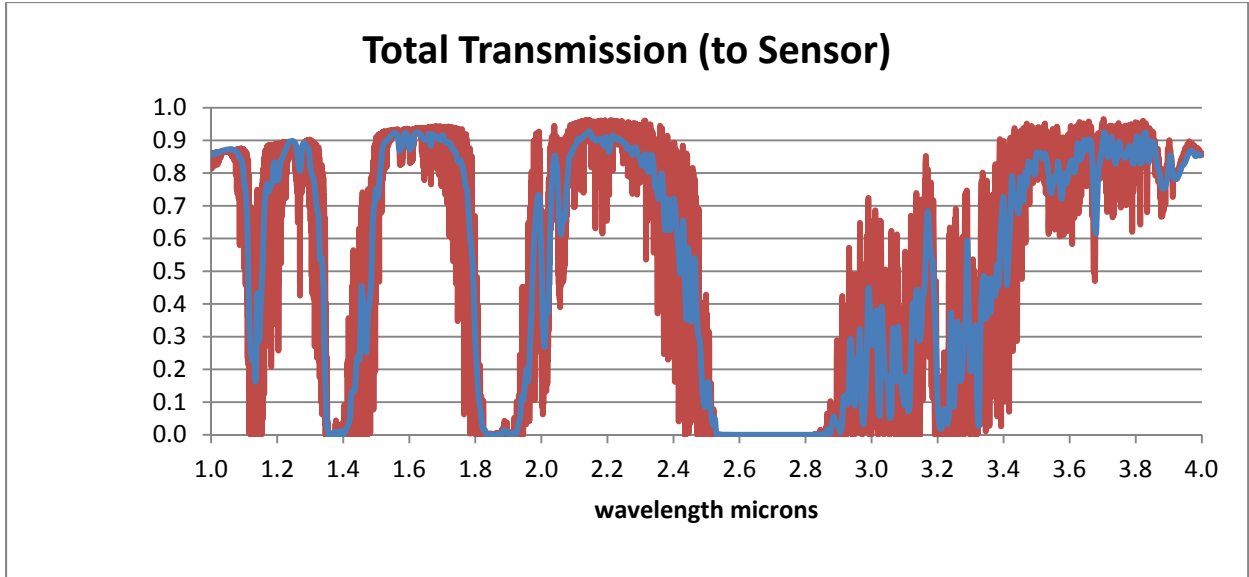


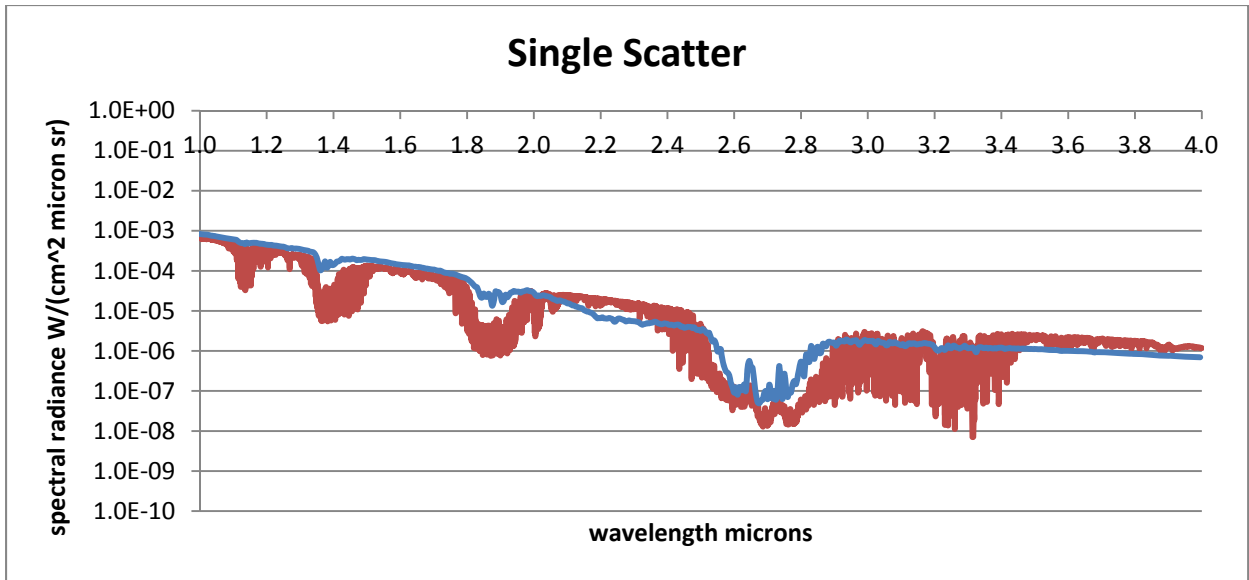


*1.0  $\mu\text{m}$  to 4.0  $\mu\text{m}$  comparison*



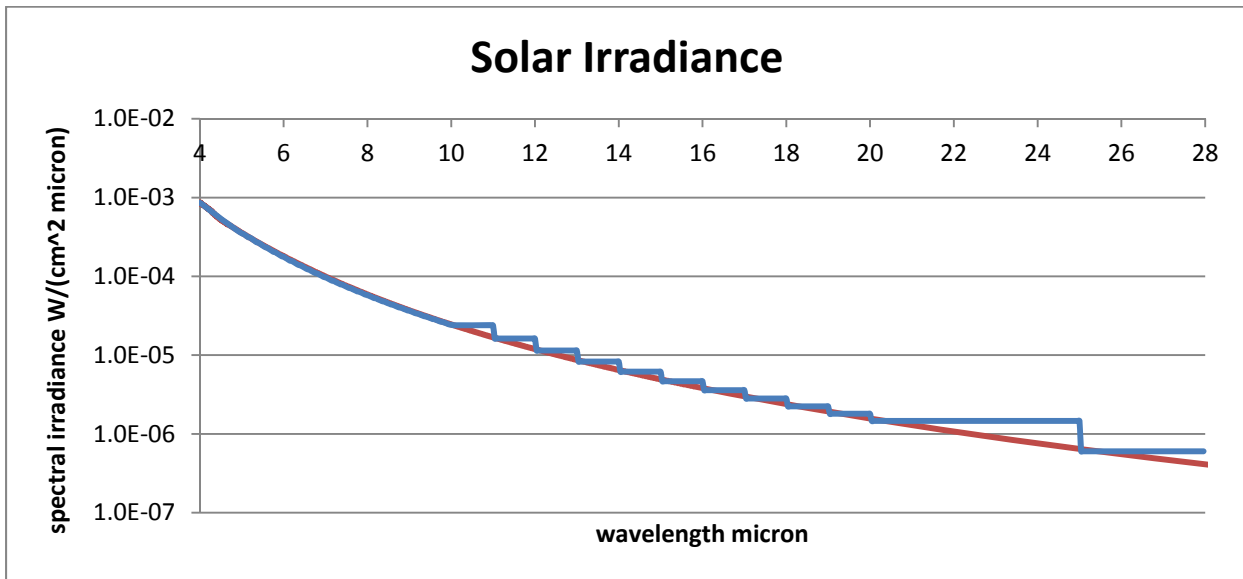
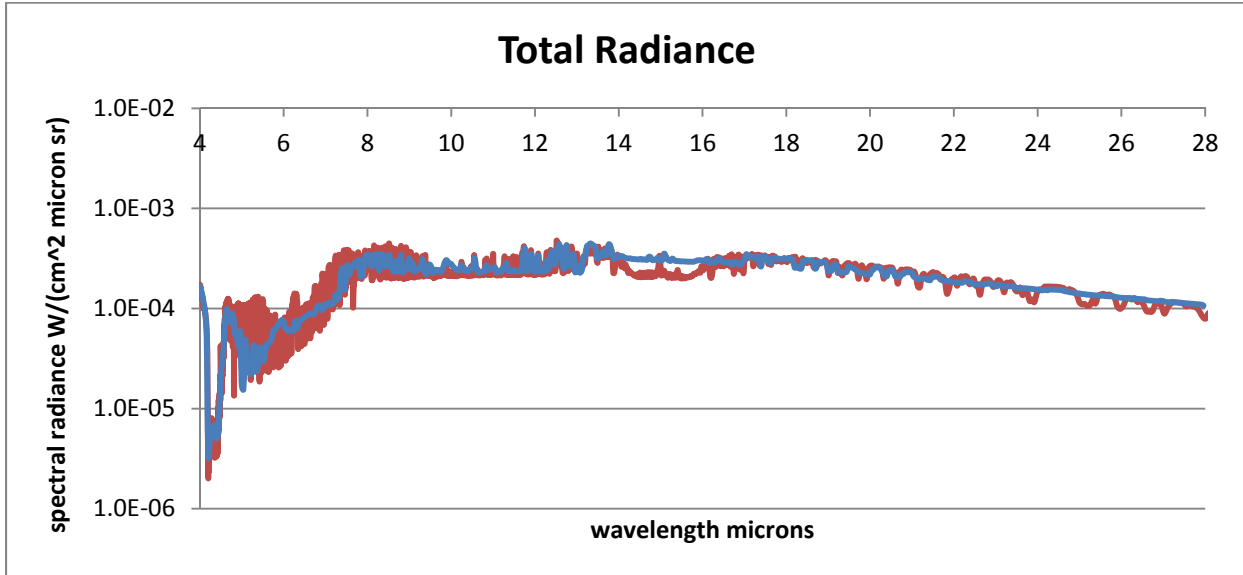


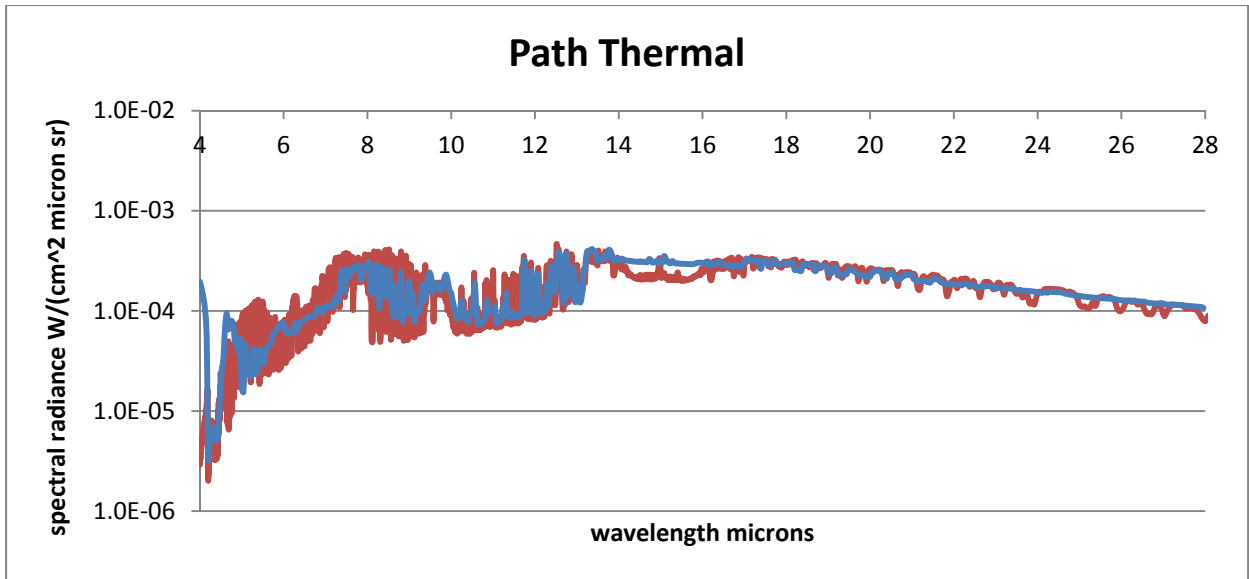
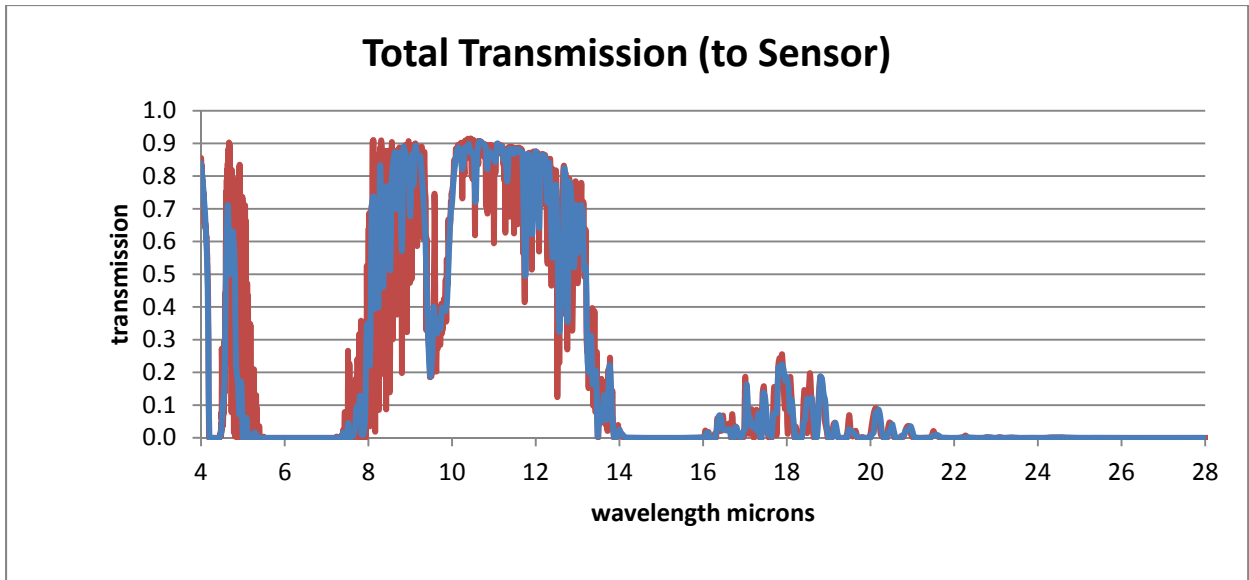


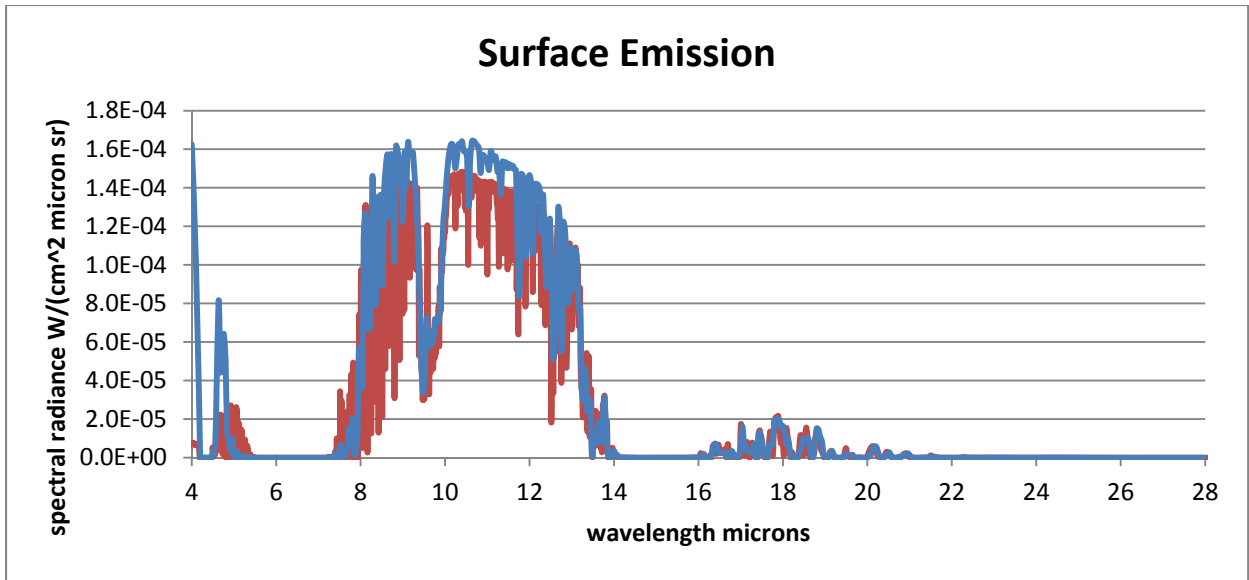


**4.0  $\mu\text{m}$  to 28.0  $\mu\text{m}$  comparison**

[This spectral region needs additional work]

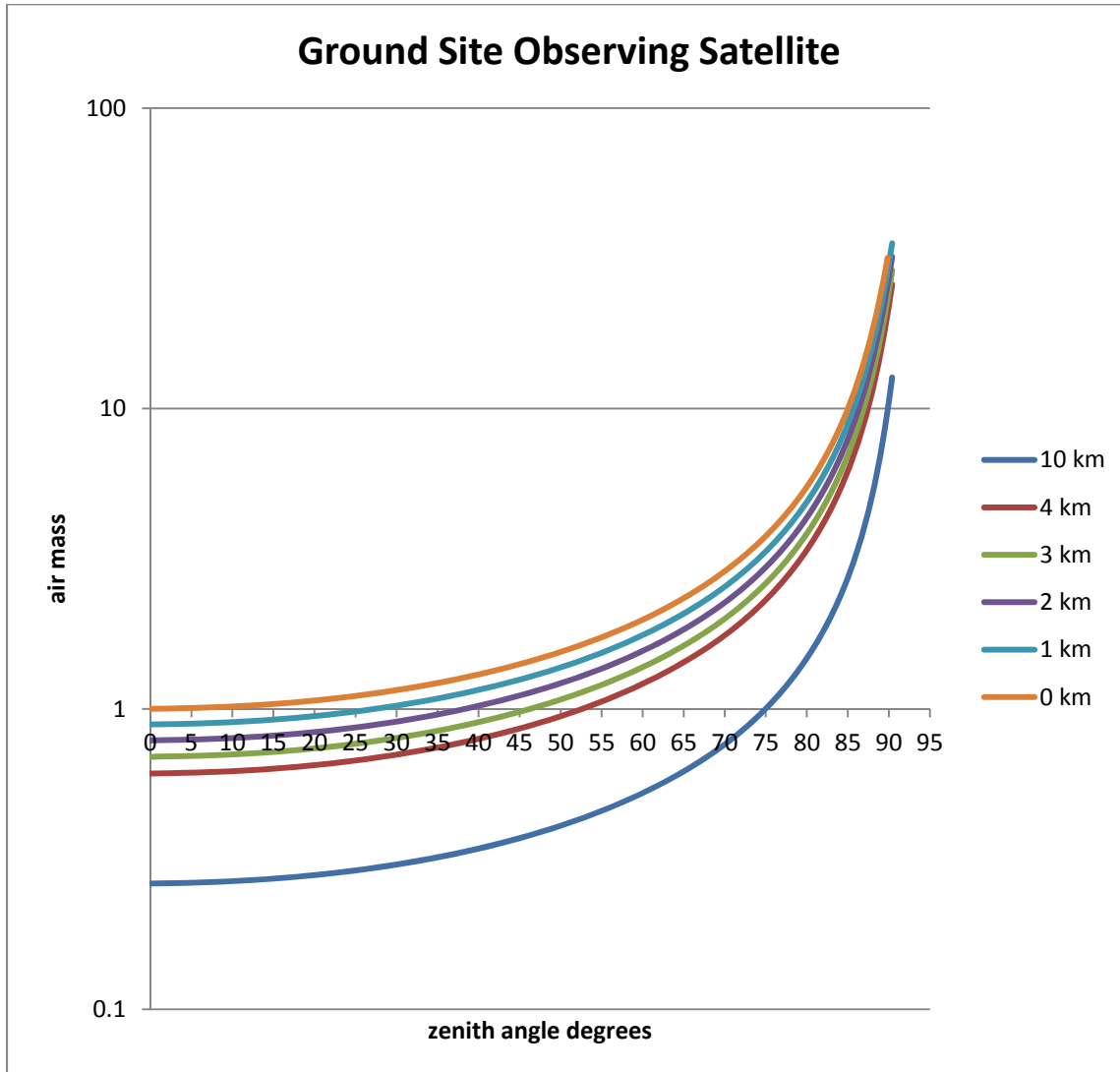




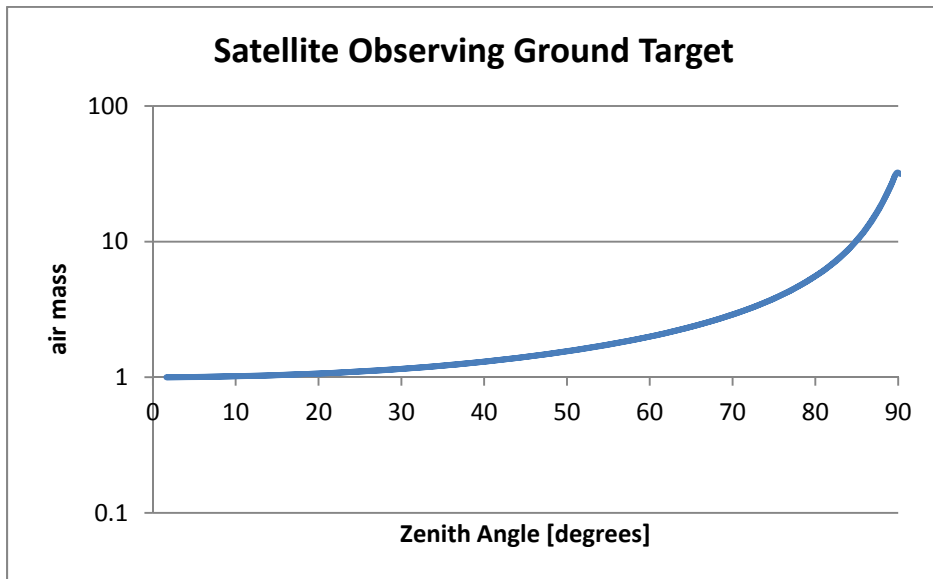
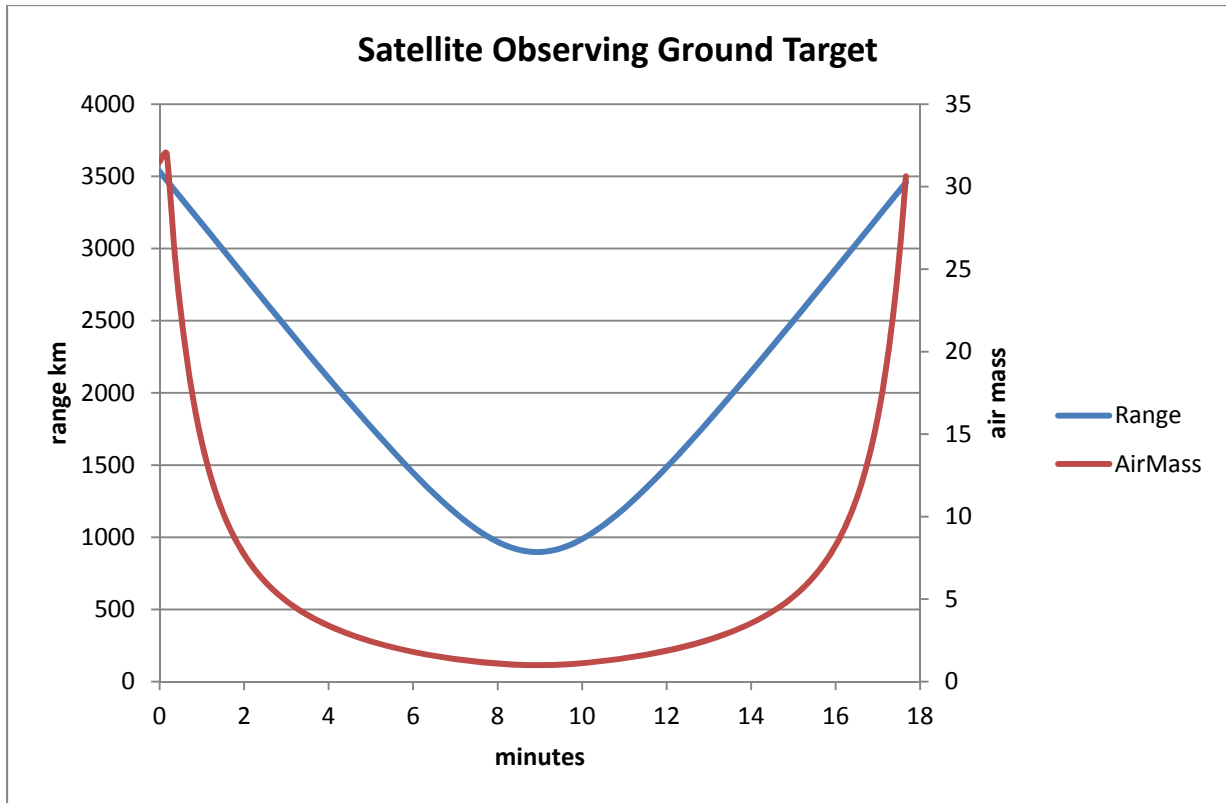


Calculating the Air Mass being looked through from sensor to target is the first major step of the atmosphere model. Looking straight up from the Earth's surface to space [zenith angle = 0], a sensor looks through 1 Air Mass. The Air Mass variable is currently accessible to debug versions of EOIR.

The following chart is the modeled result of looking from an EOIR sensor to a satellite flying overhead. The ground sensor is placed at a succession of altitudes from 0 km to 10 km. Local Zenith (LZA) 0° is looking straight up. LZA 90° is looking at the horizon. At altitude, the horizon recedes to greater distance, so it's possible to look through a greater amount of atmosphere.



The following charts shows the converse, where a sensor on a satellite is observing a ground target



---

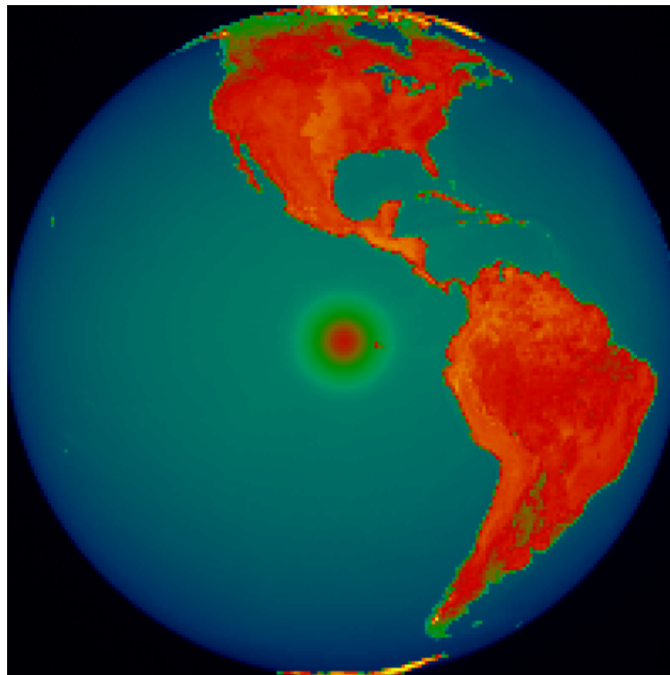
## 7. SENSOR MODEL VALIDATION

The procedures listed below exercise several aspects of the sensor model. In some cases a particular aspect of the model is validated against theoretical behavior, in other cases an aspect of the model is characterized to show to what extent the model matches expected behavior. In the scenarios employed, the sensor parameters are set so as to easily exercise the sensor aspects of interest and may not necessarily represent physically realistic sensors.

### 7.1 ANGULAR EXTENT OF FIELD OF VIEW

This procedure validates that the angular extent of the sensor field of view (FOV) is correct.

1. Run STK EOIR.
2. Open the scenario Valid\_Sens\_FOVextent. This scenario contains a sensor on a geosynchronous satellite viewing the earth in the visible wavelength region (0.4 – 0.7  $\mu\text{m}$ ). The sun is illuminating the earth from directly behind the sensor. The sensor FOV is set to  $17.401^\circ$  in the horizontal direction which is the angular extend of the Earth in the horizontal direction from geosynchronous orbit [ $2*\text{asin}(6378.1 \text{ km}/42164.2 \text{ km})$ ]. The sensor FOV in the vertical direction is set to  $17.342^\circ$  which is the angular extend of the Earth in the vertical direction from geosynchronous orbit [ $2*\text{asin}(6356.8 \text{ km}/42164.2 \text{ km})$ ].
3. Display the EOIR Sensor Scene window.
4. Note that the Earth exactly fills the sensor FOV.



### 7.2 IDEAL FIELD OF VIEW

An ideal sensor field of view (FOV) has a spatial response which is unity within the nominal FOV and zero outside of the nominal FOV. This procedure is used to characterize the extent to



---

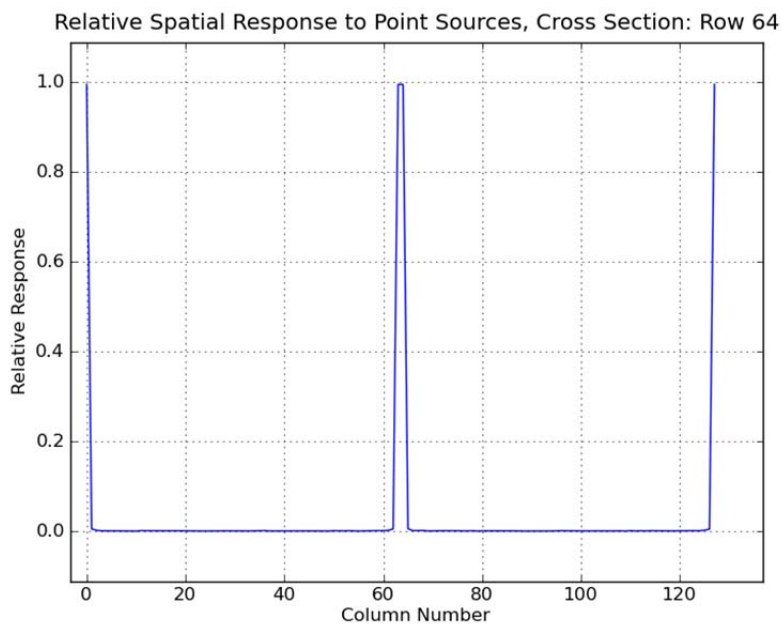
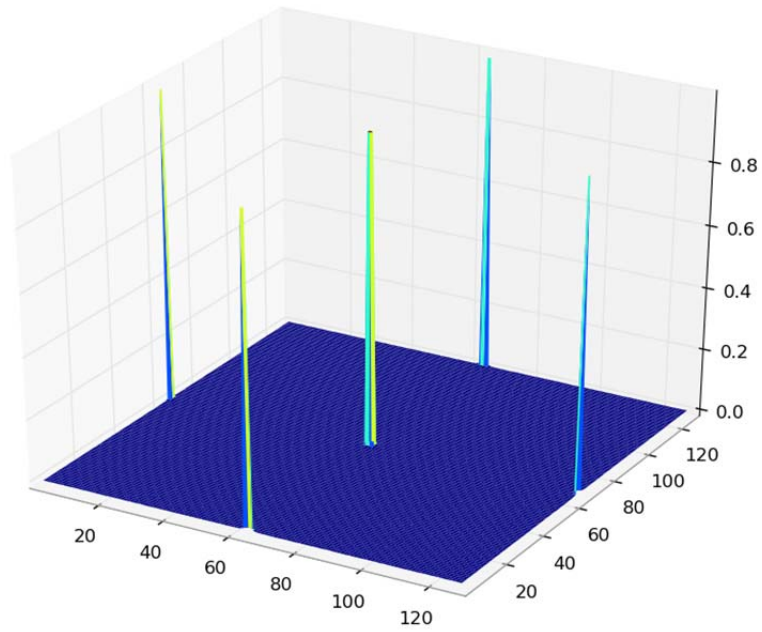
which the STK EOIR spatial response matches that of an ideal FOV for both point and extended area sources.

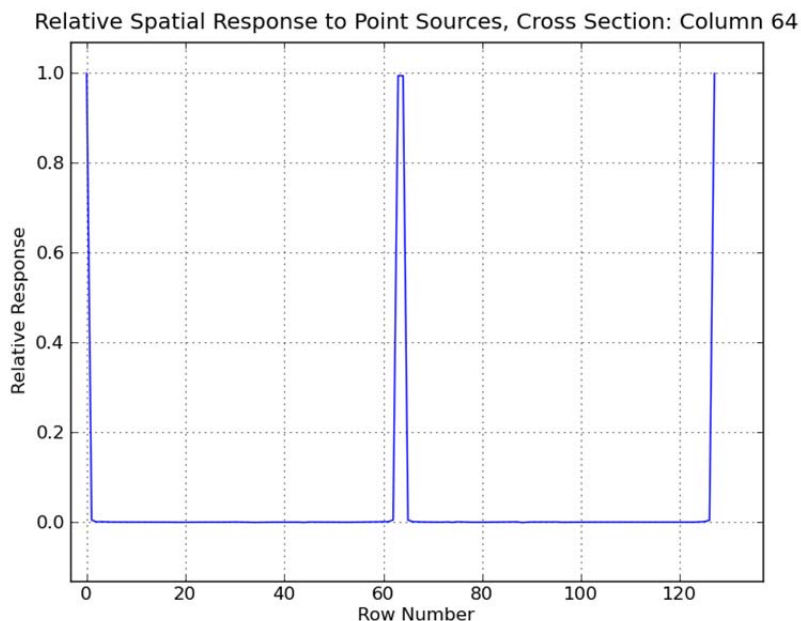
### 7.2.1 Point Source

This procedure validates that the sensor spatial response to point sources is uniform over the nominal sensor FOV and zero outside the nominal sensor FOV.

1. Run STK EOIR.
2. Open the scenario Valid\_Sens\_IdealFOV\_PointSrc. This scenario contains a sensor viewing five separate aircraft. The dimensions of the five aircraft and the viewing geometry are such that the angular extent of each aircraft is small compared with a single sensor pixel. One of the aircraft is located along the sensor line of sight 100 km from the sensor. The other four aircraft are located 5.0 degrees from the sensor line-of-sight in the horizontal and vertical directions and are also 100 km from the sensor. Because the sensor full-angle field of view (FOV) is 10.0 x 10.0 degrees these four aircraft should be exactly at the edges of the FOV. The five aircraft in the sensor's FOV have identical EOIR properties (shape, dimensions, material, reflectance, and temperature).
3. Display the EOIR Sensor Scene window. There should be five objects in the FOV, one in the center and one on each of the four edges.
4. Use the STK Report & Graph Manager to determine the position vector of Sensor1 using the 'Points(Fixed)-Center-x', 'Points(Fixed)-Center-y', and 'Points(Fixed)-Center-z' Data Providers. Record the Sensor1 position vector: (6378.137 km, 0.0 km, 0.0 km). In this coordinate system the  $x$ -axis is along sensor LOS, the  $y$ -axis is along the sensor FOV horizontal direction and the  $z$ -axis is along the sensor FOV vertical direction.
5. Use the STK Report & Graph Manager to determine the Sensor1 line-of-sight (LOS) vector using the 'Vectors(Fixed)-Boresight-x', 'Vectors (Fixed)- Boresight -y', and 'Vectors (Fixed)- Boresight -z' Data Providers. Record the Sensor1 LOS unit vector: (1, 0, 0).
6. Use the STK Report & Graph Manager to determine the position vectors of Aircraft2, Aircraft3, Aircraft4, Aircraft5, and Aircraft6 using the 'Points(Fixed)-Center-x', 'Points(Fixed)-Center-y', and 'Points(Fixed)-Center-z' Data Providers. Record the position vectors: e.g. for Aircraft2 (6477.75646981 km, -8.71557432 km, 0.0 km).
7. Using the reported position vectors and sensor LOS vector calculate the distance from the sensor to each aircraft and the angle between the sensor LOS and each aircraft. Confirm that each aircraft is 100 km from the sensor and that Aircraft2, Aircraft3, Aircraft4, and Aircraft5 are 5.0 degrees from the sensor LOS.
8. Save the sensor image data to a file.
9. Import the sensor image data file into MATLAB or Python.
10. Peak-normalize the sensor image data.
11. Create a surface plot and plots of cross sections through row 64 and column 64 of the sensor image data. These plots demonstrate that the sensor responds uniformly to identical point sources at different locations in the FOV. (Note that the locations of the point sources have been carefully selected such that the alignment of a given point source with respect to a pixel is the same in all five cases, i.e. each of the point source is at the corners of adjacent pixels. If one of the point sources is repositioned such that it is aligned differently with respect to a pixel, for example the pixel center, the sensor response to that point source will be different.)

- 
12. Change the Longitude of Aircraft3 to be slightly larger and observe that Aircraft3 is no longer visible in the sensor FOV. Change the Latitude of Aircraft5 to be slightly larger and observe that Aircraft5 is no longer visible in the sensor FOV.

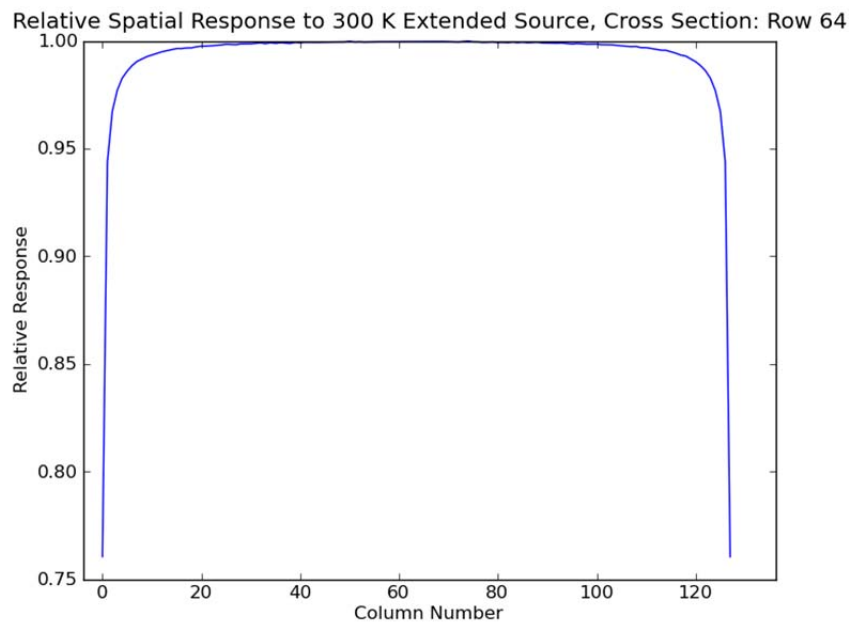
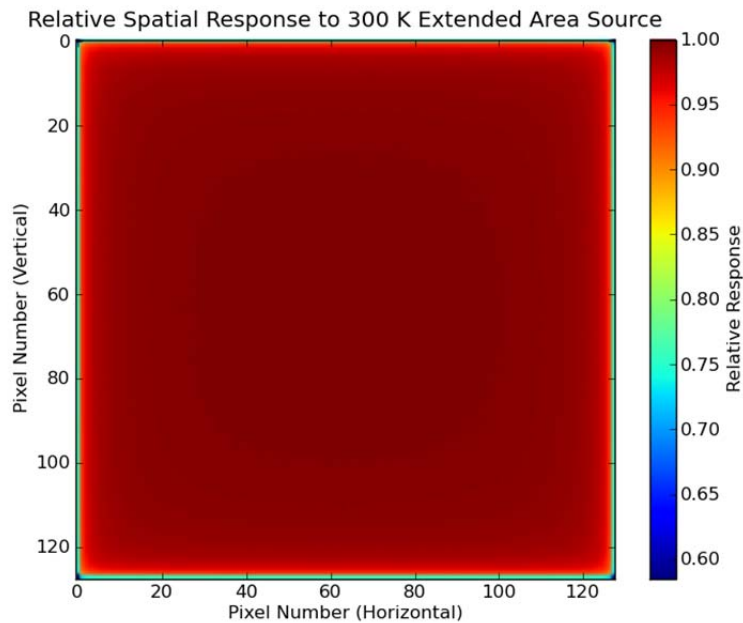




### 7.2.2 Extended Area Source

This procedure characterizes the extent to which the sensor spatial response to extended area sources is ideal.

1. Run STK EOIR.
2. Open the scenario Valid\_Sens\_UniformExtAreaSrc. This scenario contains a sensor viewing a uniform extended source blackbody (Satellite2) in the 8 – 12  $\mu\text{m}$  infrared band. The dimensions of Satellite2 and the viewing geometry are such that the angular extent of Satellite2 is large compared with the sensor’s field of view. The material of Satellite2 is set to Gray Body and the reflectance is set to 0 %.
3. Set the number of intervals on the Spectral tab of the sensor properties page to 50 so that errors in numerical integration over wavelength are minimized.
4. Set the temperature of Satellite2 to 300 K.
5. Display the EOIR Sensor Scene window.
6. Right-click on the image and select the “Details...” context menu. Click on the EOIR Sensor Scene window and confirm using the EOIR Scene Visual Details dialog that the object in the sensor’s field of view is Satellite2 and that its temperature is set appropriately.
7. Save the sensor image data to a file.
8. Import the sensor image data file into MATLAB or Python.
9. Peak-normalize and plot the sensor output image. The spatial response is generally uniform but falls off at the edges and corners due to a processing artifact. The response at the edges is ~75% of the peak response and the response in the corners is ~60% of the peak response. Note that this non-ideal spatial response only applies to extended area sources in the scene, the spatial response to point sources is ideal.



Extended Area Source Outside of Nominal Field of View

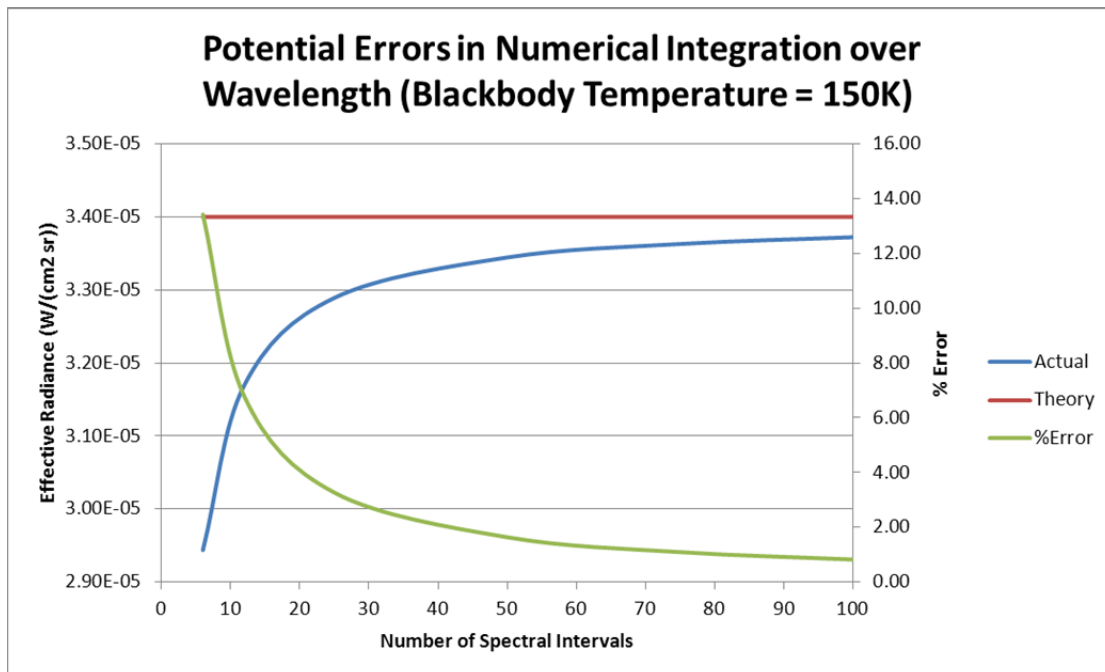
### 7.3 NUMERICAL INTEGRATION OVER WAVELENGTH

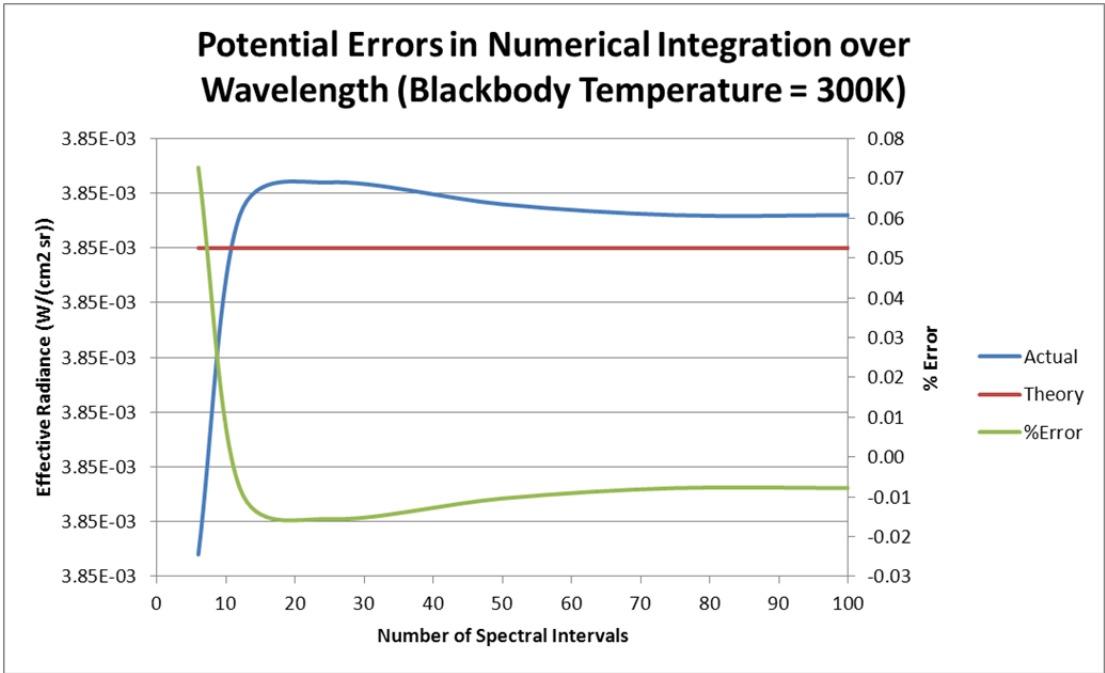
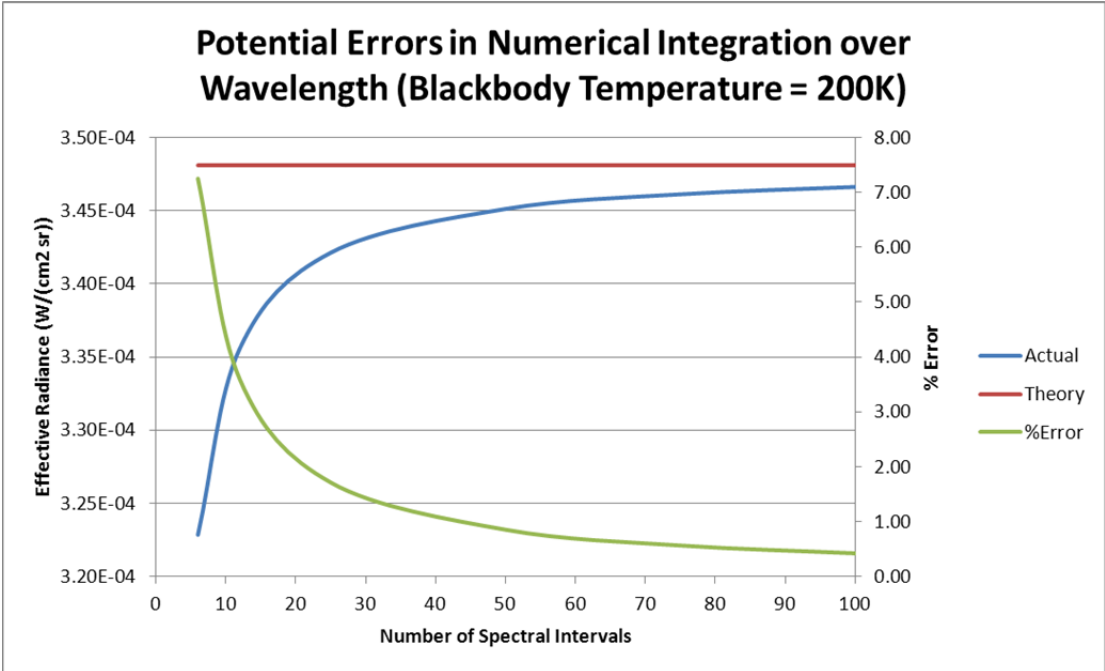
This procedure demonstrates errors in the numerical integration over wavelength when using the model with a small number of spectral intervals, and that the errors can be reduced by using a larger number of spectral intervals.

1. Run STK EOIR.

2. Open the scenario Valid\_Sens\_UniformExtAreaSrc. This scenario contains a sensor viewing a uniform extended source blackbody (Satellite2) in the 8 – 12  $\mu\text{m}$  infrared band. The dimensions of Satellite2 and the viewing geometry are such that the angular extent of Satellite2 is large compared with the sensor's field of view. The material of Satellite2 is set to Gray Body and the reflectance is set to 0 %.
3. Set the temperature of Satellite2 to 150 K.
4. Set the number of spectral intervals on the Sensor Properties Spectral tab to 6.
5. Display the EOIR Sensor Scene window.
6. Right click on the EOIR Sensor View window and invoke the Details... dialog. Click on the Sensor View window and confirm that the temperature of Satellite2 is set appropriately.
7. Click on the image and observe the reported band-integrated radiance shown in the EOIR Scene Visual Details dialog. Record the reported in-band radiance.
8. Repeat steps 4 through 7 using 12, 25, 50, 75, and 100 for the number of spectral intervals.
9. Plot the reported band-integrated radiance vs. the number of spectral intervals. Also compare the reported band-integrated radiances with the true band-integrated radiance (the true band-integrated radiance for the Planck function at 150 K from 8 – 12  $\mu\text{m}$  is  $3.40\text{E-}5 \text{ W}/(\text{cm}^2 \text{ sr})$ ).
10. Repeat steps 3 through 9 for Satellite2 temperatures of 200 K and 300 K.

(NOTE: The errors in numerical integration depend on the spectral bandpass of the sensor as well. If the spectral bandpass of the sensor is changed and this procedure is repeated different results are obtained.)s





**7.4 UNIFORM EXTENDED SOURCE RESPONSE**

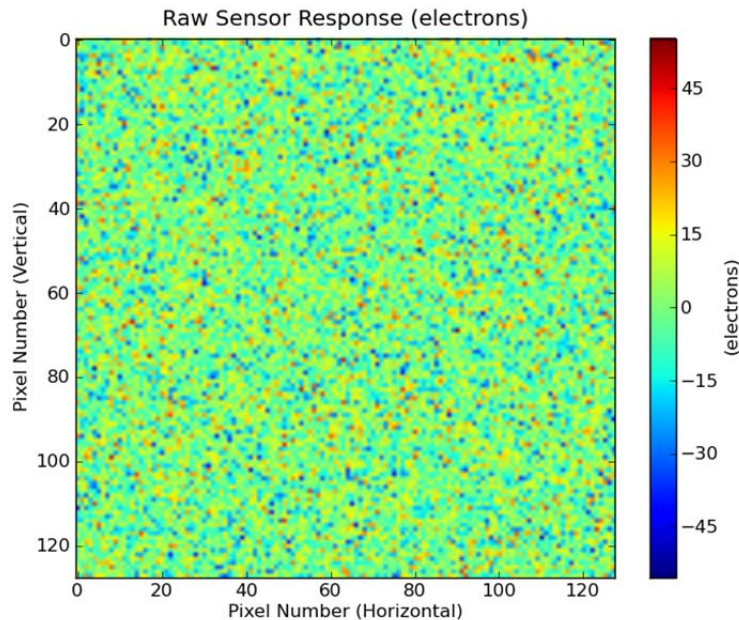
Several aspects of the sensor model are validated using a spatially uniform extended area source which overfills the sensor FOV including: dark offset, peak radiance responsivity, sensor dark noise, scene photon noise, and saturation. These are addressed in the following sections.

---

### 7.4.1 Dark Offset

This procedure validates that the dark offset in the modeled sensor response is zero.

1. Run STK EOIR.
2. Open the scenario Valid\_Sens\_UniformExtAreaSrc. This scenario contains a sensor viewing a uniform extended source blackbody (Satellite2) in the 8 – 12  $\mu\text{m}$  infrared band. The dimensions of Satellite2 and the viewing geometry are such that the angular extent of Satellite2 is large compared with the sensor's field of view. The material of Satellite2 is set to Gray Body and the reflectance is set to 0 %.
3. Set the temperature of Satellite2 to 0.0 K.
4. Display the EOIR Sensor Scene window. Right click on the EOIR Sensor Scene window and invoke the Details... dialog. Click on the Sensor Scene window and confirm that the temperature of Satellite2 is set appropriately.
5. Save the raw sensor image data to a file.
6. Import the sensor image data file into MATLAB or Python.
7. Compute the mean sensor response using the 20 rows and columns in the center of the sensor image data to avoid the edge artifacts discussed in Section 7.2.1.2. The theoretical mean should be zero. The units for the sensor image data are electrons. Confirm that the mean is close to zero thereby demonstrating that for zero radiometric input the mean sensor output is zero.



### 7.4.2 Peak Radiance Responsivity

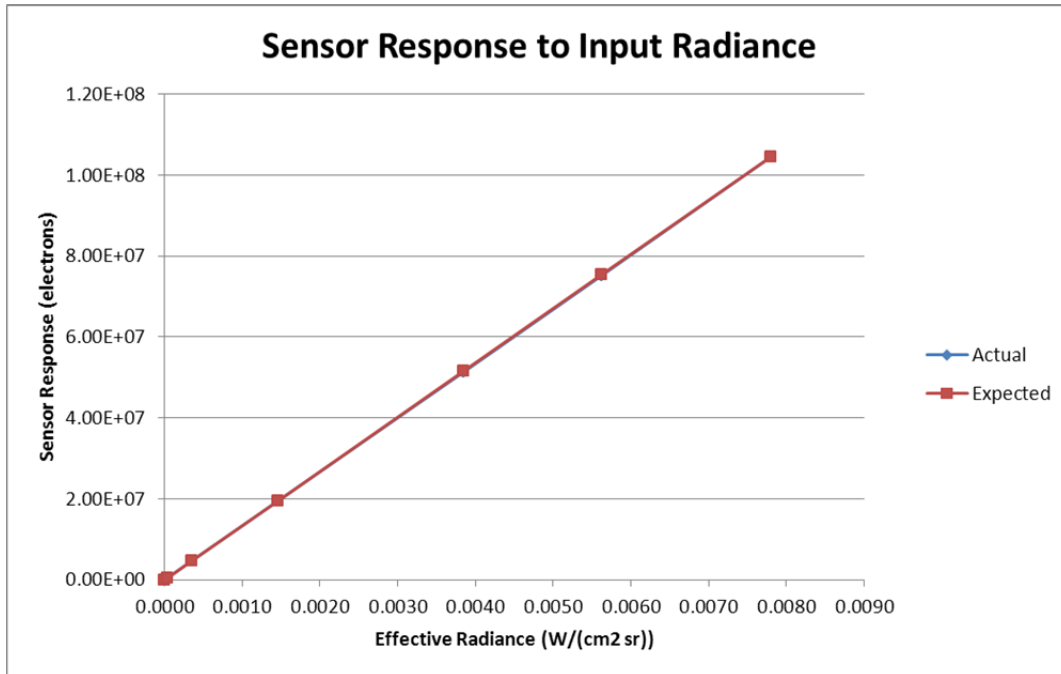
This procedure validates that the sensor peak radiance responsivity computed from simulated sensor output data matches the expected peak radiance responsivity based on user selectable sensor parameters. The peak radiance responsivity is defined as the ratio of the mean sensor output to the effective radiance input to the sensor, and the effective radiance is defined as the

---

spectral radiance input to the sensor weighted by the sensor relative spectral response and integrated over wavelength.

1. Run STK EOIR.
2. Open the scenario Valid\_Sens\_UniformExtAreaSrc. This scenario contains a sensor viewing a uniform extended source blackbody (Satellite2) in the 8 – 12  $\mu\text{m}$  infrared band. The dimensions of Satellite2 and the viewing geometry are such that the angular extent of Satellite2 is large compared with the sensor's field of view. The material of Satellite2 is set to Gray Body and the reflectance is set to 0 %.
3. Set the number of spectral intervals to 50 so that errors in numerical integration over wavelength are minimized.
4. Set the temperature of Satellite2 to 0.0 K.
5. Display the EOIR Sensor Scene window. Right click on the EOIR Sensor Scene window and invoke the Details... dialog. Click on the Sensor Scene window and confirm that the temperature of Satellite2 is set appropriately.
6. Save the raw sensor image data to a file.
7. Import the sensor image data file into MATLAB or Python.
8. Compute the mean sensor response using the 20 rows and columns in the center of the sensor image data to avoid the edge artifacts discussed in Section 7.2.1.2. Record the mean sensor response.
9. Compute the true value of the effective radiance (integral of the input spectral radiance from 8 to 12  $\mu\text{m}$ ). For a blackbody at a temperature of 200 K the effective radiance should be  $3.481\text{E-}4 \text{ W}/(\text{cm}^2 \text{ sr})$ . Record the effective radiance.
10. Repeat steps 4 – 8 for Satellite2 temperatures of 150, 200, 250 300, 325, and 350 K.
11. Plot the mean sensor response vs. effective radiance.
12. Calculate the peak radiance responsivity, which by definition is ratio of the change in sensor output to change in sensor input, i.e. the slope of line in the plot of the mean sensor response vs. the effective radiance.
13. Run a report containing the peak radiance responsivity data provider and confirm that the calculated peak radiance responsivity is approximately equal to the peak radiance responsivity given in the report. For the scenario above the theoretical peak radiance responsivity is  $1.3395\text{E}10 \text{ electrons}/(\text{W}/(\text{cm}^2 \text{ sr}))$  and the peak radiance responsivity calculated from the synthetic sensor output data is  $1.3391\text{E}10 \text{ electrons}/(\text{W}/(\text{cm}^2 \text{ sr}))$ .





### 7.4.3 Sensor Dark Noise

This procedure validates that the simulated sensor dark noise is correct. The dark noise is defined as the sensor noise for zero radiometric input to the sensor.

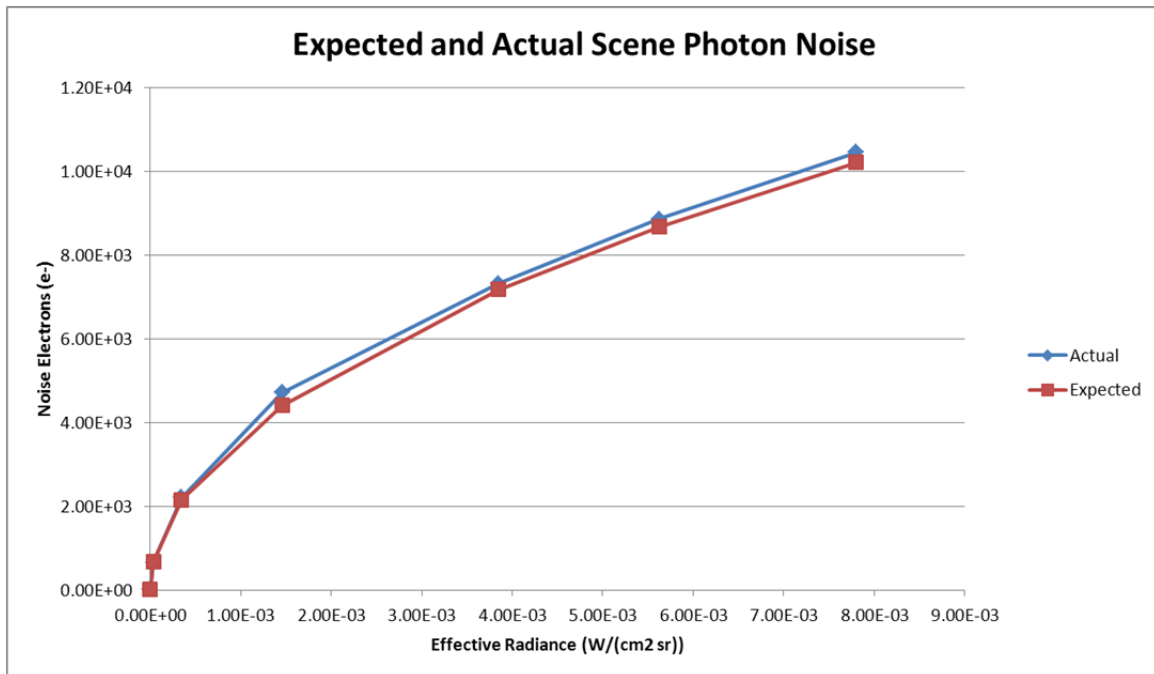
1. Run STK EOIR.
2. Open the scenario Valid\_Sens\_UniformExtAreaSrc. This scenario contains a sensor viewing a uniform extended source blackbody (Satellite2) in the 8 – 12  $\mu\text{m}$  infrared band. The dimensions of Satellite2 and the viewing geometry are such that the angular extent of Satellite2 is large compared with the sensor's field of view. The material of Satellite2 is set to Gray Body and the reflectance is set to 0 %.
3. Set the sensor dark noise equivalent radiance (NER) to  $2\text{E-}8 \text{ W}/(\text{cm}^2 \text{ sr})$ .
4. Set the temperature of Satellite2 to 0.0 K.
5. Display the EOIR Sensor Scene window. Right click on the EOIR Sensor Scene window and invoke the Details... dialog. Click on the Sensor Scene window and confirm that the temperature of Satellite2 is set appropriately.
6. Save the raw sensor image data to a file.
7. Import the sensor image data file into MATLAB or Python.
8. Compute the standard deviation of the sensor response using the 20 rows and columns in the center of the sensor image data to avoid the edge artifacts discussed in Section 7.2.1.2. The standard deviation of the sensor response when viewing a blackbody at 0 K gives the sensor dark noise in electrons.
9. Compute the sensor dark NER by dividing the sensor dark noise in electrons by the peak radiance responsivity. Verify that the sensor dark NER computed from the sensor output data is close to  $2\text{E-}8 \text{ W}/(\text{cm}^2 \text{ sr})$ .

---

#### 7.4.4 Scene Photon Noise

This procedure validates that the simulated scene photon noise is consistent with the assumptions of the model. The raw sensor output files generated for procedure 7.4.2 may be used for this procedure if desired.

1. Run STK EOIR.
2. Open the scenario Valid\_Sens\_UniformExtAreaSrc. This scenario contains a sensor viewing a uniform extended source blackbody (Satellite2) in the 8 – 12  $\mu\text{m}$  infrared band. The dimensions of Satellite2 and the viewing geometry are such that the angular extent of Satellite2 is large compared with the sensor's field of view. The material of Satellite2 is set to Gray Body and the reflectance is set to 0 %.
3. Set the number of spectral intervals to 50 so that errors in numerical integration over wavelength are minimized.
4. Set the temperature of Satellite2 to 0.0 K.
5. Display the EOIR Sensor Scene window. Right click on the EOIR Sensor Scene window and invoke the Details... dialog. Click on the Sensor Scene window and confirm that the temperature of Satellite2 is set appropriately.
6. Save the raw sensor image data to a file.
7. Import the sensor image data file into MATLAB or Python.
8. Compute the standard deviation of the sensor response using the 20 rows and columns in the center of the sensor image data to avoid the edge artifacts discussed in Section 7.2.1.2. Record the standard deviation of the sensor response.
9. Compute the true value of the effective radiance for Satellite2 (the integral of the input spectral radiance from 8 to 12  $\mu\text{m}$ ). For example, a 200 K blackbody should produce an effective radiance of  $3.481\text{E-}4 \text{ W}/(\text{cm}^2 \text{ sr})$ . Record the effective radiance.
10. Using the effective radiance computed in step 9,  $L_{\text{eff}}$ , and the theoretical peak radiance responsivity determined in procedure 7.4.2,  $\mathfrak{R}_{\text{peak},L}$ , calculate the expected mean sensor response as  $r_{\text{exp}} = L_{\text{eff}} \mathfrak{R}_{\text{peak},L}$  and the expected number of photon noise electrons as
$$ne_{\text{ph,exp}} = \sqrt{r_{\text{exp}}} .$$
11. Calculate the expected total number of noise electrons as  $ne_{\text{total}} = \sqrt{ne_{\text{dark}}^2 + ne_{\text{ph,exp}}^2}$  where  $ne_{\text{dark}}$  is the number of dark noise electrons given by  $ne_{\text{dark}} = \text{NER}_{\text{dark}} \mathfrak{R}_{\text{peak},L}$  and  $\text{NER}_{\text{dark}}$  is the sensor noise equivalent radiance. In the Valid\_Sens\_UniformExtAreaSrc scenario  $\text{NER}_{\text{dark}} = 1\text{E-}9 \text{ W}/(\text{cm}^2 \text{ sr})$ .
12. Repeat steps 1 –11 for Satellite2 temperatures of 150, 200, 250 300, 325, and 350 K.
13. Plot the actual and expected noise electrons vs. effective radiance. For higher temperature the photon noise is much larger than the dark noise so the total noise is approximately equal to the photon noise.

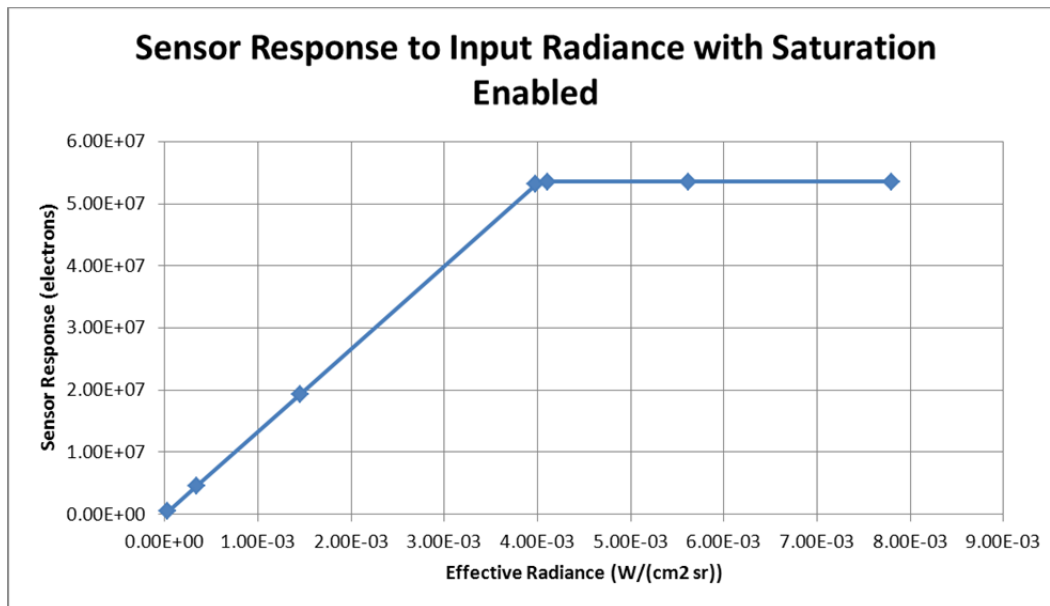


### 7.4.5 Saturation

This procedure validates that sensor saturation is simulated correctly. Saturation is defined in terms of the saturation equivalent radiance or saturation equivalent irradiance.

1. Run STK EOIR.
2. Open the scenario Valid\_Sens\_UniformExtAreaSrc. This scenario contains a sensor viewing a uniform extended source blackbody (Satellite2) in the 8 – 12  $\mu\text{m}$  infrared band. The dimensions of Satellite2 and the viewing geometry are such that the angular extent of Satellite2 is large compared with the sensor's field of view. The material of Satellite2 is set to Gray Body and the reflectance is set to 0 %.
3. Set the number of spectral intervals to 50 so that errors in numerical integration over wavelength are minimized.
4. Set the saturation equivalent radiance to  $4\text{E-}3 \text{ W}/(\text{cm}^2 \text{ sr})$ . Set the switch which enables simulating with sensor saturation.
5. Set the temperature of Satellite2 to 150 K.
6. Display the EOIR Sensor Scene window. Right click on the EOIR Sensor Scene window and invoke the Details... dialog. Click on the Sensor Scene window and confirm that the temperature of Satellite2 is set appropriately.
7. Save the raw sensor image data to a file.
8. Import the sensor image data file into MATLAB or Python.
9. Compute the mean sensor response using the 20 rows and columns in the center of the sensor image data to avoid the edge artifacts discussed in Section 7.2.1.2. Record the mean sensor response.

10. Compute the true value of the effective radiance (integral of the input spectral radiance from 8 to 12  $\mu\text{m}$ ). For a blackbody at a temperature of 200 K the effective radiance should be  $3.481\text{E-}4 \text{ W}/(\text{cm}^2 \text{ sr})$ . Record the effective radiance.
11. Repeat steps 5 – 10 for temperatures of 200, 250 302, 304, 325, and 350 K.
12. Plot the mean sensor response vs. effective radiance. The plot demonstrates that the sensor response saturates when the input effective radiance reaches the saturation equivalent radiance selected by the user ( $4\text{E-}3 \text{ W}/(\text{cm}^2 \text{ sr})$ ).



## 7.5 POINT SOURCE RESPONSE

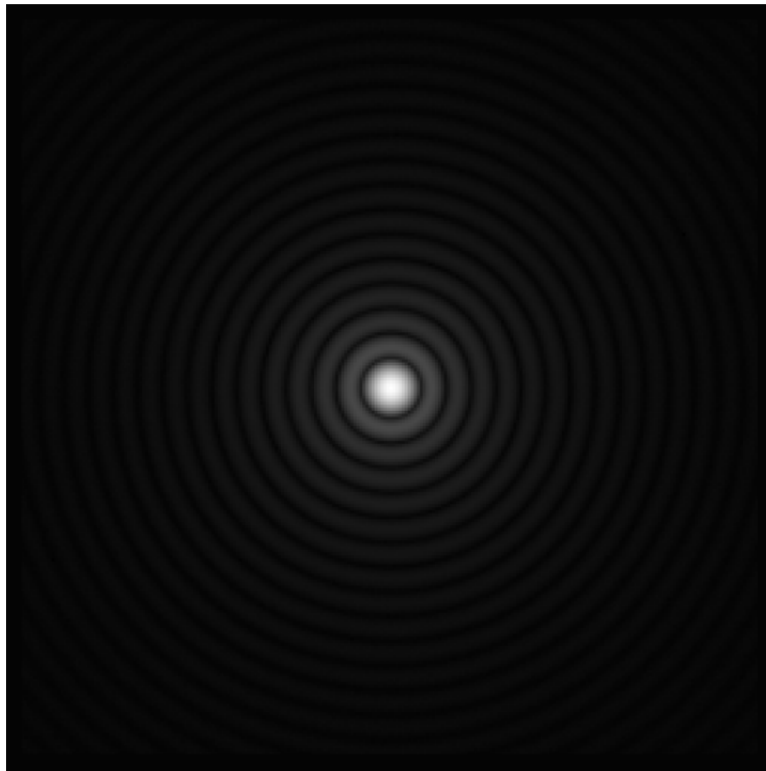
In this section several aspects of the sensor model are validated using sensor point response functions.

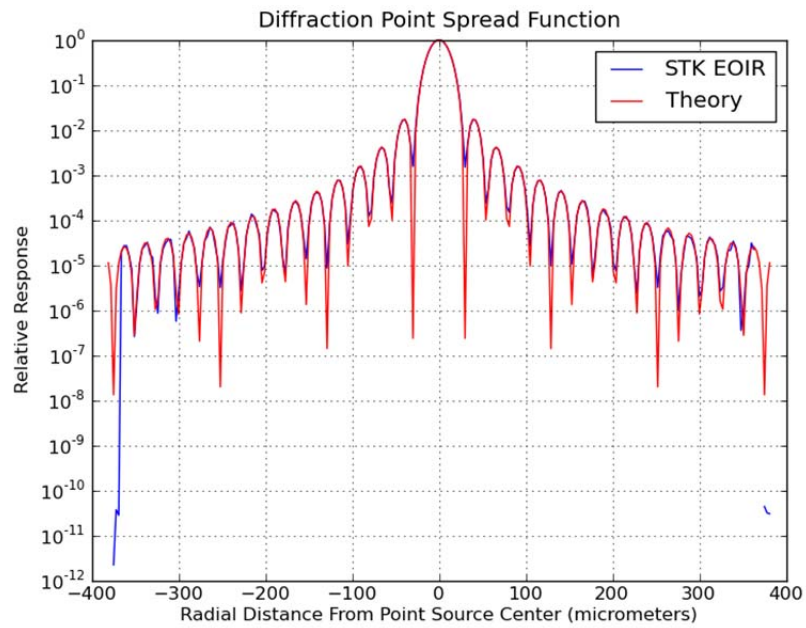
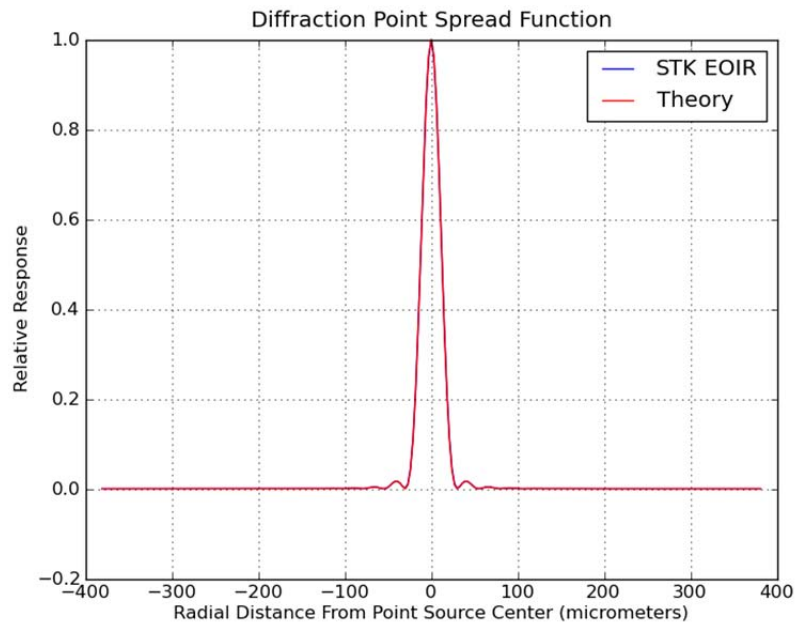
### 7.5.1 Diffraction Limited Point Spread Function

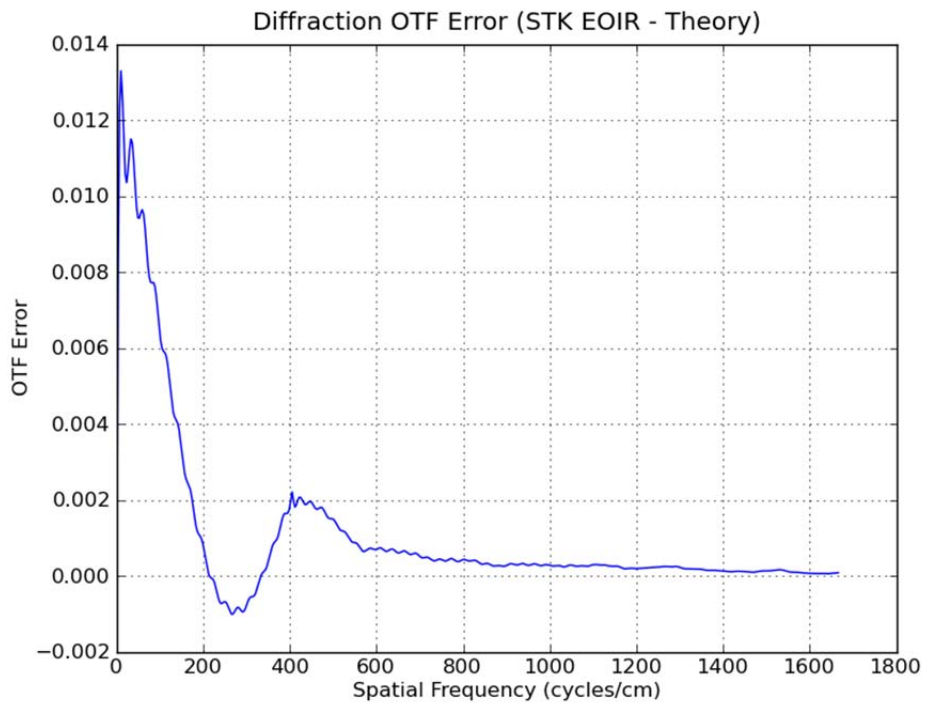
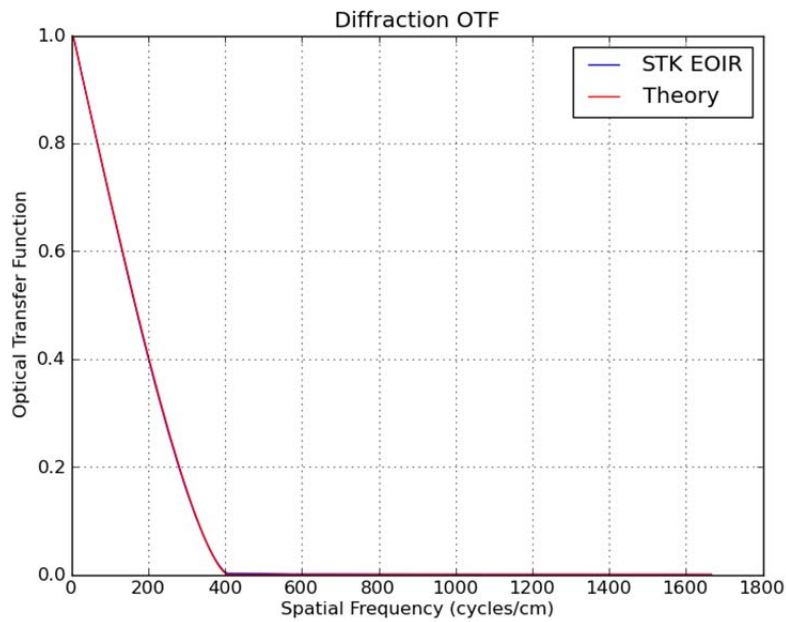
This procedure validates the modeled diffraction point spread function.

1. Run STK EOIR.
2. Open the scenario Valid\_Sens\_PSF. This scenario contains a sensor viewing a small spherical object (Aircraft2). The spectral passband of the sensor is 10 – 14  $\mu\text{m}$ . The dimensions of Aircraft2 and the viewing geometry are such that the angular extent of Aircraft2 is small compared with a single sensor pixel. The sensor parameters are set such that the Airy disk (central blur of the point spread function) covers several pixels so that the point response function is limited by optical effects rather than spatial averaging over individual pixels, i.e. the point response function is approximately the same as the point spread function. The number of pixels is set to an odd number so that the point source center will be at the center of a pixel instead of the corners of four adjacent pixels.
3. Display the EOIR Sensor Scene window. Confirm that the image appears to be that of a diffraction pattern for a circular aperture.

- 
4. Save the sensor image data to a file.
  5. Import the sensor image data file into MATLAB or Python.
  6. The point source center should be at pixel (127,127). Plot a cross section of the point response function for row 127. Overplot the theoretical diffraction point spread function.
  7. Repeat the plots in step 6 on a logarithmic scale.
  8. Compute the optical transfer function (OTF) from the sensor image data.
    - a. Zero-pad the sensor image data by a factor of four, circularly shift the data along each axis until the point source center (originally at index [127,127]) is at index [0,0], compute the 2D FFT, normalize by the transform coefficient at index [0,0], and take the real part.
  9. Plot a cross section of the 2D OTF for the first row (or first column). Overplot the theoretical diffraction OTF.
  10. Plot the error between the OTF computed from the sensor image data and the theoretical OTF.
  11. The plots confirm that the simulated diffraction point spread function matches the theoretical diffraction point spread function with acceptable error.





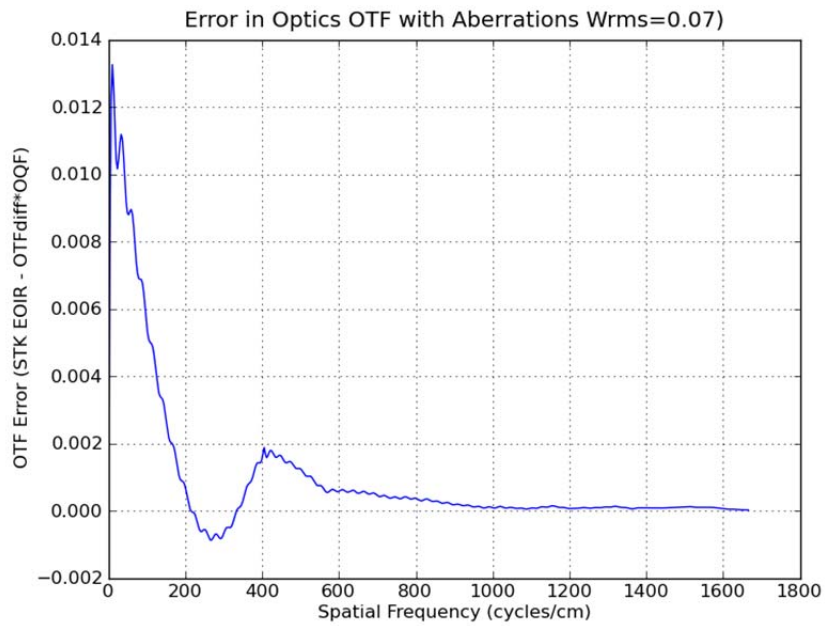
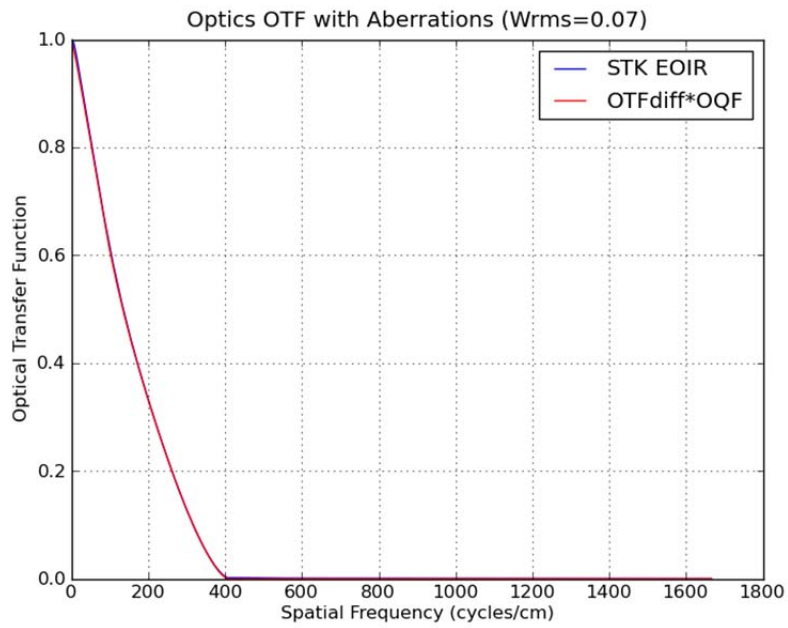


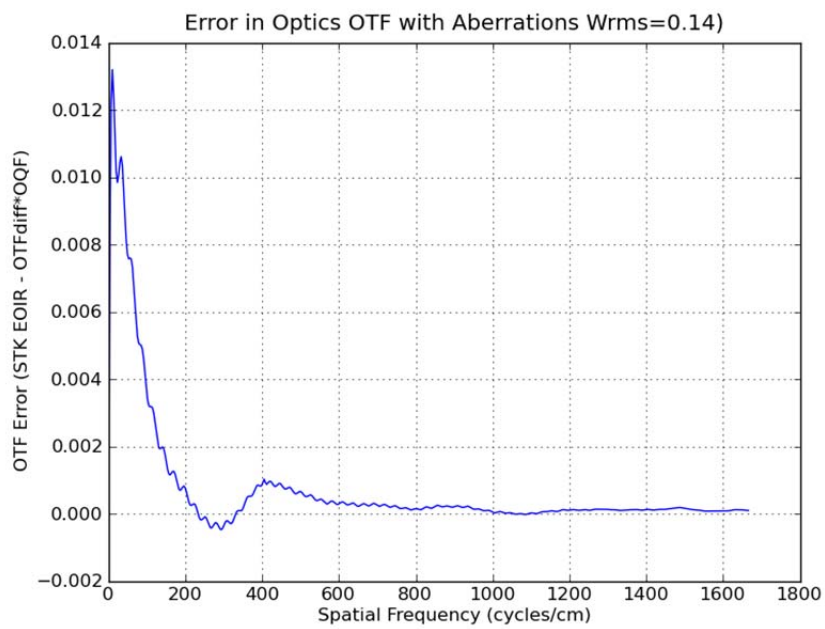
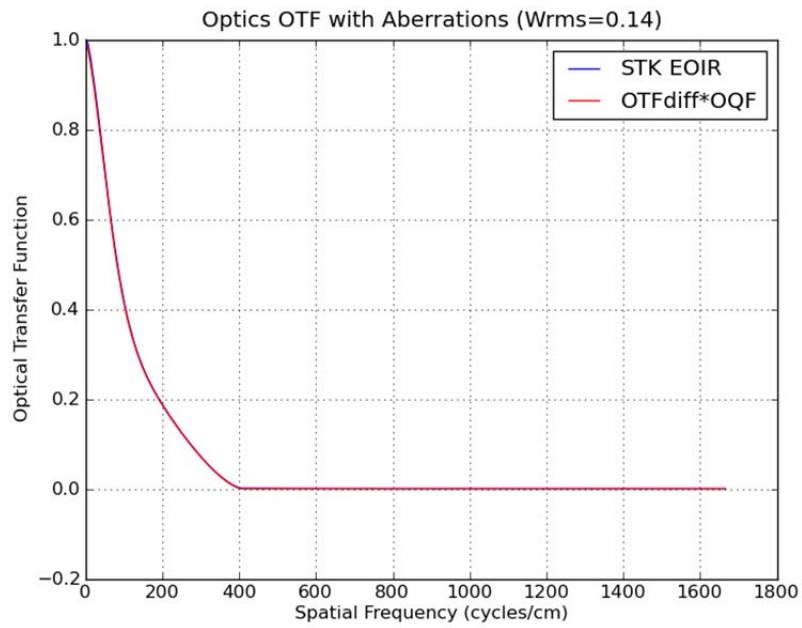
### 7.5.2 Point Spread Function with Aberrations

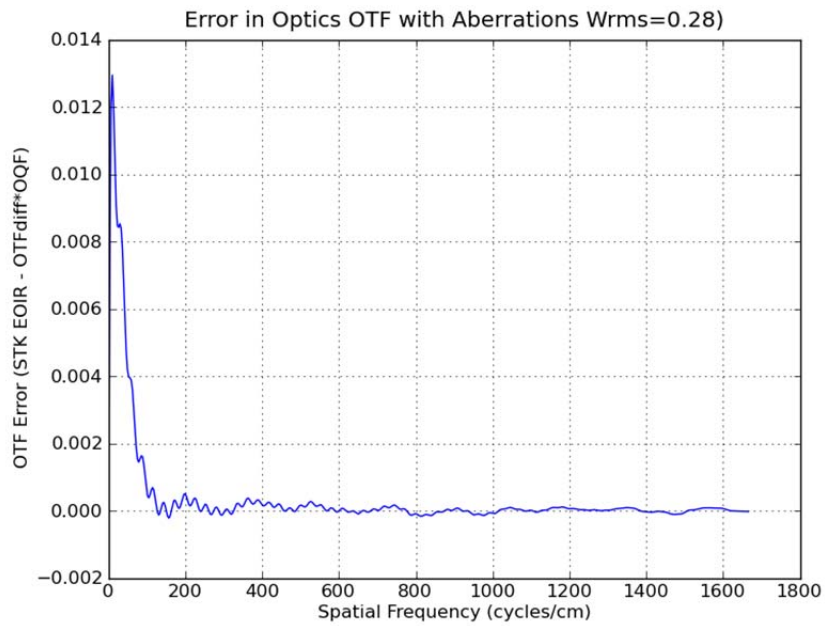
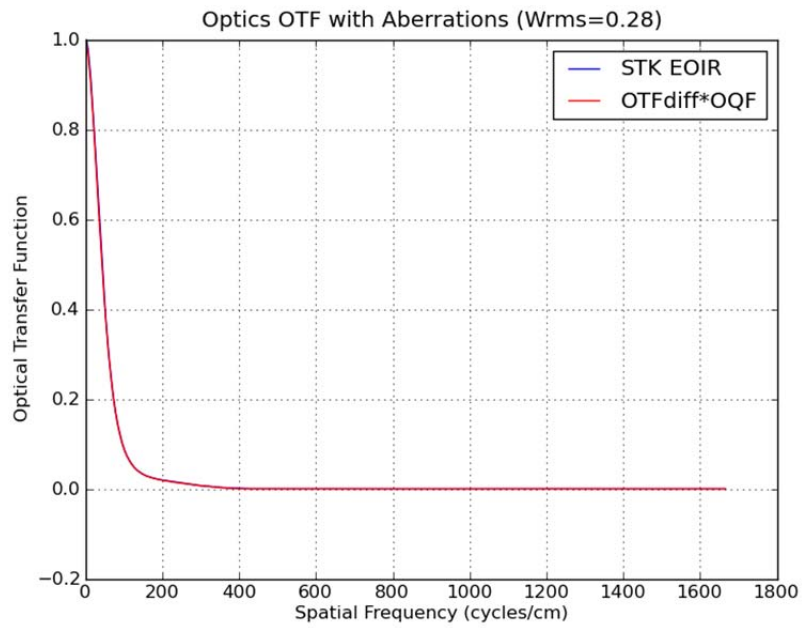
This procedure validates the modeled point spread function including aberrations.

- 
1. Run STK EOIR.
  2. Open the scenario Valid\_Sens\_PSF. This scenario contains a sensor viewing a small spherical object (Aircraft2). The spectral passband of the sensor is 10 – 14  $\mu\text{m}$ . The dimensions of Aircraft2 and the viewing geometry are such that the angular extent of Aircraft2 is small compared with a single sensor pixel. The sensor parameters are set such that the Airy disk (central blur of the point spread function) covers several pixels so that the point response function is limited by optical effects rather than spatial averaging over individual pixels, i.e. the point response function is approximately the same as the point spread function. The number of pixels is set to an odd number so that the point source center will be at the center of a pixel instead of the corners of four adjacent pixels.
  3. Change the Image Quality setting for the EOIR sensor to ‘Negligible Aberrations’.
  4. Display the EOIR Sensor Scene window.
  5. Save the sensor image data to a file.
  6. Import the sensor image data file into MATLAB or Python.
  7. Compute the optical transfer function (OTF) from the sensor image data.
    - a. Zero-pad the sensor image data by a factor of four, circularly shift the data along each axis until the point source center (originally at index [127,127]) is at index [0,0], compute the 2D FFT, normalize by the transform coefficient at index [0,0], and take the real part.
  8. Plot a cross section of the 2D OTF for the first row (or first column). Overplot the product of the theoretical diffraction OTF and the Hufnagle optical quality factor (OQF) with appropriate rms wavefront error given the Image Quality setting (see Section 5.6.1).
  9. Plot the error between the OTF computed from the sensor image data and the product of the theoretical diffraction OTF and the Hufnagle OQF.
  10. Repeat steps 3 through 9 for Image Quality settings of ‘Mild Aberrations’ and ‘Moderate Aberrations’.
  11. The plots confirm that the simulated point spread function with aberrations matches the expected point spread function using the Hufnagle approximation with acceptable error.







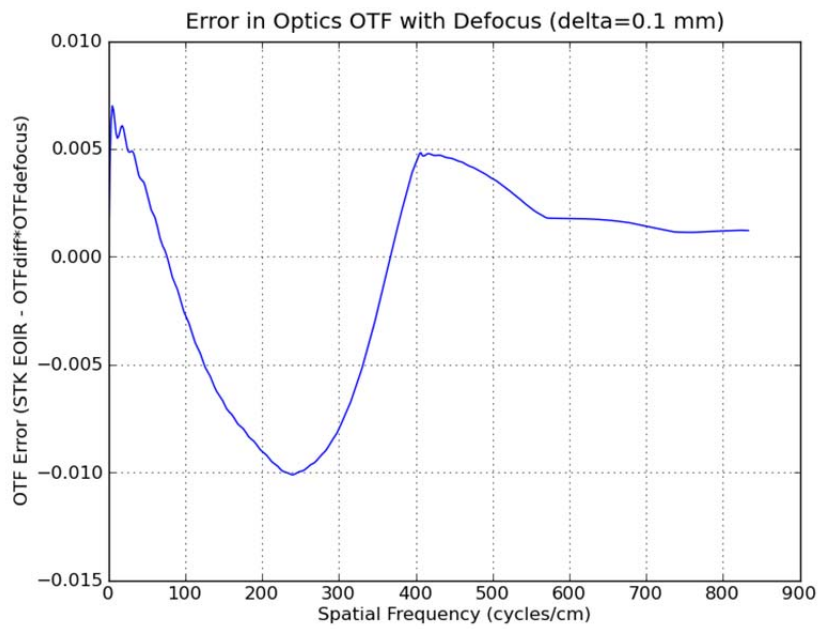
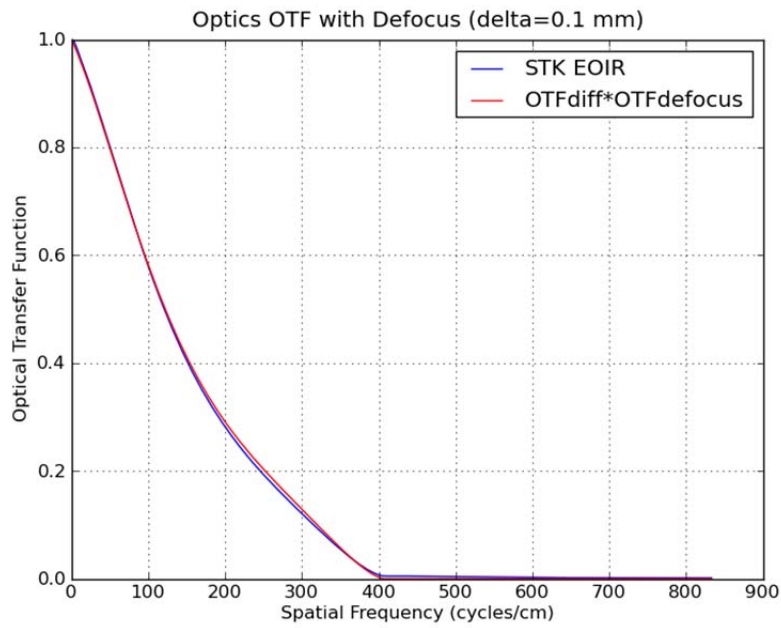


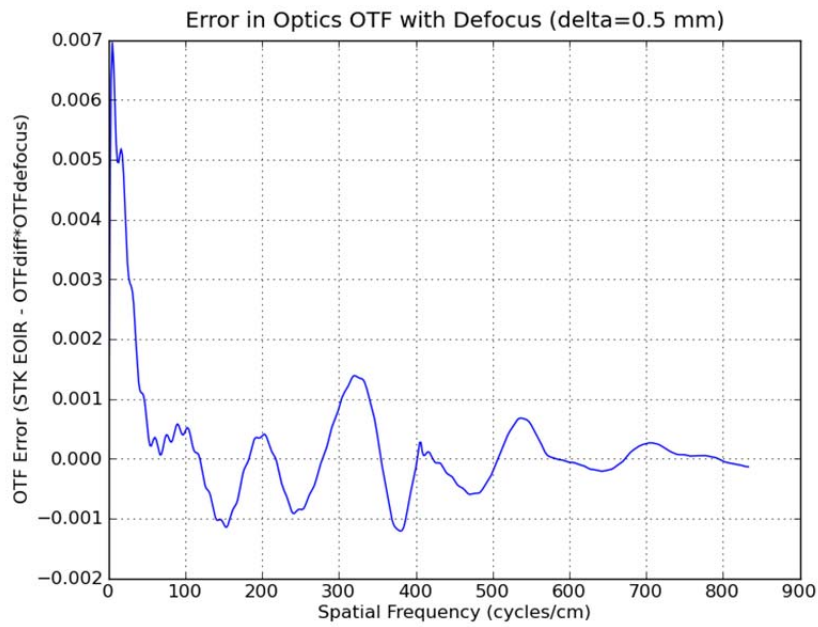
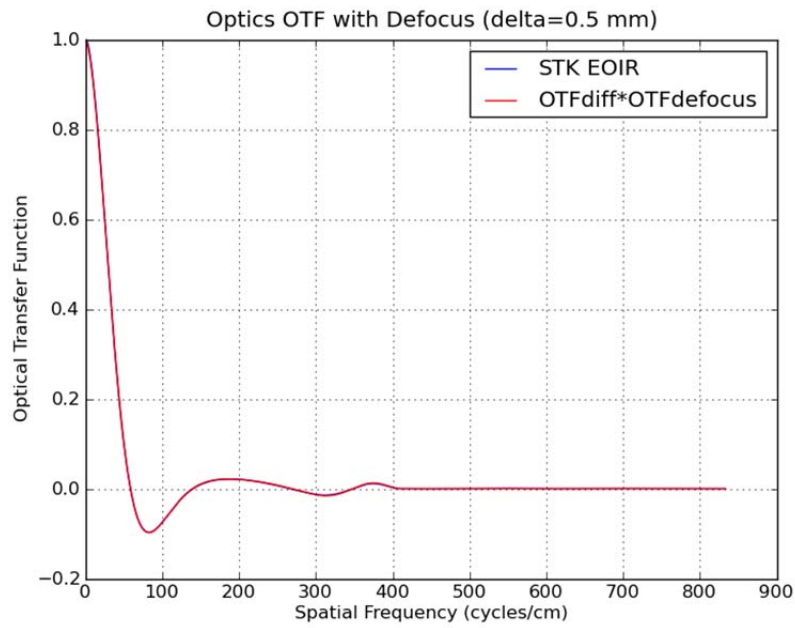
---

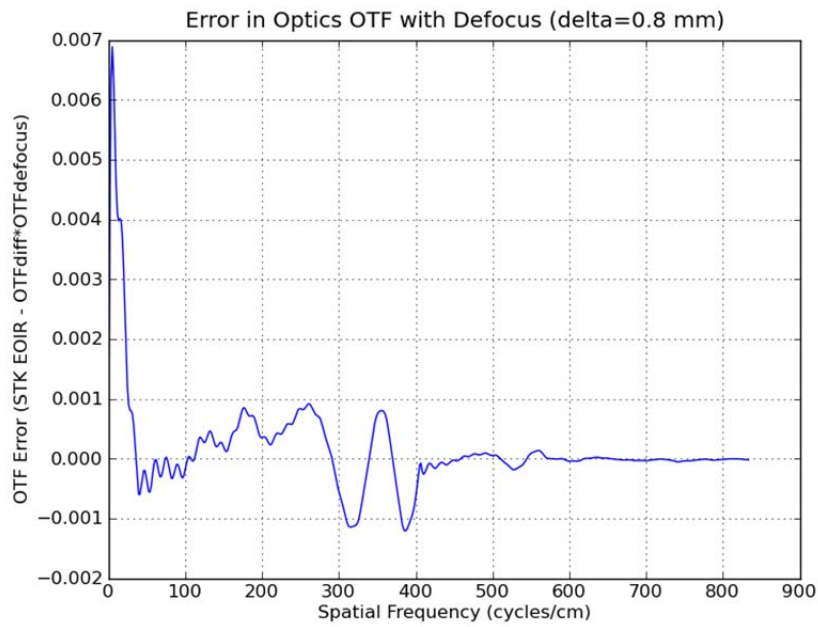
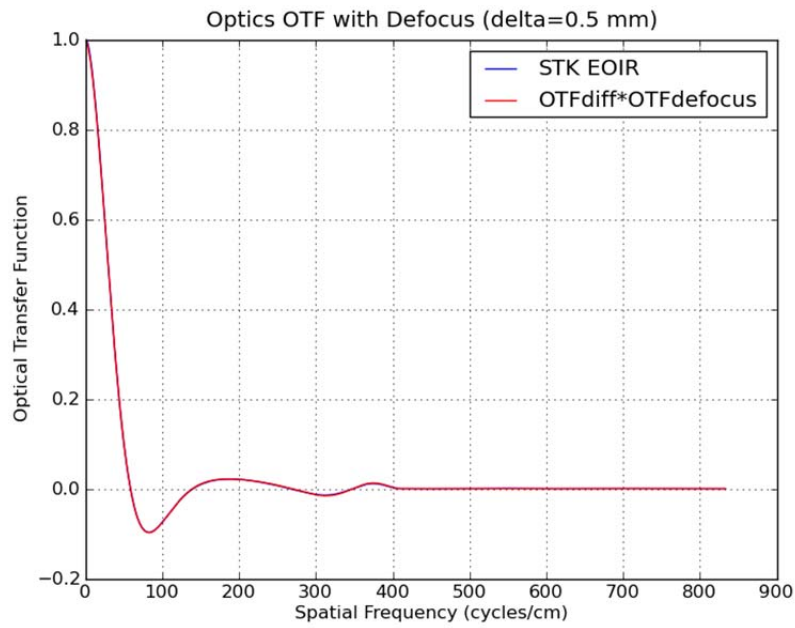
### 7.5.3 Point Spread Function with Defocus

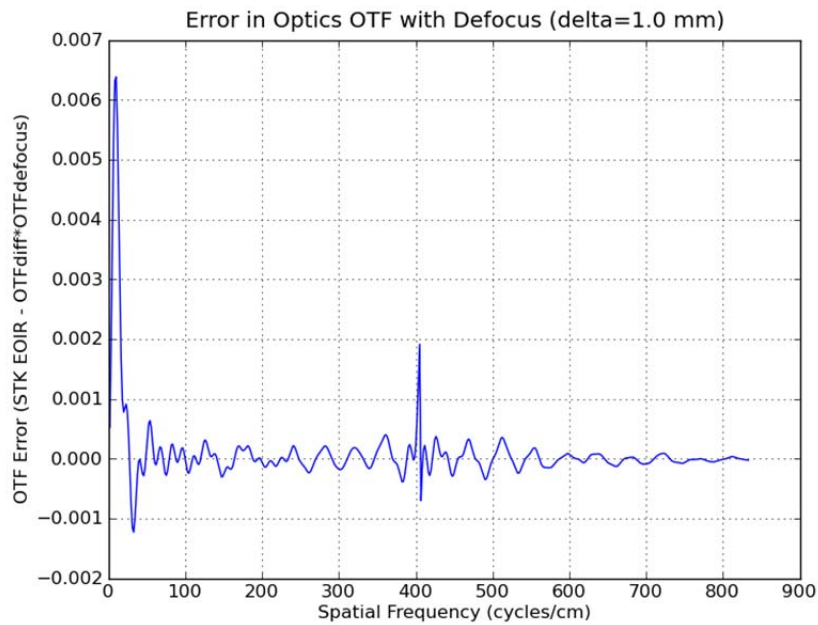
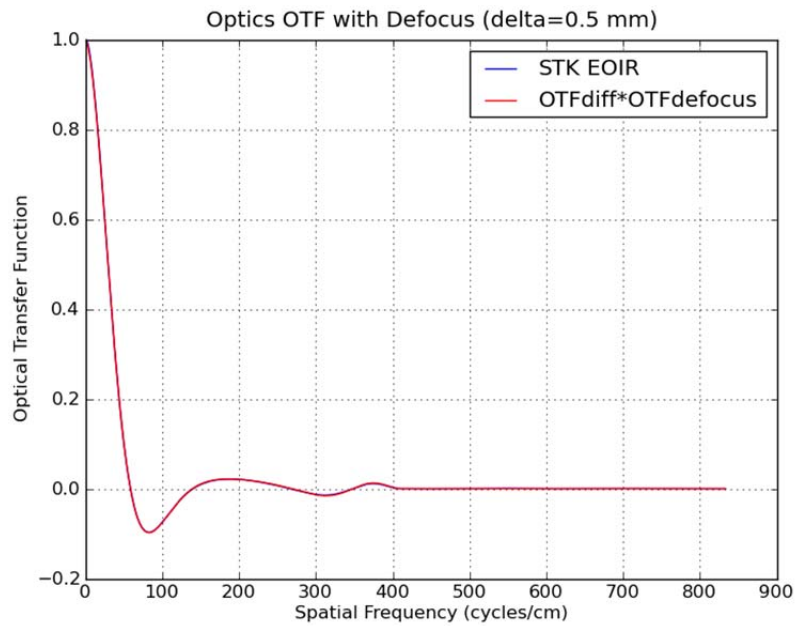
This procedure validates the modeled point spread function including defocus.

1. Run STK EOIR.
2. Open the scenario Valid\_Sens\_PSF. This scenario contains a sensor viewing a small spherical object (Aircraft2). The spectral passband of the sensor is 10 – 14  $\mu\text{m}$ . The dimensions of Aircraft2 and the viewing geometry are such that the angular extent of Aircraft2 is small compared with a single sensor pixel. The sensor parameters are set such that the Airy disk (central blur of the diffraction pattern) covers several pixels so that the point response function is limited by optical effects rather than spatial averaging over individual pixels, i.e. the point response function is approximately the same as the point spread function. The number of pixels is set to an odd number so that the point source center will be at the center of a pixel instead of the corners of four adjacent pixels.
3. Change the Effective Focal Length to 16 cm.
4. Change the Longitudinal Defocus to 0.1 mm.
5. Display the EOIR Sensor Scene window.
6. Save the sensor image data to a file.
7. Import the sensor image data file into MATLAB or Python.
8. Compute the optical transfer function (OTF) from the sensor image data.
  - a. Zero-pad the sensor image data by a factor of four, circularly shift the data along each axis until the point source center (originally at index [127,127]) is at index [0,0], compute the 2D FFT, normalize by the transform coefficient at index [0,0], and take the real part.
9. Plot a cross section of the 2D OTF for the first row (or first column). Overplot the product of the theoretical diffraction OTF and the defocus OTF with appropriate longitudinal defocus (see Section 5.6.1).
10. Plot the error between the OTF computed from the sensor image data and the product of the theoretical diffraction OTF and the defocus OTF.
11. Repeat steps 4 through 10 for Longitudinal Defocus settings of 0.5 mm, 0.8 mm, and 1.0 mm.
12. The plots confirm that the simulated point spread function with defocus matches the expected point spread function using the defocus OTF approximation (Section 5.6.1) with acceptable error.









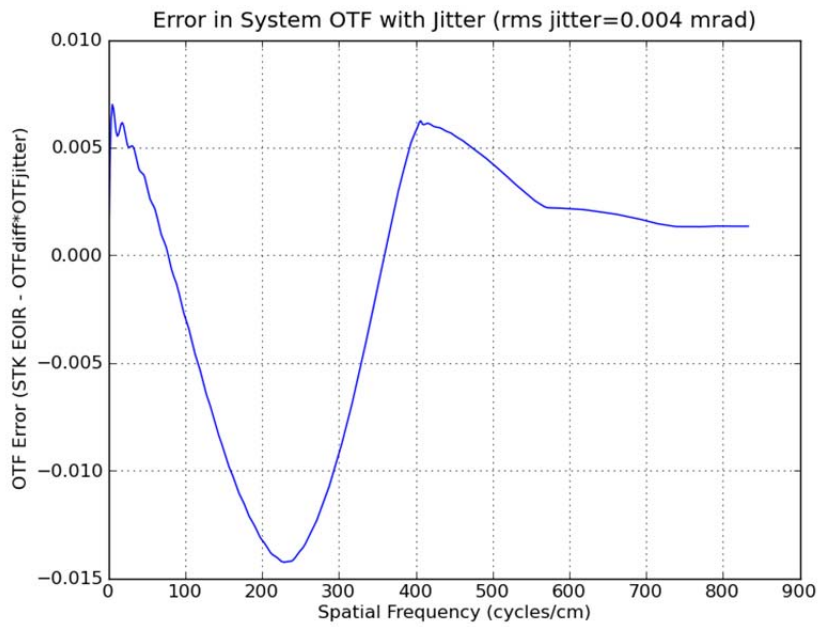
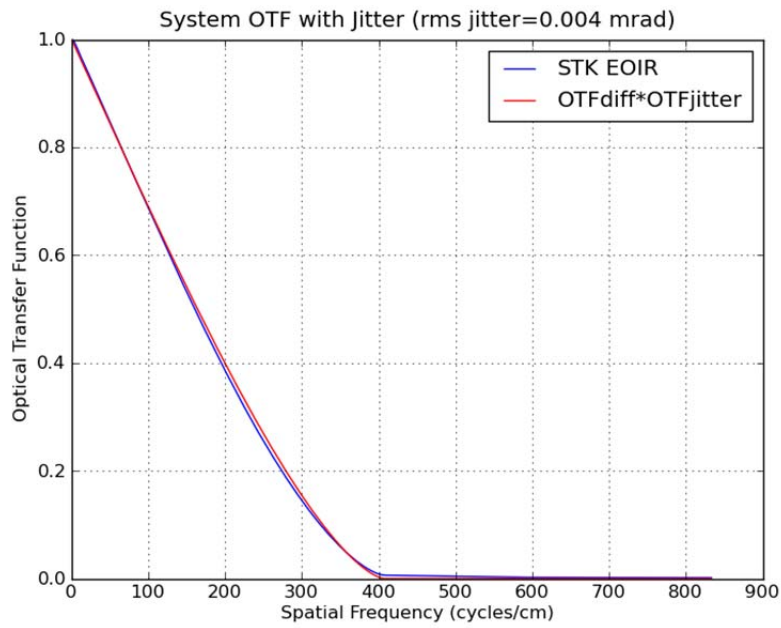
### 7.5.4 Point Spread Function with Line-of-Sight Jitter

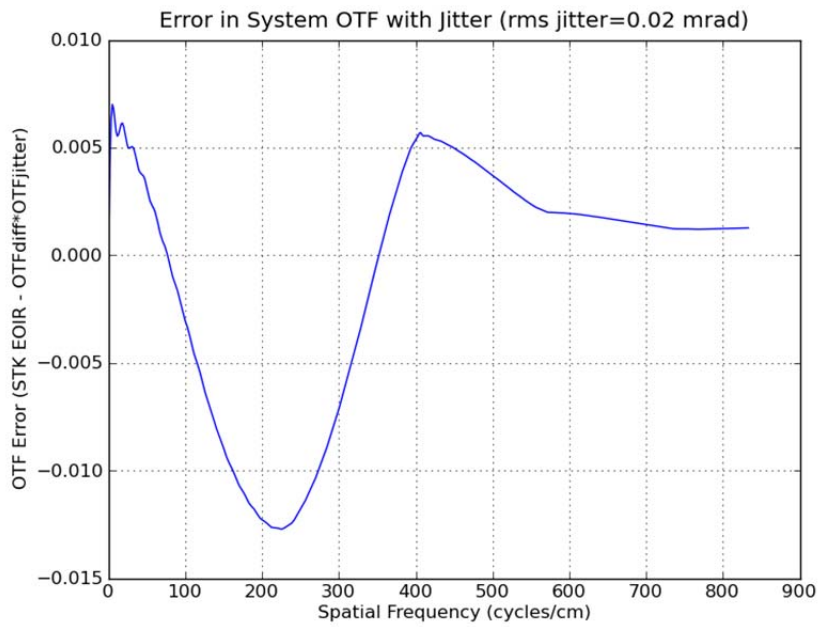
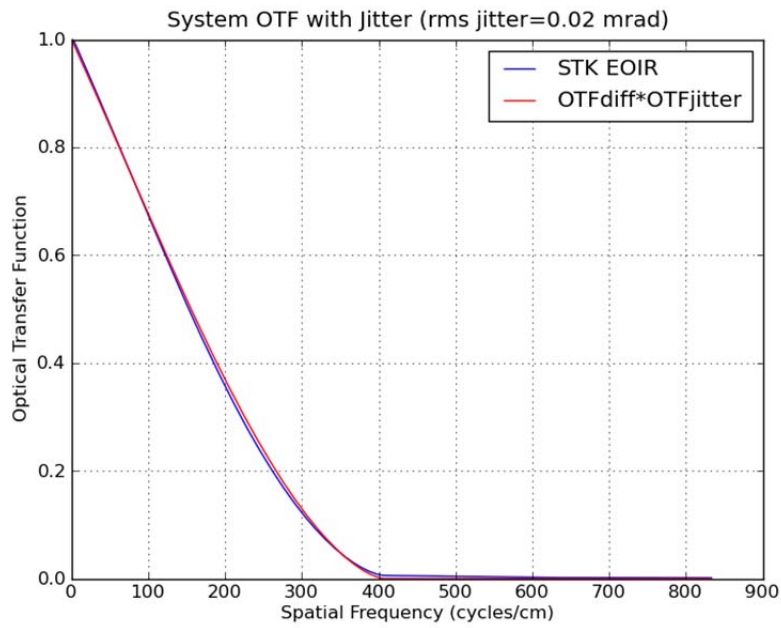
This procedure validates the modeled point spread function including high-frequency line-of-sight jitter.

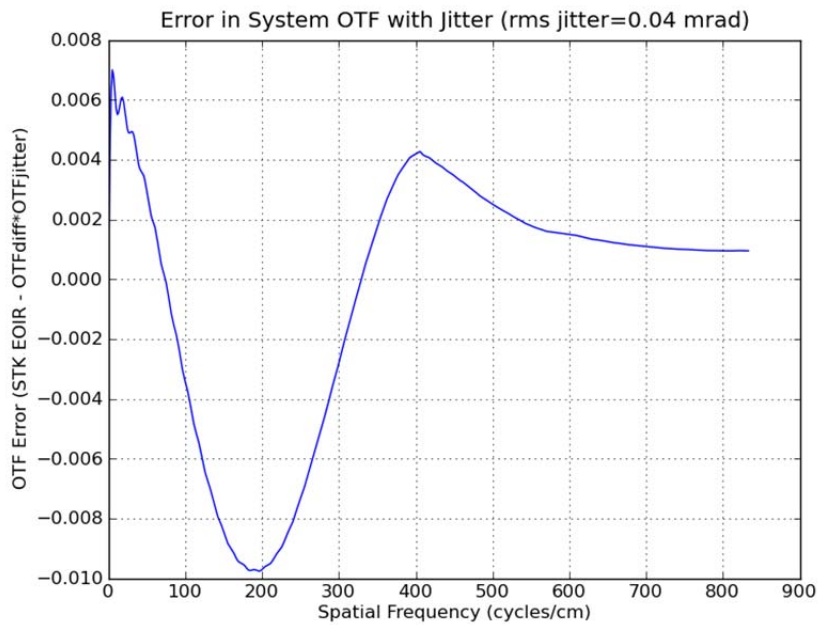
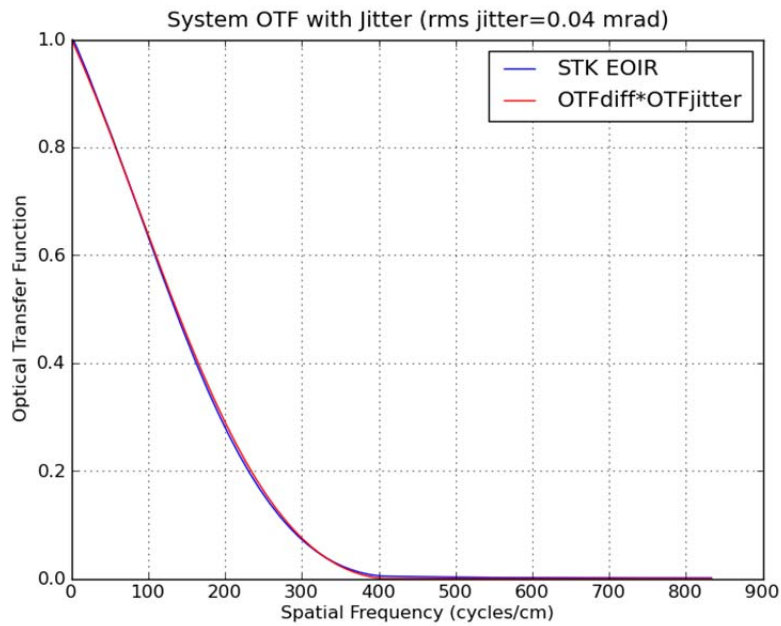
1. Run STK EOIR.



- 
2. Open the scenario Valid\_Sens\_PSF. This scenario contains a sensor viewing a small spherical object (Aircraft2). The spectral passband of the sensor is 10 – 14  $\mu\text{m}$ . The dimensions of Aircraft2 and the viewing geometry are such that the angular extent of Aircraft2 is small compared with a single sensor pixel. The sensor parameters are set such that the Airy disk (central blur of the diffraction pattern) covers several pixels so that the point response function is limited by optical effects rather than spatial averaging over individual pixels, i.e. the point response function is approximately the same as the point spread function. The number of pixels is set to an odd number so that the point source center will be at the center of a pixel instead of the corners of four adjacent pixels.
  3. Change the Effective Focal Length to 16 cm.
  4. Change the Line of Sight Jitter to 0.004 mrad (approximately one-tenth of one IFOV).
  5. Display the EOIR Sensor Scene window.
  6. Save the sensor image data to a file.
  7. Import the sensor image data file into MATLAB or Python.
  8. Compute the optical transfer function (OTF) from the sensor image data.
    - a. Zero-pad the sensor image data by a factor of four, circularly shift the data along each axis until the point source center (originally at index [127,127]) is at index [0,0], compute the 2D FFT, normalize by the transform coefficient at index [0,0], and take the real part.
  9. Plot a cross section of the 2D OTF for the first row (or first column). Overplot the product of the theoretical diffraction OTF and the jitter OTF with appropriate rms random angular displacement (see Section 5.6.2).
  10. Plot the error between the OTF computed from the sensor image data and the product of the theoretical diffraction OTF and the jitter OTF.
  11. Repeat steps 4 through 10 for Line of Sight Jitter settings of 0.02 mrad and 0.04 mrad.
  12. The plots confirm that the simulated point spread function with high-frequency line of sight jitter matches the expected point spread function using the jitter OTF approximation (Section 5.6.2) with acceptable error.







### 7.5.5 Ensquared Energy

This procedure validates that the ensquared energy in the synthetic sensor output image is correct and that it matches the ensquared energy reported by the EOIR Sensor Optics-Ensquared Energy data provider.

1. Run STK EOIR.

- 
2. Open the scenario Valid\_Sens\_PointSrcTarget. This scenario contains a sensor viewing a small spherical object (Satellite2). The spectral passband of the sensor is 8 – 12  $\mu\text{m}$ . The dimensions of Satellite2 and the viewing geometry are such that the angular extent of Satellite2 is small compared with a single sensor pixel. The sensor parameters are set such that the diameter of the Airy disk (central blur of the diffraction pattern) is the equal to the pixel pitch in both horizontal and vertical directions. The number of pixels is set to an odd number so that the point source center will be at the center of a pixel instead of the corners of four adjacent pixels.
  3. Display the EOIR Sensor Scene window. If the EOIR Sensor Scene window says “Sensor Unavailable” click the ‘Step Forward’ button to advance the scenario time by one time step.
  4. Save the sensor image data to a file.
  5. Import the sensor image data file into MATLAB or Python.
  6. Compute the ensquared energy from the sensor image data.
    - a. Obtain the sensor response in the pixel centered on the point source (index [63,63] in Python).
    - b. Obtain the total response to the point source over a window approximately 25 x 25 pixels centered on the point source.
    - c. Compute the fractional ensquared energy as the ratio of Step (a) to Step (b).
  7. Because the Airy disk contains 84% of the energy in the diffraction pattern and the pixel pitch is matched to the Airy disk diameter, the fractional ensquared energy should be slightly larger than 0.84.
  8. Run a report which includes the EOIR Sensor Optics-Ensquared Energy data provider. Verify that the fractional ensquared energy is  $\sim 0.84$ .
  9. Compare the ensquared energy in the report with the ensquared energy calculated from the sensor output data in Step 6. The difference should be on the order of  $\sim 1\%$ .

## 7.6 STATIC METRICS

This procedure is used to validate all static metrics except ensquared energy which is validated in Section 7.5.5, and the modulation transfer functions.

1. Run STK EOIR
2. Open the scenario Valid\_Sens\_StaticMetrics. This scenario contains a sensor on a satellite. The sensor parameters are set as follows.
  - a. Number of Pixels (Horizontal) = 128
  - b. Number of Pixels (Vertical) = 128
  - c. Field of View (Horizontal) = 0.5 degrees
  - d. Field of View (Vertical) = 0.5 degrees
  - e. Low Spectral Band Edge Wavelength = 1.0  $\mu\text{m}$
  - f. High Spectral Band Edge Wavelength = 4.0  $\mu\text{m}$
  - g. F-number = 3.5
  - h. Effective Focal Length = 147.0 cm
  - i. Longitudinal Defocus = 0.0 mm

- j. Image Quality = “Diffraction Limited”
  - k. Diffraction Wavelength = 2.5  $\mu\text{m}$  (Band Center)
  - l. Current Integration Time = 10 msec
  - m. Sensitivity Reference Pair = (10 msec, 1.0E-18 W/cm<sup>2</sup>)
  - n. Saturation Reference Pair = (10 msec, 1.0E-15 W/cm<sup>2</sup>)
  - o. Line-of-Sight Jitter = 0.0 mrad
3. The ensquared energy for this sensor configuration is 0.9683. Confirm this by running a report which includes the EOIR Sensor Optics-Ensquared Energy data provider.
  4. Given the sensor settings above and the static metric definitions in Table 1, the expected values for the static metrics are as follows.

**Table 3. Expected Values of Static Metrics**

<b>Metric</b>	<b>Expected Value</b>
Number of Pixels in Horizontal Direction	128
Number of Pixels in Vertical Direction	128
Geometric Field of View (FOV) Solid Angle	7.6154E-5 sr
Geometric FOV in Horizontal Direction	0.5 degrees
Geometric FOV in Vertical Direction	0.5 degrees
Geometric Instantaneous Field of View (IFOV) Solid Angle	4.648E-9 sr
Geometric IFOV in Horizontal Direction	6.818E-2 mrad
Geometric IFOV in Vertical Direction	6.818E-2 mrad
Effective FOV Solid Angle	7.865E-5 sr
Effective FOV in Horizontal Direction	0.5081 degrees
Effective FOV in Vertical Direction	0.5081 degrees
Effective Instantaneous Field of View (IFOV) Solid Angle	4.80E-9 sr

Effective IFOV in Horizontal Direction	6.928E-2 mrad
Effective IFOV in Vertical Direction	6.928E-2 mrad
Low Band Edge Wavelength	1.0 $\mu\text{m}$
High Band Edge Wavelength	4.0 $\mu\text{m}$
Peak Irradiance Responsivity	5.295E19 $\text{e}^- / (\text{W}/\text{cm}^2)$
Sensor NEI	1.0E-18 $\text{W}/\text{cm}^2$
Sensor SEI	1.0E-15 $\text{W}/\text{cm}^2$
Peak Radiance Responsivity	2.542E11 $\text{e}^- / (\text{W}/(\text{cm}^2 \text{ sr}))$
Sensor NER	2.083E-10 $\text{W}/(\text{cm}^2 \text{ sr})$
Sensor SER	2.083E-7 $\text{W}/(\text{cm}^2 \text{ sr})$
Effective Focal Length	147.0 cm
F-number	3.5
Diffraction Wavelength	2.5 $\mu\text{m}$
Airy Disk Diameter	1.452E-2 mrad
Rayleigh Resolution	7.262E-3 mrad
Sparrow Resolution	5.952E-3 mrad

5. Run the following reports in the Installed Styles: EOIR Sensor Spatial Performance, EOIR Sensor Spectral Performance, EOIR Radiometric Performance, and EOIR Sensor Optics.
6. Verify that the values in the reports match expected values in Table 3 above.

## 7.7 DYNAMIC METRICS INVOLVING A TARGET

These procedures validate the dynamic metrics involving a sensor-target pair under various circumstances.

### 7.7.1 Stationary Target against a Uniform Background

This procedure is used to validate the dynamic metrics involving a target under a controlled and very simple scenario: a stationary target against a uniform background.

1. Run STK EOIR
2. Open the scenario Valid\_Sens\_PtSrcTgtUniformBkg. This scenario contains a sensor on an aircraft (Aircraft3) viewing a small spherical object (Aircraft2) against a uniform background (Aircraft1). The radius of Aircraft2 is initially set to 1.0 m. Aircraft1 is positioned further

---

away from the sensor than Aircraft2 and the dimensions of Aircraft1 are such that Aircraft1 completely fills the sensor field of view. The temperature of Aircraft2 (the target) is initially set to 350K and the temperature of Aircraft1 (the background) is initially set to 300K. For both aircraft the material is set to Gray Body and the reflectance is set to 0 %, i.e. both aircraft will act as blackbody emitters. All aircraft are located at the same latitude and longitude with Aircraft1 at an altitude of 0.0 km, Aircraft2 at an altitude of 1.6 km, and Aircraft3 at an altitude of 100.0 km. Relevant sensor parameters (or derived parameters) are set as follows:

- a. Spectral band low wavelength = 8  $\mu\text{m}$
  - b. Spectral band high wavelength = 12  $\mu\text{m}$
  - c. Sensor dark NEI =  $1\text{E-}18 \text{ W/cm}^2$
  - d. Peak irradiance responsivity  $3.779\text{E}20 \text{ electrons / (W/cm}^2)$
  - e. Pixel pitch = 100.2207  $\mu\text{m}$  in both horizontal and vertical directions
  - f. Focal length = 147.0 cm.
  - g. Ensquared energy = 0.86396
  - h. Number of spectral intervals is set to 50 to minimize errors in numerical integration.
3. Select the sensor and display the Report and Graph Manager. Select the EOIR Sensor-to-Target metrics report in the Installed styles. Before running the report change the Time Properties to “Specify properties”, change the Stop time to “25 Aug 2010 18:05:00.00 UTCG”, and set the step size to 60.0 sec. Run the report and select Aircraft2 as the target.
  4. For this scenario the values of the metrics in the report should be constant as a function of time. Verify that the values in the report are close to the following (these expected values can be calculated using the model equations referred to in Table 2):
    - a. Range to target = 98.4 km (100.0 km – 1.6 km)
    - b. Effective target irradiance =  $2.53\text{E-}12 \text{ W/cm}^2$
    - c. Point target solid angle =  $3.24\text{E-}10 \text{ sr}$
    - d. Scene photon NEI =  $2.34\text{E-}16 \text{ W/cm}^2$
    - e. Total NEI =  $2.34\text{E-}16 \text{ W/cm}^2$
    - f. Effective target radiance = (not applicable but set to 0.0 in report)
    - g. Effective background radiance =  $3.85\text{E-}3 \text{ W/(cm}^2 \text{ sr)}$
    - h. Scene photon NER =  $4.35\text{E-}8 \text{ W/(cm}^2 \text{ sr)}$
    - i. Total NER =  $4.35\text{E-}8 \text{ W/(cm}^2 \text{ sr)}$
    - j. Signal to noise ratio = 5479
    - k. Geometric IFOV footprint = 45.006  $\text{m}^2$
    - l. Effective IFOV footprint = 46.481  $\text{m}^2$
  5. Change the temperature of Aircraft2 (the target) to 300 K. After this change the temperatures of the target and background are the same.
  6. Re-run or refresh the report.
  7. Verify that the SNR is now 0.0.
  8. Turn the atmosphere on (use default atmospheric properties).



- 
9. Note that SNR is now non-zero<sup>3</sup>.
  10. Turn the atmosphere off.
  11. Change the temperature of Aircraft1 (the background) to 0.0 K.
  12. Re-run or refresh the report.
  13. Verify that the scene photon NEI is now 0.0 and the total NEI is equal to the sensor dark NEI (1.0E-18 W/cm<sup>2</sup>).
  14. Change the temperature of Aircraft1 back to 300 K and the temperature of Aircraft2 back to 350 K.
  15. The effective IFOV solid angle of the sensor  $\Omega_{EIFOV} = 5.38E-9$  sr. Change the radius of Aircraft2 to 4.072 m. This will make the solid angle subtended by the target at the sensor  $\Omega_T = 5.3799E-9$  sr, i.e. just smaller than  $\Omega_{EIFOV}$ . (NOTE: the Point Target Solid Angle shown in the report may not match the exact value of  $\Omega_T = 5.3799E-9$  sr.)
  16. Re-run or refresh the report.
  17. Confirm that the target is treated as a point source (effective target irradiance and point target solid angle are non-zero and effective target radiance is zero). Record the value of SNR.
  18. Change the radius of Aircraft2 to 4.073 m. This will make the solid angle subtended by the target at the sensor  $\Omega_T = 5.383E-9$  sr, i.e. just larger than  $\Omega_{EIFOV}$ .
  19. Re-run or refresh the report.
  20. Confirm that the target is now treated as an extended area source (effective target irradiance and point target solid angle are zero and effective target radiance is non-zero). Record the value of SNR.
  21. Note that the SNR decreases slightly when the target transitions from a point source to extended area source. This is caused by the fact that the point source solid angle computed internally by the model is slightly larger than the true solid angle of the point source causing the irradiance from the point source to be slightly larger than it should be. However, the errors are small (~1%).
  22. Confirm that the effective target radiance is  $\sim 7.80E-3$  W/(cm<sup>2</sup> sr).

### 7.7.2 Satellite Point Source Target

This procedure is used to validate the SNR for a moving point source satellite target.

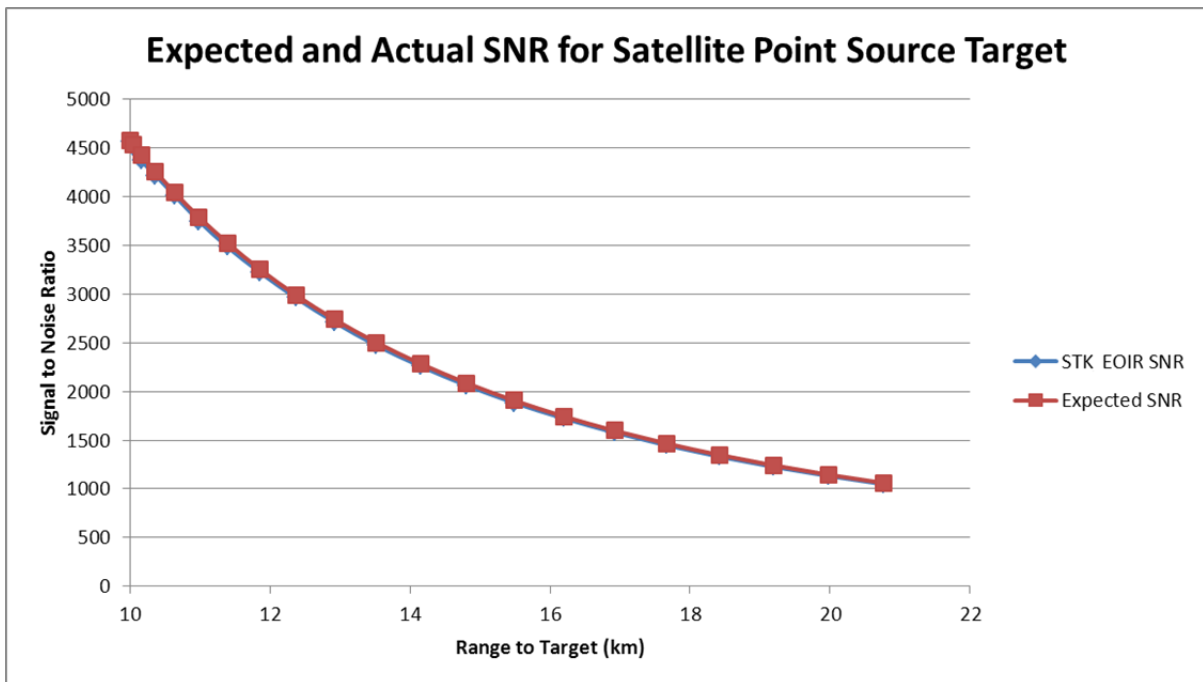
1. Run STK EOIR
2. Open the scenario Valid\_Sens\_PointSrcTarget. This scenario contains a sensor on a satellite (Satellite1) viewing a small spherical object (Satellite2). The radius of Satellite2 is set to 1 cm. The semi-major axis of Satellite1's orbit is 7300 km and the semi-major axis of Satellite2's orbit is 7310 km. Thus when the scenario begins the target satellite is 10 km away from the sensor and as the scenario progresses it gets further away. Because the sensor is lower than the target satellite the background is space. The temperature of Satellite2 (the

---

<sup>3</sup> The SNR should be 0.0 in this case but isn't because the point source irradiance calculated with Eqn. (9) doesn't include path radiance while the background radiance calculated with Eqn. (11) does include path radiance. This inconsistency will be fixed in a future release of STK EOIR.

target) is set to 250K, its material is set to Gray Body, and its reflectance is set to 0 %, i.e. the target satellite will act as a blackbody emitter at 250 K. Relevant sensor parameters (or derived parameters) are set as follows:

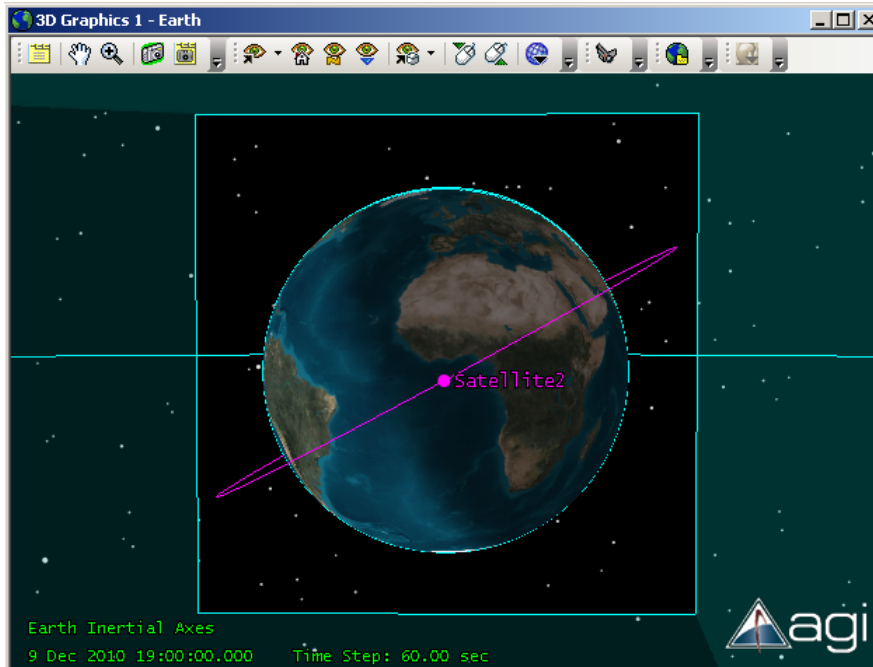
- a. Spectral band low wavelength = 8  $\mu\text{m}$
  - b. Spectral band high wavelength = 12  $\mu\text{m}$
  - c. Sensor dark NEI =  $1\text{E-}18 \text{ W/cm}^2$
3. Select the sensor and display the Report and Graph Manager. Select the EOIR Sensor-to-Target metrics report in the Installed styles. Before running the report change the Time Properties to “Specify properties”, change the Stop time to “3 Aug 2010 16:20:00.00 UTCG”, and set the step size to 60.0 sec. Run the report and select Satellite2 as the target.
  4. Save the report as a .csv file and import into Excel.
  5. From the scenario parameters calculate the expected SNR vs. range.
  6. Plot the actual and expected SNR vs. range.



## 7.8 SNR ACCESS CONSTRAINT

This procedure validates that the SNR Access constraint works as expected.

1. Run STK EOIR
2. Open the scenario Valid\_Sens\_SNR\_Access. This scenario contains a nadir-pointing wide-angle (24 x 24 degrees full-angle) sensor on a geosynchronous satellite (Satellite2) and a low Earth orbiting satellite (Satellite2). The spectral bandpass of the sensor is 8 – 12  $\mu\text{m}$ . The temperature of Satellite2 is 300 K.



3. Select the sensor and display the Report and Graph Manager. Select the EOIR Sensor-to-Target Metrics report in the Installed styles. Before running the report change the Time Properties to “Specify properties”, change the Stop time to “9 Dec 2010 22:00:00.00 UTCG”, and set the step size to 60.0 sec. Run the report and select Satellite2 as the target. (This report will take several minutes to run.) Save the report as a .csv file.
4. The report shows periods of time where the SNR is  $\sim 0.0$  and periods of time when the SNR is a small non-zero value ( $\sim 5 - 9$ ). Because the temperature of Satellite2 is similar to terrestrial temperatures when Satellite2 is viewed against the Earth background there is very little contrast between the target and the background and the SNR is  $\sim 0.0$ . Thus, the periods of time when the SNR is  $\sim 0$  correspond to times when Satellite2 viewed against the Earth background, or when Satellite2 is behind the Earth. The periods of time when the SNR is  $\sim 5 - 9$  correspond to times when Satellite2 viewed against the space background.
5. Run an Access Report using the same Time Period used for the EOIR Sensor-to-Target metrics report. Save the Access Report.
6. The Access Report shows two different Access periods.

Report: Satellite-Satellite1-Sensor-Sensor1-To-Satellite-Satellite2 - Access

Jump To: Top

Start: 9 Dec 2010 19:00:00.000 UTCG Stop: 9 Dec 2010 22:00:00.000 UTCG

10 Dec 2010 12:08:31

Satellite-Satellite1-Sensor-Sensor1-To-Satellite-Satellite2: Access Summary Report

Sensor1-To-Satellite2

Access	Start Time (UTC)	Stop Time (UTC)	Duration (sec)
1	9 Dec 2010 19:00:00.000	9 Dec 2010 19:54:26.866	3266.866
2	9 Dec 2010 20:40:14.742	9 Dec 2010 22:00:00.000	4785.258

Global Statistics

Min Duration	1	9 Dec 2010 19:00:00.000	9 Dec 2010 19:54:26.866	3266.866
Max Duration	2	9 Dec 2010 20:40:14.742	9 Dec 2010 22:00:00.000	4785.258
Mean Duration				4026.062
Total Duration				8052.123

- Change the EOIR Constraints such that the SNR minimum constraint is set to 6. When the change is applied the Access Report will automatically be recalculated. Save the new Access Report.
- Verify that the Access periods have changed to correspond to times when the SNR is greater than or equal to 6. (NOTE: The Access Start and Stop times are found by interpolating between time steps. Thus the Access Start and Stop times should be between time steps in the EOIR Sensor-to-Target Metrics report where the SNR changed from <6 to >6 or from >6 to <6.)

Report: Satellite-Satellite1-Sensor-Sensor1-To-Satellite-Satellite2 - Access

Jump To: Top

Start: 9 Dec 2010 19:00:00.000 UTCG Stop: 9 Dec 2010 22:00:00.000 UTCG

10 Dec 2010 11:54:31

Satellite-Satellite1-Sensor-Sensor1-To-Satellite-Satellite2: Access Summary Report

Sensor1-To-Satellite2

Access	Start Time (UTC)	Stop Time (UTC)	Duration (sec)
1	9 Dec 2010 19:15:38.451	9 Dec 2010 19:42:22.504	1604.053
2	9 Dec 2010 20:52:28.693	9 Dec 2010 21:20:51.801	1703.109
3	9 Dec 2010 21:49:08.905	9 Dec 2010 22:00:00.000	651.095

Global Statistics

Min Duration	3	9 Dec 2010 21:49:08.905	9 Dec 2010 22:00:00.000	651.095
Max Duration	2	9 Dec 2010 20:52:28.693	9 Dec 2010 21:20:51.801	1703.109
Mean Duration				1319.419
Total Duration				3958.257

## APPENDIX A. SPECTRAL REFLECTANCE FUNCTIONS

EOIR simulates spectral reflectance for the 17 International Geosphere Biosphere Program (IGBP) Global Land Cover types plus Tundra as type 18. The data utilized to create the SRF's came from the spectral reflectance libraries of the United States Geological Survey and John's Hopkins University. The various land cover types were created as linear combinations of simpler materials. NASA/TP-1999-209362, "Surface Emissivity Maps for Use in Satellite Retrievals of Longwave Radiation", provided a general guideline for proceeding, but the combinations utilized by EOIR are as follows:

No.	Land Cover Type	Combination Description
1	Evergreen Needle Leaf Forest	0.4*JHU:Conifer + 0.3*USGS:Blue Spruce + 0.3*USGS:Douglas Fir
2	Evergreen Broadleaf Forest	IGBP:1
3	Deciduous Needle Leaf Forest	0.4*JHU:Deciduous + 0.3*USGS:Oak + 0.3*USGS:Maple
4	Deciduous Broadleaf Forest	IGBP:3
5	Mixed Forest	0.5*IGBP:1 + 0.5*IGBP:3
6	Closed Shrubland	0.1*IGBP:16 + 0.2*Dirt + 0.7*IGBP:5
7	Open Shrubland	0.35*IGBP:16 + 0.25*Dirt + 0.4*IGBP:5
8	Woody Savannas	0.41*IGBP:10 + 0.14*USGS:Rangeland + 0.45*IGBP:3
9	Savannas	0.6*IGBP:10 + 0.2*USGS:Rangeland + 0.2*IGBP:3
10	Grasslands	0.4*JHU:Green Grass + 0.3*USGS:Lawn Grass + 0.3*USGS:Dry Grass
11	Permanent Wetlands	0.25*IGBP:10 + 0.25*IGBP:17 + 0.5*USGS:Wet Lands
12	Croplands	IGBP:10
13	Urban	0.1*Dirt + 0.1*IGBP:3 + 0.3*USGS:Concrete + 0.3*USGS:Asphalt + 0.2*USGS:Brick
14	Cropland/Mosaic	0.5*IGBP:12 + 0.5*IGBP:5
15	Snow and Ice	0.25*Fine Snow + 0.25*Medium Snow + 0.25*Coarse Snow + 0.25*Ice [see end of table]
16	Barren	0.3*USGS:Rangeland + 0.3*USGS:Hematite Quartz + 0.3*JHU:Quartz
17	Water Bodies	0.8*USGS:Sea Water + 0.2*JHU:Sea Water
18	Tundra	0.25*IGBP:11 + 0.25*USGS:Lichen + 0.125*IGBP:1 + 0.125*IGBP:15
<b>Convenient Building Blocks</b>		
	Dirt	0.4*USGS:Rangeland + 0.3*JHU:Brown Loamy Fine Sand + 0.3*JHU:Light Yellowish Brown Loamy Sand
	Fine Snow	0.5*JHU:Fine Snow + 0.5*USGS:Snow 1a
	Medium Snow	JHU:Medium Snow

Coarse Snow	0.5*JHU:Coarse Snow + 0.5*USGS:Snow 3
Ice	JHU:Ice

Where one or more datasets lacked values, the remaining dataset contributions are utilized with re-normalized fractional contributions. Since the available datasets mostly only go to 15.0  $\mu\text{m}$ , the last provided value is either propagated out to 28.0  $\mu\text{m}$  or forced to some low value. Generally, materials become much more emissive (less reflective) at longer wavelengths.

Some examples:

